

TECHNICAL UNIVERSITY OF CRETE
SCHOOL OF ENVIRONMENTAL ENGINEERING
Laboratory of Toxic and Hazardous Waste Management



PhD DISSERTATION

“Integrated development of treatment and management technologies of asbestos containing materials”

Aikaterini Valouma

Rural and Surveying Engineer, MSc

Chania, 2019

ΠΟΛΥΤΕΧΝΕΙΟ ΚΡΗΤΗΣ
ΣΧΟΛΗ ΜΗΧΑΝΙΚΩΝ ΠΕΡΙΒΑΛΛΟΝΤΟΣ
Εργαστήριο Διαχείρισης Τοξικών και Επικίνδυνων Αποβλήτων



ΔΙΔΑΚΤΟΡΙΚΗ ΔΙΑΤΡΙΒΗ

«Ολοκληρωμένη ανάπτυξη τεχνολογιών
αποτοξικοποίησης και διαχείρισης αμιαντούχων υλικών»

Αικατερίνη Βαλουμά

Αγρονόμος-Τοπογράφος Μηχανικός, MSc

Χανιά, 2019

Examination Committee

Evangelos Gidakos – Supervisor Professor

School of Environmental Engineering
Technical University of Crete

Konstantinos Komnitsas - Advisory committee

Professor
School of Mineral Resources Engineering
Technical University of Crete

Pagona-Noni Maravelaki - Advisory committee

Professor
School of Architecture
Technical University of Crete

Mihalis Galetakis

Professor
School of Mineral Resources Engineering
Technical University of Crete

Apostolos Gianni

Assistant Professor
School of Environmental Engineering
Technical University of Crete

Evangelos Diamadopoulos

Professor
School of Environmental Engineering
Technical University of Crete

George Karatzas

Professor
School of Environmental Engineering
Technical University of Crete

Dedicated to my father

He didn't tell me how to live.
He lived and let me watch him do it.

ΕΥΧΑΡΙΣΤΙΕΣ

Ολοκληρώνοντας την Διδακτορική Διατριβή θα ήθελα να ευχαριστήσω όλους τους ανθρώπους που με βοήθησαν στην διεκπεραίωσή της, χωρίς τη συμβολή των οποίων δε θα είχα φτάσει στο τέλος της διαδικασίας.

Η διδακτορική αυτή διατριβή θα ήταν αδύνατο να έχει ολοκληρωθεί χωρίς την πολύτιμη βοήθεια και στήριξη που έλαβα, από την αρχή των μεταπτυχιακών μου κιόλας σπουδών, από τον επιβλέποντα Καθηγητή κ. Ευάγγελο Γιδαράκο, που με εμπιστεύτηκε προσφέροντάς μου τη δυνατότητα να ασχοληθώ με ένα αντικείμενο εξαιρετικού ενδιαφέροντος. Θα ήθελα να τον ευχαριστήσω από καρδιάς για την συνεχή υποστήριξη, πνευματική, επιστημονική, ηθική και οικονομική. Επιπλέον, του οφείλω το πιο ειλικρινές ευχαριστώ για την καθολική και αμέριστη συμπαράστασή και το ενδιαφέρον που μου έδειξε σε προσωπικό επίπεδο. Σας ευχαριστώ πολύ για την εξαιρετική συνεργασία καθ' όλη τη διάρκεια της πενταετούς παρουσίας μου στο Εργαστήριο Διαχείρισης Τοξικών και Επικίνδυνων Αποβλήτων.

Ειδικές θερμές ευχαριστίες θα ήθελα να αποδώσω στα μέλη της συμβουλευτικής μου επιτροπής, τον Καθηγητή κ. Κωνσταντίνο Κομνίτσα και την Καθηγήτρια κα. Νόνη Μαραβελάκη, οι οποίοι πάντα μου προσέφεραν ανιδιοτελώς πολύτιμες επιστημονικές συμβουλές και ειλικρινές ενδιαφέρον για την πορεία αυτής της διδακτορικής διατριβής. Η παραμονή μου στο Πολυτεχνείο Κρήτης είναι άρρηκτα συνδεδεμένη και με τους δύο αυτούς καθηγητές που στάθηκαν για μένα αρωγοί, ο καθένας με τον τρόπο του, από τις μεταπτυχιακές μου σπουδές έως το τέλος του διδακτορικού μου. Ευχαριστώ για τις ευκαιρίες που μου δώσατε.

Επίσης, θα ήθελα να ευχαριστήσω τα μέλη της επταμελούς εξεταστικής επιτροπής, τον Καθηγητή κ. Μιχάλη Γαλετάκη, τον Επίκουρο Καθηγητή κ. Απόστολο Γιαννή, τον Καθηγητή κ. Ευάγγελο Διαμαντόπουλο και τον Καθηγητή κ. Γεώργιο Καρατζά, για το χρόνο που αφιέρωσαν στη μελέτη και αξιολόγηση της παρούσας διδακτορικής διατριβής.

Οφείλω να ευχαριστήσω το προσωπικό των εργαστηρίων του Πολυτεχνείου Κρήτης που με βοήθησε για την διεξαγωγή της πειραματικής διαδικασίας και των αναλύσεων κατά τη διάρκεια της διατριβής. Θα ήθελα να ευχαριστήσω το Εργαστήριο Υλικών Πολιτιστικής Κληρονομιάς και Σύγχρονης Δόμησης, την Dr. Αναστασία Βεργανελάκη και τη Dr. Χρυσή Καπριδάκη, το Εργαστήριο Πετρολογίας & Οικονομικής Γεωλογίας, την κα. Παυλίνα Ροτόντο και τον Dr. Γεώργιο Τριανταφύλλου, τα Εργαστήρια Ανάλυσης Ρευστών & Πυρήνων Υπογείων Ταμειυτήρων και Χημείας & Τεχνολογίας Υδρογονανθράκων, με ιδιαίτερες ευχαριστίες στην κα. Ελένη Χαμηλάκη, το εργαστήριο Εξευγενισμού & Τεχνολογίας Στερεών Καυσίμων, εργαστήριο Υδρογεωχημικής Μηχανικής και Αποκατάστασης Εδαφών και το εργαστήριο Μικροκοπής & Κατασκευαστικής Προσομοίωσης. Ευχαριστώ θερμά τον Dr. Αντώνη Στρατάκη και το Εργαστήριο Γενικής & Τεχνικής Ορυκτολογίας για τη βοήθειά που

μου προσέφερε. Ιδιαίτερες ευχαριστίες οφείλω στον Διευθυντή Καθηγητή του εργαστηρίου Ελέγχου Ποιότητας - Υγιεινής & Ασφάλειας στη Μεταλλευτική Καθηγητή κ. Μιχάλη Γαλετάκη που πάντα με δεχόταν με συμβουλές και ενδιαφέρον, καθώς και στη συνεργάτιδά του Υπ. Διδάκτορα κα. Αθανασία Σουλτανά που δε σταμάτησε να με βοηθάει από την πρώτη ημέρα της γνωριμίας μας. Ευχαριστώ από καρδιάς το προσωπικό των εργαστηρίων Εμπλουτισμού, Τεχνολογίας Κεραμικών & Υάλου και Τεχνολογιών Διαχείρισης Μεταλλευτικών & Μεταλλουργικών Αποβλήτων & Αποκατάστασης Εδαφών τις φίλες και συναδέλφους μου Dr. Αικατερίνη Βαβουράκη, Βασιλική Καρμάλη και Αθανασία Σουλτανά, την Dr. Άννα Κρητικάκη, την κα. Όλγα Παντελάκη, και τον Dr. Ευάγγελο Πετράκη για την εξαιρετική συνεργασία. Τους ευχαριστώ όλους θερμά για τη βοήθεια και τις διευκολύνσεις που μου προσέφεραν σε διάφορα στάδια της διδακτορικής διατριβής.

Ιδιαίτερη αναφορά και ευχαριστίες οφείλω στα μέλη, φίλους και συναδέλφους, του Εργαστηρίου Διαχείρισης Τοξικών και Επικίνδυνων Αποβλήτων, Μαρία Αϊβαλιώτη, Ελένη Καστανάκη, Αργυρώ Κουκουτσάκη, Αθανασία Κουσαϊτή, Ιωάννη Μουκαζή, Ιωάννα Παπαγγελή, Φραντζέσκα-Μαρία Πελλέρα, Βασιλική Σαββιλωτίδου, Φωτεινή Σημαντηράκη, Ιωάννη Τετώρο, Παναγιώτη Χαζιράκη, Ιωάννη Χαχλαδάκη, Γιώργο Χρυσικό για την άψογη συνεργασία και τις όμορφες στιγμές που ζήσαμε όλα αυτά τα χρόνια.

Ευχαριστώ πραγματικά, τους φίλους μου για τη σημαντική συμπαράσταση και υπομονή που έδειξαν σε κάθε μου απογοήτευση. Ξεχωριστά ευχαριστώ τη Λορέτα, τη Ναταλία, το Χάρη και το Χρήστο που όσο μακριά και να βρίσκονται τους νιώθω πάντα δίπλα μου.

Τέλος, τίποτα από όλα αυτά δε θα είχε πραγματοποιηθεί εάν δεν είχα δίπλα μου την οικογένειά μου, σε κάθε μου βήμα. Θέλω να εκφράσω βαθιά ευγνωμοσύνη μέσα από την καρδιά μου για την απόλυτη στήριξη και υπομονή, σε κάθε μου απόφαση και δύσκολη στιγμή, προσφέροντάς μου άνευ όρων αγάπη. Ήταν πάντα δίπλα μου υποδεικνύοντάς μου να ακολουθώ τα όνειρά μου. Θα είμαι πάντα ευγνώμων σε αυτούς. Παρόντες και απόντες.

ΠΕΡΙΛΗΨΗ

Ο σκοπός της παρούσας διδακτορικής διατριβής είναι η αποτοξικοποίηση και διαχείριση επικινδύνων αποβλήτων που περιέχουν αμιάντο. Τα Απόβλητα Εκσκαφών Κατασκευών & Κατεδαφίσεων (ΑΕΚΚ) αποτελούν ένα σημαντικό περιβαλλοντικό πρόβλημα στον τομέα διαχείρισης αποβλήτων. Τα ορυκτά του αμιάντου, λόγω της διαδεδομένης τους χρήσης στον κατασκευαστικό τομέα, καθιστούν τα υλικά που περιέχουν αμιάντο ένα αυξανόμενο ρεύμα αποβλήτων, ως μέρος που προέρχονται από ανακαινίσεις και κατεδαφίσεις κτιρίων.

Η διατριβή προσεγγίζει το πρόβλημα διαχείρισης των κυματοειδών φύλλων στέγης αμιαντοτσιμέντου (ΕΛΕΝΙΤ). Τα ΕΛΕΝΙΤ είναι κατασκευαστικά υλικά με συνδετικό υλικό το τσιμέντο, ενισχυμένα με ίνες αμιάντου. Ως υλικά στέγης υπόκεινται σε διάβρωση λόγω της έκθεσης σε καιρικές συνθήκες, καθώς η βροχή, η υγρασία, η όξινη βροχή και οι διακυμάνσεις της θερμοκρασίας προκαλούν φθορά. Σημαντικές φάσεις του τσιμέντου, όπως ο πορτλανδίτης, ο ετρινγκίτης, η γύψος και οι ασβεστοπυριτικές ενώσεις (C-S-H) διαβρώνονται λόγω της έκθεσης στις ατμοσφαιρικές συνθήκες με αποτέλεσμα οι μηχανικές ιδιότητες των ΕΛΕΝΙΤ να υποβαθμίζονται, τα υλικά να διαβρώνονται και ως εκ τούτου διευκολύνεται η απελευθέρωση των ινών του αμιάντου. Η ορυκτολογική και χημική πολυπλοκότητα των εν λόγω υλικών καθιστά αναγκαίο τον λεπτομερή και πλήρη χαρακτηρισμό των αποβλήτων, προκειμένου να προσδιοριστεί η σύστασή τους. Δύο τύποι αμιάντου εντοπίστηκαν στα απόβλητα αμιαντοτσιμέντου, ο χρυσοτίλης και ο κροκιδόλιθος σε ποσοστά 8 και 2 %κ.β., αντίστοιχα.

Αρχικά, μελετάται η επίδραση διαφορετικών συγκεντρώσεων οξαλικού οξέος, ως προς την δυνατότητα αποτοξικοποίησης των ΕΛΕΝΙΤ. Οι ίνες του αμιάντου είναι εφικτό να διασπαστούν μετά από εκχύλιση με διάλυμα οξαλικού οξέος, επιτυγχάνοντας τον διαχωρισμό του εξωτερικού στρώματος βρουσίτη $[Mg(OH)_2]$ και των ινών του χρυσοτίλη από την μήτρα πυριτίου. Επιπλέον, το οξαλικό οξύ αντιδρά με το υδροξείδιο του ασβεστίου παράγοντας οξαλικό ασβέστιο. Το οξαλικό ασβέστιο είναι ένα υλικό που χρησιμοποιείται στην αποκατάσταση μνημείων καθώς είναι εξαιρετικά ανθεκτικό στη διάβρωση λόγω καιρικών συνθηκών. Καθώς το οξαλικό οξύ τείνει να αντιδρά και με τις ίνες αμιάντου αλλά και με τις φάσεις του τσιμέντου που περιέχουν υδροξείδιο του ασβεστίου, γίνεται η παραδοχή πως θα απαιτείται μεγαλύτερη συγκέντρωση οξέος για την αποτοξικοποίηση των ΕΛΕΝΙΤ σε σύγκριση με τη διεργασία αποτοξικοποίησης χρυσοτίλη. Μελετάται λοιπόν δυνατότητα του οξαλικού οξέος να αντιδρά με τις ίνες του αμιάντου παρουσία τσιμέντου.

Κατόπιν, γίνεται αξιοποίηση της πυριτικής μήτρας του αμιάντου ενσωματώνοντάς της σε ένα δίκτυο πυριτίου. Το τετρα-αιθοξυ-σιλάνιο ($Si(OC_2H_5)_4$, TEOS) είναι υλικό που χρησιμοποιείται στην παραγωγή πυριτικού δικτύου με τη μέθοδο λύματος-πηκτής (sol-gel). Η αποτοξικοποίηση των αποβλήτων οδήγησε στην παραγωγή μιας μη τοξικής πυριτικής γέλης. Η γέλη αυτή είναι προϊόν που παράχθηκε αναμιγνύοντας ΕΛΕΝΙΤ σε υδατικό διάλυμα οξαλικού οξέος, στο οποίο στη συνέχεια προστέθηκε TEOS. Η όλη διαδικασία έλαβε χώρα σε

θερμοκρασία δωματίου, υπό συνεχή ανάδευση. Στη διαδικασία αυτή το οξαλικό οξύ είναι το βασικό αντιδραστήριο που ευθύνεται για τη διαλυτοποίηση των ινών του αμιάντου, αλλά παράλληλα είναι και καταλύτης στη διαδικασία παραγωγής της πυριτικής γέλης. Μελετήθηκε επιπλέον, η επίδραση της ακτινοβολίας μικροκυμάτων στη διαδικασία προκειμένου να διαπιστωθεί τυχόν επιτάχυνση της επεξεργασίας των αποβλήτων. Επιπλέον, μελετήθηκε ο συνδυασμός οξαλικού οξέος με πυριτικό κάλιο (K_2SiO_3) προς τη διάσπαση των ινών του αμιάντου και τη μετατροπή των αποβλήτων σε μη επικίνδυνη μορφή.

Πραγματοποιήθηκε χαρακτηρισμός των επεξεργασμένων αποβλήτων ως προς τον προσδιορισμό των ορυκτών αμιάντου, των φάσεων κρυσταλλικών και άμορφων φάσεων του αμιαντοτσιμέντου, καθώς και των νέων φάσεων που δημιουργήθηκαν μετά τις επεξεργασίες. Χρησιμοποιήθηκαν αναλυτικές τεχνικές όπως XRPD, FTIR, XRF και TG-DTG. Τα αποτελέσματα υποδεικνύουν ότι ο συνδυασμός του οξαλικού οξέος είτε με το TEOS είτε με το πυριτικό κάλιο επιτυγχάνει την πλήρη αποτοξικοποίηση των αποβλήτων και τη διάσπαση της δομής των ΕΛΕΝΙΤ, ενώ παράλληλα παράγεται οξαλικό ασβέστιο λόγω της αντίδρασης του οξαλικού οξέος με τις φάσεις του τσιμέντου και μεγάλη ποσότητα άμορφου πυριτίου μέχρι και 90 %κ.β.

Στη συνέχεια διερευνώνται καινοτόμες επιλογές ανακύκλωσης των επεξεργασμένων αποβλήτων, βάσει των χαρακτηριστικών των παραγόμενων δευτερευουσών πρώτων υλών, σε συμμόρφωση με την Οδηγία 2008/98/ΕΚ για τη διαχείριση αποβλήτων που προτείνει την αξιοποίηση των ΑΕΚΚ ως δευτερεύουσες πρώτες ύλες με στόχο τη μείωση της χρήσης των φυσικών πόρων. Επιπλέον, σύμφωνα με την Οδηγία 2009/125/ΕΚ για τη θέσπιση πλαισίου για τον καθορισμό απαιτήσεων οικολογικού σχεδιασμού όσον αφορά τα συνδεδεμένα με την ενέργεια προϊόντα, η οικονομική αξία των παραγόμενων αποβλήτων πρέπει επίσης να αξιολογείται μέσω ανάκτησης και επαναχρησιμοποίησης, έναντι της ταφής σε ΧΥΤΑ. Ανάλογα με τη σύστασή τους, τα ΑΕΚΚ αποτελούν πιθανές δευτερεύουσες πρώτες ύλες για επαναχρησιμοποίηση ως πρόσθετο τσιμέντο στην παραγωγή κονιαμάτων ή σκυροδέματος. Ο περιβαλλοντικός αντίκτυπος της παραγωγής τσιμέντου σε συνδυασμό με τις τεράστιες απαιτήσεις της αγοράς, καθιστούν αναγκαία την προσπάθεια ενσωμάτωσης ανακυκλώσιμων υλικών στο τσιμέντο, με κύριο στόχο την προστασία του περιβάλλοντος και την διατήρηση των φυσικών πόρων.

Συστατικά με συγκεκριμένα χαρακτηριστικά ενσωματώνονται στα αρχικά μίγματα κονιαμάτων, ώστε να αντιδράσουν με το τσιμέντο προσδίδοντας καλύτερες ιδιότητες στα τελικά προϊόντα. Πυρίτιο σε μικρο- και νάνο- σωματίδια προτιμάται ως ενισχυτικό τσιμέντου, λόγω της άμορφης δομής του και της μεγάλης ειδικής επιφάνειας των κόκκων, χαρακτηριστικά που βοηθούν την ποζολανική αντίδραση. Τα υλικά που προέκυψαν από την επεξεργασία των αποβλήτων μελετώνται για τυχόν ποζολανικές ιδιότητες, λόγω του μεγάλου περιεχομένου σε άμορφο πυρίτιο (90 %κ.β.) και της λεπτότητά τους.

Ο προσδιορισμός της ποζολανικότητας αξιολογείται με πρότυπες μεθόδους. Η άμεση αντίδραση των υλικών με το υδροξείδιο του ασβεστίου προσδιορίζεται μέσω της μεθόδου NF P 18 – 513 που ποσοτικοποιεί την κατανάλωση του ασβεστίου από τα μελετώμενα υλικά. Η μακροπρόθεσμη ποζολανική αντίδραση των υλικών εκτιμάται σύμφωνα με το Δείκτη

Δραστικότητας Αντοχής (Strength Activity Index, EN 450-1) σε δοκίμια κονιάματος τσιμέντου, που παράγονται αντικαθιστώντας ποσοστό τσιμέντου με το επεξεργασμένο απόβλητο ως πρόσθετο υλικό. Επιπλέον, διεξάγεται θερμοβαρυμετρική ανάλυση στα δοκίμια προκειμένου να προσδιορισθεί η κατανάλωση υδροξειδίου του ασβεστίου και ο σχηματισμός C-S-H, λόγω της ποζολανικής αντίδρασης. Παρατηρείται πως το υλικό που προκύπτει από την επεξεργασία με οξαλικό οξύ και TEOS παρουσιάζει ιδιότητες ποζολάνης, και συνεπώς χαρακτηρίζεται ως τεχνητή ποζολάνη.

Στη συνέχεια, μελετάται η δυνατότητα ανακύκλωσης των υλικών ως δευτερεύουσες πρώτες ύλες με ποζολανικές ιδιότητες για την παραγωγή δομικών στοιχείων με προηγμένα χαρακτηριστικά. Για την παραγωγή των δοκιμίων χρησιμοποιούνται δύο εμπορικοί τύποι τσιμέντου, τα CEM I 42.5N και CEM III/A-LL 42.5N, πρότυπη άμμος ως αδρανές, και πυριτική παιπάλη (για λόγους σύγκρισης) ως υλικό αντικατάστασης τσιμέντου. Διερευνάται η επίδραση της μερικής αντικατάστασης τσιμέντου (1.5-5 %κ.β.) με την τεχνητή ποζολάνη. Η όλη διαδικασία παραγωγής των δοκιμίων διεξάγεται με βάση στην πρότυπη μέθοδο EN 196-1. Τα δοκίμια παραμένουν προς ωρίμανση για 90 ημέρες, αρκετές ώστε να τους προσδοθούν χαρακτηριστικά λόγω της ποζολανικής αντίδρασης, και ελέγχονται ως προς την αντοχή σε θλίψη, προκειμένου να προσδιορισθεί η επίδραση της τεχνητής ποζολάνης στο μείγμα. Επιπλέον, προσδιορίζεται το πορώδες, η πυκνότητα και απορροφητικότητα των παραγόμενων δοκιμίων.

Τα σωματίδια πυριτίου έχουν την τάση να αντιδρούν με το ελεύθερο υδροξείδιο του ασβεστίου της πάστας τσιμέντου, με αποτέλεσμα να βελτιώνουν τα φυσικά και χημικά χαρακτηριστικά που σχετίζονται με τη μικροδομή των κονιαμάτων τσιμέντου. Αυτή η αντίδραση έχει ως αποτέλεσμα την παραγωγή ένυδρου πυριτικού ασβεστίου, τη μείωση του υδροξειδίου του ασβεστίου (πορτλανδίτη), και ως αποτέλεσμα την αύξηση της αντοχής σε θλίψη. Η μεγάλη ειδική επιφάνεια των εξεταζόμενου υλικού διευκολύνει την ποζολανική αντίδραση.

Η αντοχή των κονιαμάτων που παρασκευάστηκαν με τσιμέντο CEM I ως βασική συνδετική κονία και την τεχνητή ποζολάνη ως υλικό αντικατάστασης τσιμέντου, μειώθηκε κατά 1-13% μετά από 28 ημέρες ωρίμανσης, ενώ αυξήθηκε μέχρι και 21% έπειτα από 90 ημέρες ωρίμανσης. Αυτό αποδίδεται στη μεγάλη απαιτούμενη διάρκεια για την διεκπεραίωση των ποζολανικών αντιδράσεων καθώς συνεχίζονται για 365 από την παραγωγή των δοκιμίων, παράγοντας δευτερεύουσες φάσεις ένυδρου πυριτικού ασβεστίου, που οδηγούν στη συμπύκνωση της δομής του υλικού και την αύξηση της αντοχής σε θλίψη.

EXECUTIVE ABSTRACT

This dissertation aims to develop a new technology concerning the detoxification and management of asbestos containing waste (ACW). Asbestos minerals were extensively used as raw materials in the construction sector, rendering asbestos containing materials (ACM) an increasingly hazardous waste stream, mainly due to renovation and demolition waste.

The purpose of this thesis is to manage asbestos cement (AC) corrugated sheets. The AC corrugated sheets are cementitious materials reinforced with asbestos fibers. They are subjected to long term deterioration due to weathering in the natural environment. Since they are roofing materials, rain, humidity, acid rain and temperature variation cause weakening of their composites. Important cement phases, such as portlandite, ettringite, gypsum and C-S-H bonds are corroded due to leaching by rain water, and, as a result, the mechanical properties of ACM are downgraded and asbestos fibers are released. The mineralogical and chemical complexity of the material necessitates a detailed and complete characterization of ACW in order to identify the mineralogical and morphological characteristics of weather-deteriorated samples. Two classes of asbestos minerals, chrysotile and magnesioriebeckite (mineral phase of the commercially used crocidolite asbestos) are identified at proportions of 8% and 2%wt., respectively.

Initially, the effect of different concentrations of the moderate organic acid, oxalic acid, on the detoxification of AC corrugated sheets is investigated. Oxalic acid is able to achieve dissolution of chrysotile fibers. The external layer of the fiber, brucite $[Mg(OH)_2]$ is separated from the valuable silica matrix. Oxalic acid is also reactive with calcium hydroxide, producing calcium oxalate, which is commonly used in monuments patina due to its remarkable weathering resistance, in particular as a calcium oxalate-silica combination. Since oxalic acid is reactive with both chrysotile fibers and cement phases, it is assumed that a higher concentration of oxalic acid is necessary in order to achieve ACM transformation, compared to oxalic acid concentration on pure chrysotile treatment. AC was added to oxalic acid solutions of different concentrations in order to investigate the ability of asbestos fibers to react with oxalic acid in the presence of cement.

Then, the use of tetraethyl orthosilicate (TEOS) on the simultaneous effect of asbestos cement detoxification and transformation of silica matrix into silica network is studied. This research is focused on the development of a nontoxic sol-gel. The gel is a product of ACW mixing in an aquatic solution of oxalic acid and TEOS addition, under stirring, in room temperature. The selection of the reagents of the combined treatments is based primarily on the oxalic acid's ability to destruct the fibers of chrysotile, while it is also used as acid catalyst in sol-gel processes. Furthermore, treatment with the same reagents is conducted under microwave irradiation. A combined treatment of oxalic acid and potassium silicate also achieved the transformation of ACW into harmless material.

Characterization analyses of asbestos minerals, cementitious and amorphous phases of AC, as well as newly-formed phases of treated samples, are performed with XRD, FTIR, XRF and TG-DTG. The results indicated that the combined treatment with TEOS achieves the full detoxification and transformation of AC structure. Specifically, during the treatment, calcium oxalate monohydrate is yielded, due to oxalic acid reaction with cementitious phases, and high production of silica of amorphous phase up to 90 %wt.

Novel options on recycling of the end-of-life treated asbestos cement waste are investigated, based on the quality of the produced secondary raw materials, in concurrence with the Directive 2008/98/EC, which indicates the valorization and reduction of the use of resources. Additionally, in accordance with the eco-design regulation (2009/125/EC) the economic value of the produced waste should also be evaluated via recovery and reuse, instead of landfilling. Depending on their composition, CDW constitutes a potential source of secondary raw materials for reutilization as supplementary of cement in mortars and concrete. The environmental impact of cement production in combination with the enormous quantities required by the market, results in an effort to incorporate recyclable materials into cement, aimed primarily at the protection of the environment, human health and conservation of natural resources.

Components with specific characteristics are added in the initial mixtures to react with cement and offer advantageous properties. Silica micro and nanoparticles are preferred due to their excess of reactive amorphous SiO_2 and high specific surface area, characteristics that aid the conduction of pozzolanic reaction. The properties of modified harmless ACM to amorphous silica are investigated. Due to particles fineness and high amorphous silica content (90 %wt.), pozzolanic reactivity of the secondary raw material is studied by several methods.

Pozzolanic reactivity determination is evaluated based on an accelerated method (NF P 18 - 513) that determines lime-pozzolan reaction and quantifies the pozzolanic reaction measuring $\text{Ca}(\text{OH})_2$ reduction in the presence of pozzolans. This method is a fast and accurate way to determine the pozzolanic reactivity of a material. The long-term pozzolanic reactivity of the material, as supplementary cementitious material in mortar specimens is evaluated via Strength Activity Index (EN 450-1). Thermogravimetric analysis is also conducted in the specimens in order to understand the pozzolanic reaction through the consumption of $\text{Ca}(\text{OH})_2$ and the formation of calcium silicate hydrates. It is observed that the material resulting from the treatment with oxalic acid and TEOS obtained pozzolanic properties, and it is therefore characterized as artificial pozzolan.

Subsequently, the possibility of recycling the treated material as secondary raw material with pozzolanic properties to produce building elements with advantageous characteristics is studied. Two commercial types of cement, CEMI 42.5N and CEMII/A-LL 42.5N, standard sand as aggregate and silica fume (for comparison reasons) as additive, are used for the production of the mortars. The effect of the partial cement substitution (1.5-5 %wt.) by the artificial pozzolan is investigated. Mixing of the materials, casting into moulds and curing are carried out according to the EN 196-1. After 90 days of curing, specimens are tested (according to the EN) for their strength in uniaxial compression, in order to determine the effect of artificial

pozzolan and silica fume as supplementary cementitious materials. Additionally, porosity, density and water absorption are also measured.

Silica particles are capable of reacting with free calcium hydroxide (Ca(OH)_2) of cement paste, resulting in an improvement of the physical and chemical characteristics associated with microstructure of cement pastes. This reaction leads to the formation of calcium silicate hydrate (C-S-H) gel. Free calcium hydroxide in the cement matrix is reduced, while the strength of hardened mortar is increased and permeability is decreased. The higher the specific surface area of particles, the more is the pozzolanic reaction facilitated.

The blended mortars that were produced using CEMI as a binder after 28 days of curing resulted in the decrease of compressive strength in a range of 1-13%, while after 90 days of curing the compressive strength is increased up to 21% using STG as cement replacement. This is attributed to the slow rate of the pozzolanic reaction that continues after the 28 days of cement hydration, producing secondary CSH, resulting in the densification of pore structure and increased compressive strength of the mortars.

NOMENCLATURE

AC, Asbestos Cement
ACM, Asbestos Containing Materials
ACW, Asbestos Containing Waste
C₂S, dicalcium silicate
C₃A, tricalcium aluminate
C₃S, tricalcium silicate
C₄AF, tetracalcium aluminoferrite
CDW, Construction and Demolition Waste
Cs, compressive strength
CSH, calcium silicate hydrate
EC, European Commission
EU, European Union
FTIR, Fourier Transform Infrared Spectroscopy
ISP, isopropanol
Ox, oxalic acid
SAI, Strength Activity Index
SEM, Scanning Electron Microscopy
SF, silica fume
TEOS, tetraethyl orthosilicate
TG, Thermogravimetric Analysis
UPV, Ultrasonic Pulse Velocity
w/b, water/binder
w/c, water/cement
WA, water absorption
WG, potassium silicate
XRD, X-ray Diffraction
XRF, X-Ray Fluorescence

CONTENTS

EΥΧΑΡΙΣΤΙΕΣ.....	i
ΠΕΡΙΛΗΨΗ.....	iii
EXECUTIVE ABSTRACT.....	vi
NOMENCLATURE.....	ix
1. Introduction.....	5
1.1 Background and motivation.....	5
1.2 Aim and objectives of PhD thesis.....	6
1.3 Outline of the thesis.....	7
1.4 Contribution and Novelty of PhD thesis.....	9
1.5 Publications.....	10
2. Asbestos.....	15
2.1 Asbestos minerals.....	15
2.1.1 Chrysotile.....	15
2.1.2 Crocidolite.....	16
2.2 ACM and their use.....	16
2.3 Effect on human health.....	18
2.3.1 Asbestosis.....	18
2.3.2 Mesothelioma.....	18
2.3.3 Lung cancer.....	19
2.4 Current situation and future perspectives.....	19
2.5 Management of asbestos deposits and Asbestos Containing Materials (ACMs) in abandoned mining and public premises in Greece.....	21
2.6 Asbestos Containing Waste treatments.....	24
2.6.1 Thermal treatments.....	25
2.6.2 Mechanical Treatments.....	28
2.6.3 Chemical treatments and combined treatments.....	28
3. Cement: composition and supplementary cementitious materials.....	33
3.1 Binders.....	33
3.1.1 Hydraulic binders.....	33
3.1.2 Pozzolanic binders.....	33

3.1.3 Mortars	34
3.2 Portland cement	34
3.2.1 Chemical synthesis.....	35
3.2.2 Types of Portland Cement	36
3.3 Solids of hydrated cement binder	36
3.3.1 Calcium Silicate Hydrates (C-S-H)	36
3.3.2 Calcium Hydroxide.....	37
3.3.3 Sulfuric salts.....	37
3.4 Voids of hydrated cement binder	37
3.4.1 C-S-H internal layered structure voids.	37
3.4.2 Capillary voids	37
3.4.3 Air voids.....	38
3.4.4 Structure-properties relationship of hydrated cement paste.....	38
3.5 Compressive strength.....	38
3.3.1 Factors affecting compressive strength.....	38
3.6 Mineral additives	40
3.6.1 Pore fillers.....	40
3.6.2 Pozzolan.....	41
3.6.3 Silica Fume	42
4. Materials and methods	47
4.1 Experimental setup of Asbestos Containing Waste treatment.....	47
4.1.1 Materials	47
4.1.2 Experimental design: Chemical treatment process	47
4.1.3 Characterization of materials- Analytical techniques	48
4.2 Investigation of pozzolanic activity of treated materials	49
4.2.1 Materials	49
4.2.2 Pozzolanic reactivity determination.....	51
4.2.3 Properties of the mortars	54
5. Effect of the reagents on raw asbestos fibers.	59
5.1 Selection of the materials.....	59
5.2 Results of preliminary experimental investigation	60
5.2.1 The effect of different concentrations oxalic acid aquatic solution on fibers of chrysotile.....	60
5.2.2 The effect of combined treatment with oxalic acid aquatic solution and silicates	62

6. Results of Asbestos Containing Waste detoxification processes	71
6.1 Characterization of raw asbestos cement waste	71
6.1.1 Chemical composition	71
6.1.2 FTIR analysis	71
6.1.3 Mineralogical composition	72
6.1.4 Stereoscopy	74
6.2 Characterization of treatment with oxalic acid	75
6.2.1 FTIR analysis	75
6.2.2 Mineralogical composition	75
6.2.3 Stereoscopy	77
6.3 Combined treatments: Oxalic acid combined with tetraethyl orthosilicate	78
6.3.1 Selection of the materials	78
6.3.2 Chemical composition	79
6.3.3 FTIR analysis	80
6.3.4 Mineralogical composition	81
6.3.5 Stereoscopy	83
6.4 Combined treatments: Oxalic acid combined with potassium silicate	83
6.4.1 FTIR analysis	83
6.4.2 Mineralogical analysis	84
6.5 Microwave treatment	85
6.5.1 FTIR analysis	85
6.5.2 Mineralogical analysis	86
6.6 Thermal analysis of selective specimens	87
6.7 Discussion - Selection of the optimum treatment	90
7. Pozzolanic reactivity determination	95
7.1 Direct determination of calcium consumption (Chapelle test)	95
7.2 Strength activity index	96
7.3 Fineness and diffraction particle size	97
7.4 Evaluation of pozzolanic activity by thermal analysis	99
7.4.1 Ca(OH) ₂ content	99
8. Recycle of artificial pozzolan as supplementary cementitious material	106
8.1 Non-Destructive Evaluation of cement mortars using Ultrasonic Pulse Velocity	106
8.2 Compressive strength	108
8.2.1 Selection of admixtures proportions	108

8.2.2 Effect of silica fume.....	108
8.2.3 Effect of artificial pozzolan STG.....	110
8.3 Properties of selective specimens	112
8.4 Toxicity of the mortars.....	114
8.5 Discussion.....	115
9. Summary and concluding remarks	118
REFERENCES	123
APPENDIX.....	124

Chapter I: Introduction

1.1 Background and motivation

Construction and demolition waste (CDW) constitutes the largest waste stream in volume (Panizza et al., 2018). The European Union, through the Waste Framework (2008/98/EC), puts forward the CDW valorization and circular economy. Additionally, in accordance with the eco-design regulation (2009/125/EC) the economic value of the generated waste should also be evaluated for reuse, instead of landfilling. Depending on the composition, CDW is potential sources of secondary raw materials for reutilization either as aggregate (masonry, tiles, glass etc.) (Silva et al., 2017) or as a substitute of cement in mortars and concrete (Gautam et al., 2018).

Asbestos Containing Materials (ACM) represent an important hazardous waste fraction derived from the renovation and demolition of buildings. Asbestos had been extensively used as a raw material in the construction sector. Due to mechanical strength, resistance to heat and corrosive chemicals, asbestos was very popular in construction products, mostly in building materials, friction products, insulation materials and heat-resistant fabrics (Bonifazi et al., 2018). The most commonly found building materials that contain asbestos fibers are roofing materials, such as flat and corrugated sheets, gutters, floor tiles, cement pipes, boilers etc. (Virta & Flanagan, 2014, Paglietti et al., 2016). During the 20th century up until the early 90s, asbestos mining and ACM production were particularly widespread (Paglietti et al., 2012). Nowadays, the excavation of the mineral and the production of ACM have been banned by legislation in 66 countries worldwide, including the European Union (IBAS, 2018). Chrysotile remains the only commercialized asbestos form, mined in Russia, Canada, Brazil, South Africa, Zimbabwe, and Kazakhstan (Finley et al., 2012). During its peak extraction year in 1977, 4.8×10^6 tonnes of asbestos were mined (Park et al., 2012), while it is estimated that the production of asbestos fibers from 1900 to 2015 was around 2×10^8 tonnes (Spasiano & Pirozzi, 2017).

Although the use of asbestos is banned in the European Union, ACM can still be found in thousands of buildings. The concern of the scientific community is directed towards the asbestos containing waste (ACW) and its constantly increasing volume, generated by the demolition and renovation of old buildings (Yamamoto et al., 2014, Viani et al., 2013).

The asbestos cement (AC) corrugated sheets are cementitious materials that are subjected to deterioration due to weathering. Rain, humidity, acid rain and temperature variations cause weakening of cement composites. Major cement minerals, as portlandite, ettringite,

gypsum and C-S-H bonds, are corroded due to leaching by rain water (Dias et al., 2008), resulting in downgraded mechanical properties of ACM which facilitate the release of asbestos fibers in the air.

According to OVAM statistical data, it is estimated that in the next 50 years there will be 450.000 tonnes/year of ACW generated in Germany, while in the Netherlands, 70.000 tonnes/year of ACW are already being released (Wille, 2016). Considering the above mentioned huge amount of ACW, imperative need for a sustainable solution emerges. The European Union, through the European Parliament (EU-P7_TA, 2013), proposed “*to work with the social partners and other stakeholders at European, national and regional levels to develop and share action plans for asbestos removal and management*” (Spasiano & Pirozzi, 2017). Several different approaches and methods have been proposed or patented on asbestos waste management. The mineralogical and chemical complexity of the ACM leads to a variety of detoxification treatments, but the existing legislation does not designate any specific method for ACW treatment. Instead, it indicates the disposal of ACW in special hazardous waste landfills (Paglietti et al., 2016).

Several processes have been developed in laboratory scale aiming sustainable ACW treatment. Physical, chemical and biological methods are investigated by researchers in order to eliminate asbestos fibers and render safe residues for human health and the environment. The purpose is to establish a solution framework which will lead towards a substantial cooperation between the research community and the industrial sector, to a pilot plant and eventually the operation of a full scale treatment plant.

1.2 Aim and objectives of PhD thesis

The aim of this thesis is to develop a detoxification process for ACW treatment and utilization of residues in sustainable applications. It is investigated the decomposition of asbestos containing materials by the chelate agent oxalic acid with or without additives in various concentrations. Once asbestos fibers are destructed, the residues (secondary material) are exploitable in the construction industry.

The objectives of this PhD are to:

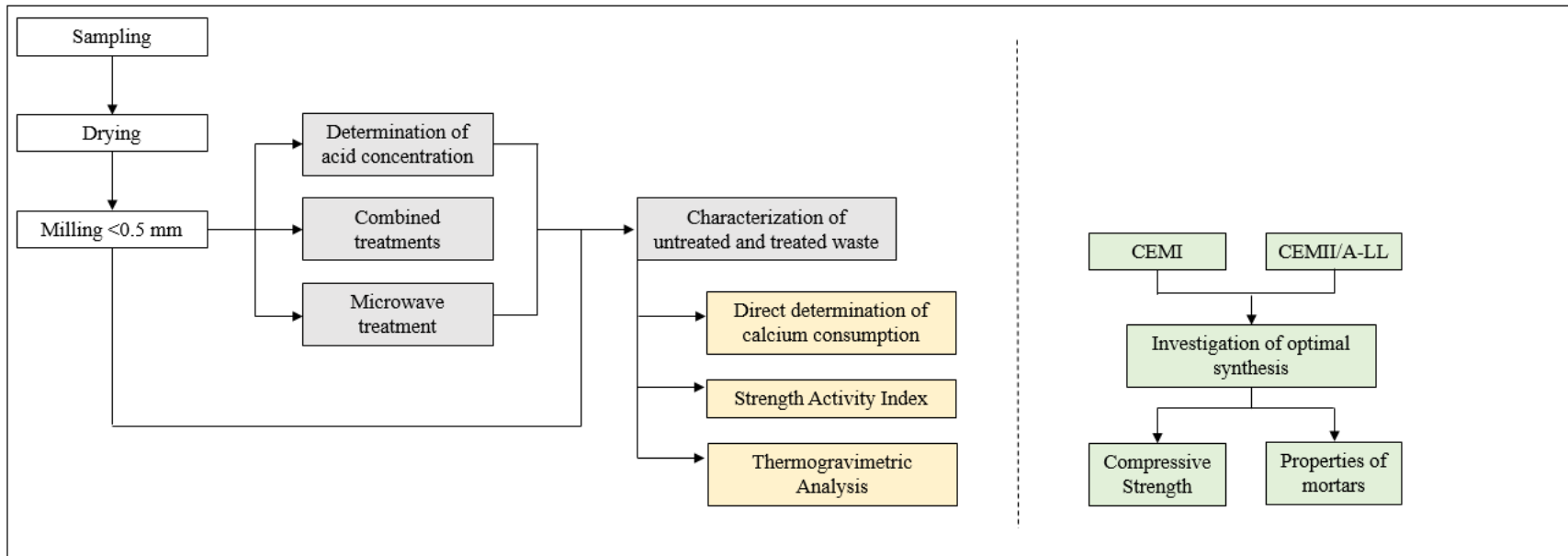
1. Determine the physical and chemical properties of ACW that was subjected to deterioration due to weathering.
2. Identify a suitable reagent in order to destroy the crystalline structure of asbestos fibers. The efficiency of the reagents in various concentrations and the treatment duration are investigated.
3. Detoxify asbestos fibers and embed the converted asbestos silica matrix into a silica network, creating a non-toxic sol-gel. The detoxification of ACW is achieved while tetraethoxysilane combined with silica matrix of asbestos fibers create the silica

- gel. Oxalic acid plays a double role. It is the main reagent that provokes the dissolution of asbestos fibers by leaching the external layer of $\text{Mg}(\text{OH})_2$ and releasing the silica matrix. Moreover, it is the catalyst of the sol-gel process aiming to complete the hydrolysis before condensation begins.
4. Use of residues (secondary material) in construction sector. Study the pozzolanic activity of asbestos-free ACM residues. Estimate the long-term pozzolanic reactivity of the secondary raw materials in cement mortars via Strength Activity Index (EN 450-1) and Thermogravimetric analysis.
 5. Estimate the optimal proportion of cement replacement to obtain mortars with advantageous properties. Study the beneficial synergistic effects between the treated waste and the binder.

1.3 Outline of the thesis

The PhD thesis is organized into nine chapters. Chapter 1 presents an introduction to the ACW topic, the aims and objectives of the research and the contribution of the current thesis. Chapter 2 describes asbestos minerals and their use in ACM, asbestos exposure effect on human health, the reason that renders asbestos a contemporary field of research and the state-of-the-art ACW management. Chapter 3 provides the necessary information to understand the synthesis and hydration of Portland cement, and the role of supplementary cementitious materials placing emphasis on pozzolans and silica fume. Chapter 4 presents the materials and describes the experimental setups, the analytic techniques and the standard methods used in this thesis. Chapter 5 discusses the selection of the reagents and different chemical pretreatments on raw asbestos fibers. In Chapter 6, the effect of the concentration and combination of the reagents is studied. Three experimental sets are evaluated varying on reagent concentration and depending on process duration, resulting in the selection of the optimum. Afterwards, the addition of silicates aims to complete elimination of asbestos fibers and the production of a non-toxic sol-gel. In Chapter 7, the pozzolanic reactivity of materials is investigated, by measuring the reaction rate between the relevant material and calcium hydroxide. Chapter 8 investigates the possibility to recycle the treated material as secondary raw material with pozzolanic properties to produce building elements with advantageous characteristics. Finally, the conclusions are drawn in Chapter 9.

Diagram of the experimental procedure



Detoxification process
Determination of pozzolanic properties of secondary raw materials
Recycle of artificial pozzolan on cement mortars

1.4 Contribution and Novelty of PhD thesis

This dissertation aims to develop a sustainable solution concerning the detoxification and management of asbestos containing waste (ACW). The objective of the present study is the conversion of asbestos cement corrugated sheets to non-hazardous material according to the circular economy approach. It is considered that the transformation of the material to a non-hazardous and valuable product has not been extensively studied before, in terms of evaluating the most suitable reagents to convert asbestos containing waste to secondary raw materials. In this line, economic and environmental feasibility are evaluated, through the examination of the most effective reagents concentration, temperature and treatment time.

The selection of the reagents of the combined treatments is based primarily on the oxalic acid ability to destruct the fibers of chrysotile. The acid leaching treatment with oxalic acid dihydrate ($\text{H}_2\text{C}_2\text{O}_4 \cdot 2\text{H}_2\text{O}$) is studied. The oxalic acid is characterized as moderate organic acid, in terms of acidity and toxicity and it was chosen due to its low environmental impact and cost, in comparison with other strong acids reported in literature (HF, HCl, HNO_3 etc.). The effectiveness of different concentrations of oxalic acid is investigated.

The combined influence of oxalic acid and TEOS/ISP mixture is also studied. ISP addition is selected to increase TEOS hydrolysis rate. ISP as a solvent preserves a complex role in sol-gel systems. The combined treatment has as a main objective the transformation of asbestos fibers, and the encapsulation of the treated ACW in TEOS silica network. Additionally, oxalic acid is used as an acid catalyst in sol-gel processes. Sol-gel processes compose a research area aiming at the production of silicate composites, characterized by homogeneity, large surface area and low density. Such characteristics are considered advantageous in various applications.

The proposed combined treatments achieve the detoxification of asbestos containing waste and its transformation to a harmless material, while a non-toxic amorphous silica network is formatted aided by the silica matrix of treated asbestos containing waste. The oxalic acid concentration (0.3 M) was chosen that ensues asbestos fibers destruction, while the pH of the medium was 1.49 ensuring that the esterification would not be facilitated. TEOS/ISP mixture addition to the oxalic acid – ACW solution resulted in the increase of pH at 1.91.

Novel options on recycling of the end-of-life treated asbestos cement waste are presented, based on the quality of the produced secondary raw materials. There is a lack of studies regarding the fate of the by-products of ACW treatment processes. The obtained properties of the secondary raw materials render them valuable for the construction sector. High pozzolanic reactivity of treated waste leads to the valorization of the by-products.

In this regard, the major contribution of this dissertation is the integrated approach of ACW management. The valorization of the secondary raw materials occurs exploiting them as

cementitious supplementary materials in the production of cement mortars with advantageous characteristics. Specifically, the compressive strength of modified mortars increased up to 21% using treated ACW as cement replacement.

1.5 Publications

Publications in scientific journals

Directly related to the PhD Thesis

Valouma, A., Verganelaki, A., Maravelaki-Kalaitzaki, P., & Gidakos, E. (2016). Chrysotile asbestos detoxification with a combined treatment of oxalic acid and silicates producing amorphous silica and biomaterial. *Journal of hazardous materials*, 305, 164-170.

Valouma, A., Verganelaki, A., Tektoros, I., Maravelaki-Kalaitzaki, P., & Gidakos, E. (2017). Magnesium oxide production from chrysotile asbestos detoxification with oxalic acid treatment. *Journal of hazardous materials*, 336, 93-100.

Under review

Valouma A. & Gidakos E. Asbestos containing waste transformation into harmless secondary raw material in the context of circular economy, *Waste Management*.

In preparation

Valouma A. & Gidakos E. Influence of artificial pozzolan derived from treated waste as supplementary cementitious material on composition of C-S-H in cement mortar pastes. *Cement and Concrete Composites*

Related to the PhD Thesis area of research

Mymrin V, Presotto P., Alekseev K. Avanci M., Petukhov V., Taskin A., Gidakos E., Valouma A., Yu G. Application of hazardous serpentine rocks' extraction wastes in composites with glass waste and clay-sand mix to produce environmentally clean construction materials, *Construction & Building Materials* (**Under Review**)

Publications in international conferences

Directly related to the PhD Thesis

Valouma, A., Gidakos, E. (2015). Management of asbestos deposits and Asbestos Containing Material (ACM) in abandoned mining and manufacturing sites in Greece. *Modern technologies and the development of polytechnic education*, 14-18th September, Vladivostok, Russia. ISBN 978-5-7444-3608-7

Papangelis, I., Valouma, A., Gidakos, E. (2016) Asbestos cement treatment via silylation processes using microwave radiation 5th International Conference on Industrial and

Hazardous Waste Management, 27 30 September, Chania, Crete, Greece.

Valouma, A., Verganelaki, A., Maravelaki-Kalaitzaki, P., & Gidarakos, E. (2016). Chrysotile asbestos detoxification and transformation to amorphous silica and oxalate. 5th International Conference on Industrial and Hazardous Waste Management, 27 30 September, Chania, Crete, Greece.

Koukoutsaki A. Valouma A. & Gidarakos E. (2018) Reuse of treated asbestos containing waste as artificial pozzolan and comparison with commercial microsilica, 6th International Conference on Industrial and Hazardous Waste Management 4-7 September, Chania, Crete, Greece

Valouma A., Triantafyllou G. & Gidarakos E. (2018), Asbestos treated material characterization and its potential application on hydraulic mortars for restoration applications, 6th International Conference on Industrial and Hazardous Waste Management 4-7 September, Chania, Crete, Greece

Valouma A. & Gidarakos E., Chrysotile and asbestos containing materials treatment with organic acid and silicates resulting high amorphous silica production. The 7th Annual Conference of AnalytiX-2019 (Europe), Berlin, Germany, November 2019.

Valouma A. & Gidarakos E., Mechanical treatment of asbestos containing waste and safe recycling on the production of alkali activated materials. Accepted to be presented in the 17th International waste management and landfill symposium (SARDINIA 2019), Cagliari, Italy, October 2019.

Research activity during PhD

Participation in National Project entitled: “Dismantling of asbestos containing materials in the building of Old General Hospital of Chania”

06/2014-08/2014

Participation in European Project: “TIWaSiC: Advanced Training in Integrated Sustainable Waste Management for Siberian Companies and Authorities”

05/2014-10/2016

- Conference Publication: Valouma, A., Gidarakos, E. (2014). Management for Siberian Companies and Authorities for Tempus Project TIWaSiC: Advanced Training in Integrated Sustainable Waste. 4th International Conference on Industrial and Hazardous Waste Management, 3 – 5th September, Chania, Crete, Greece.
- Report submitted to EACEA entitled: Mining and Mineral Processing Industry
- Contribution: Final Report Project nr. 543962-TEMPUS-1-2013-1-DE-JPHES (2013-5066)

Training Courses in the context of research project TIWaSiC

1. Management of waste from extractive industries in EU (Irkutsk, Russia)
2. Extractive industry: best available technologies in mining waste management (Irkutsk, Russia)
3. Environmental rehabilitation of the Asbestos Mine of Northern Greece (Ulan Ude, Russia)
4. Waste legislation in EU (Vladivostok, Russia)
5. Treatment methods of asbestos and asbestos cement containing waste materials (Chania)

Participation in project “Restriction of free oil phase of land and coastline of PYRKAL area”

04/2017-01/2018.

Participation in INVALOR project: Research Infrastructure for Waste Valorization and Sustainable Management of Resources (INVALOR)

02/2018-07/2019

Conference Publications:

A. Soultana, A. Valouma, A.I. Vavouraki, K. Komnitsas, Mechanical and durability properties of alkali activated materials produced from brick waste and metallurgical slag. 7th International Conference on Sustainable Solid Waste Management, Crete Island, Greece, June 2019.

A. Σουλτανά, Α. Βαλουμά, Κ. Κομνίτσας, Μ. Γαλετάκης, Συν-αξιοποίηση αποβλήτων κατασκευών και κατεδαφίσεων (ΑΚΚ) και μεταλλουργικής σκωρίας για την παραγωγή ανόργανων πολυμερών, “5ο Πανελλήνιο Συνέδριο: Αξιοποίηση Παραπροϊόντων στη Δόμηση”, Θεσσαλονίκη, Οκτώβριος 2019.

Publication in scientific journal

Soultana, A., Valouma, A., Bartzas, G., & Komnitsas, K. (2019). Properties of Inorganic Polymers Produced from Brick Waste and Metallurgical Slag. *Minerals*, 9(9), 551.

Chapter II: Asbestos

Abstract

The mineralogical term “asbestos” referred to a group of naturally occurring silicate minerals of fibrous form, which in chemical perspective are hydrated silicates in crystalline structure.

Asbestos minerals are known for their unique physical and chemical properties: electrical, thermal and sound insulation, flexibility, excellent mechanical strength, as well as resistance to chemical attack. All these exceptional characteristics and its low cost, have contributed decisively to establish asbestos as one of the most commonly used materials worldwide. Asbestos extensive use continued up to the verification of its harmful consequences to human health.

More than 98% of asbestos containing materials were manufactured using asbestos fibers bonded with organic and/or inorganic materials. Asbestos cement is a building and construction material extensively used in construction sector. Asbestos fibers are embedded to cement mortar matrix in percentage range of 10-18 %wt. Mainly chrysotile and crocidolite are used as reinforcement materials. AC is resistant to fire and acid rain, while in parallel its mechanical and insulation properties are advantageous comparing to conventional cement. It is used for the production of roof sheets (ETERNIT), pipes of water supply and sewerage network, tiles etc.

Most frequent harmful consequences due to asbestos exposure are related with inhalation of fibers. Asbestos fibers of specific dimensions are easily inhaled and carried into lung region and they are responsible for lung related cancer.

In 2005 asbestos ban has been applied throughout the whole EU. Except from 28 member states of EU, there are only 38 more countries that have applied asbestos ban. Although asbestos mining and asbestos containing materials production remains active mainly in developing countries, the problem incurs in developed nations also. The common opinion nowadays is concerned about demolition asbestos containing waste, produced by building renovation.

2. Asbestos

The mineralogical term “asbestos” refers to a group of naturally occurring silicate minerals of fibrous form, which from a chemical perspective are hydrated silicates in crystalline structure. It can be found in two classes, each with different physical characteristics; serpentine and amphibole. All six asbestos mineral types consist of a silica matrix and, depending on their type, they may also contain Magnesium (Mg), Iron (Fe), Calcium (Ca) or Sodium (Na). The mineral class of amphiboles includes 5 asbestos types: actinolite $[\text{Ca}_2(\text{Mg,Fe})_5\text{Si}_8\text{O}_{22}(\text{OH})_2]$, tremolite $[\text{Ca}_2\text{Mg}_5\text{Si}_8\text{O}_{22}(\text{OH})_2]$, anthophyllite $[(\text{Mg,Fe})_7\text{Si}_8\text{O}_{22}(\text{OH})_2]$, amosite $[(\text{Fe,Mg})_7\text{Si}_8\text{O}_{22}(\text{OH})_2]$ and crocidolite $[\text{Na}_2(\text{Fe}^{2+}_3\text{Fe}^{3+}_2)\text{Si}_8\text{O}_{22}(\text{OH})_2]$. Chrysotile asbestos $[\text{Mg}_3(\text{Si}_2\text{O}_5)(\text{OH})_4]$ belongs to the serpentine class.

The primary applications of asbestos have been recorded in history since ancient times, in the production of lamp wicks, clothing and as reinforcement of ceramic ware. Its name, “asbestos”, derives from the Greek word “ἀσβεστος” due to its use in wicks, and it means “unquenchable”. Asbestos minerals are known for their unique physical and chemical properties: electrical, thermal and sound insulation, flexibility, excellent mechanical strength, as well as resistance to chemical attack. All these exceptional characteristics and its low cost, have contributed decisively to establish asbestos as one of the most commonly used materials worldwide.

The extensive use of asbestos continued up to the verification of its harmful consequences to human health. It has been very well documented in literature (Markowitz et al. 2013) that exposure to asbestos leads to several diseases, such as lung cancer, asbestos signature disease, mesothelioma cancer and asbestosis. Asbestos fibers of specific characteristics (length > 5 mm and diameter < 3 μm, and a length/diameter ratio ≥ 3) are hazardous to human health. Asbestos products that are corroded tend to release fibers in the air. Long term inhalation of those fibers results in the aforementioned diseases (Schreier, 1989). Asbestos irreversible implication to human health was recognized in the 1960s, but it was only in the 1980s that legislative restrictions have been introduced with the aim of prohibiting the mineral extraction and ACM production.

2.1 Asbestos minerals

2.1.1 Chrysotile

Chrysotile mineral, also known as “white asbestos”, is the most common type of asbestos and the form with the largest deposits worldwide. Its Greek origin name indicates its color but also its friable fibrous structure. It is a hydrated silicate mineral of serpentine class, with ideal chemical formula $\text{Mg}_3(\text{Si}_2\text{O}_5)(\text{OH})_4$ and molecular weight 277.11 g (Roskill, 1986).

Chrysotile fibers are flexible, their length range from 10 to 40 mm and they tend to break into smaller fibers. When fibers obtain specific characteristics (length > 5 mm, diameter < 3 mm, length/diameter ratio $\geq 3:1$), they are dangerous to human health. The structure of the fibers is tubular, consisting of two layers. Specifically, there is a silicate matrix of silicon tetrahedra (SiO_4), strongly bonded with Mg octahedra, which is called brucite $[\text{Mg}(\text{OH})_2]$. SiO_4 tetrahedra

dimensions are smaller than brucite's octahedra in a percentage of 9%, resulting in incompatibility of the connection of the individual layers. The ideal width of magnesium octahedra is 9.43 Å, whereas the ideal width of silicon tetrahedra is 9.1 Å. This difference between layers is responsible for the coil structure of chrysotile fibers, creating curvature, leading to spiroid cylindrical fibers (Veblen&Wylie, 1993). The brucite layer covers the outer surface of the fibers.

The properties of chrysotile that render it different from other asbestos types are related to solubility and thermal conductivity. All asbestos types are insoluble in water. The solubility of minerals depends on the pH and the temperature that they will be exposed to. The fibers of chrysotile decompose when exposed to acidic conditions and/or high temperatures. Solubility of chrysotile results in weight loss of up to 56% (Anastasadou, 2011). The external layer of fibers, brucite, consists of magnesium hydroxide. Even though brucite is insoluble in water, it is soluble in acids. Thus, the structure of chrysotile can be destructed. Magnesium hydroxide layer is dissolved in the presence of acids and separated from the silicate matrix of the fibers. Chrysotile's fiber structure is unstable in high temperatures. Specifically, dihydroxylation could occur at 500-600°C, and at around 800-850°C the mineral is recrystallized in harmless forsterite.

Table 2.1: Resistance of asbestos minerals to chemical attack

Resistance to chemical attack
Tremolite > Anthophyllite > Crocidolite > Actonolite > Amosite > Chrysotile

2.1.2 Crocidolite

Crocidolite is also known as “*blue asbestos*”, with fibers that are characterized by elasticity, needle-like form and blue color. Under a mineralogical perspective it is found as magnesioriebeckite, calcium-riebeckite and riebeckite. Crocidolite term represents the commercial form of this type of asbestos. The length of the fibers ranges from 0.5 to 2.5 cm, but, nonetheless, very long fibers up to 7 cm have rarely been recorded, too. Crocidolite's structure is characterized by double chain corner-linked tetrahedra that extends infinitely (Gualtieri et al., 2004). It is considered to be the most dangerous asbestos type concerning human health, besides its outstanding properties. The largest deposits are found in South Africa, as well as in Australia and Bolivia.

2.2 ACM and their use

Asbestos use has been recorded since ancient times in thermal protection and fire prevention (Schreier, 1989). Its commercial exploitation began between 1860 and 1875 (Skinner et al., 1988), in textile production, ropes and thermal insulation boards. These innovative products were presented in “Exposition Universelle” in Paris, 1878, and that was the stimulus for the growing demand of asbestos containing materials. For more than a century, asbestos use was extensive, especially as a raw material in the construction sector.

ACM wide application was established during the 19th century, and was increased during the 1930s. The reason for that is associated with the increased need for ship construction, which arose during the Second World War. That sector used ACM mainly as insulator in boilers, tanks and pipelines. In the years following the war, the rapid development of the construction industry resulted in the extensive use of asbestos. The excellent mechanical and insulating properties led to its multiple applications.

More than 98% of ACM were manufactured using asbestos (mainly chrysotile and crocidolite) bonded with organic and/or inorganic materials. Cementitious, magnesium and calcium based inorganic materials were used in combination with asbestos to produce flat and corrugated sheets, pipelines and insulation products. On the other hand, asbestos reinforcement to organic materials, such as oils, plastics and resins was used for the production of gaskets, plastic sheets, thermoplastics, thermosets etc. Furthermore, it was also used as textile fiber and insulation foam. ACM were used as raw materials in schools, public buildings, hospitals, industrial plants etc. (Paglietti et al., 2012).

The most commonly found industrial commercialized asbestos products are:

- Asbestos cement
- Asbestos Sprayed Coatings
- Insulation materials
- Asbestos Textile Cloths and Textile Garments.

Asbestos cement (AC): AC is a building and construction material extensively used in the construction sector. It is a mixture of asbestos fibers, cement, sand and water. Asbestos fibers are embedded to cement mortar matrix in a percentage range of 10-18 % wt. Chrysotile and crocidolite are mainly used as reinforcement materials. AC is resistant to fire and acid rain, while, simultaneously, its mechanical and insulation properties are advantageous compared to conventional cement. It is used for the production of roof sheets (ETERNIT), pipes for water supply and sewerage network, tiles etc.

Asbestos Sprayed Coatings: It is mainly used for thermal insulation, sound insulation, fire protection, reinforcement of concrete beams/columns and decoration. It is extremely dangerous because it contains up to 85% asbestos in brittle form. It is spray-applied, creating a layer of 10 – 150 mm thickness.

Insulation materials: Besides coating, asbestos insulation boards are also commonly used. Their main application concerns fireproofing, while, at the same time, sound and thermal insulation is achieved. They are also applied in the outer surfaces of boilers, tanks and heat exchangers in order to improve their resistance to weathering. This type of insulation is also found in ship installations and ovens. Asbestos sheets or asbestos papers are used for thermal and electrical insulation in cables and air-conditioning systems.

Asbestos Textile Cloths and Textile Garments: Mainly found in protective clothing of firefighters and foundry workers. Asbestos fireproofing properties, in combination with its

fibrous nature, render it suitable as a raw material for textile fabrication for specialized uses. It attributes to textiles resistance to high temperature, fire and corrosive substances.

2.3 Effect on human health

In 1960 one of the primary investigation studies (Wagner et al., 1960) was conducted, concerning the association between asbestos exposure and its consequences on human health (Goswami et al., 2013). This study was the first that identified the domestic and neighborhood asbestos exposure.

Asbestos penetrates the human body via ingestion or inhalation. Ingestion penetration takes place through drinking water or food intake, and the swallowed fibers end up to the intestine through the digestive system. The most frequent harmful consequences due to asbestos exposure are related to the inhalation of fibers. Asbestos fibers of specific dimensions are easily inhaled and carried into the lung region and they are responsible for lung related cancer. The penetration of asbestos in the lungs depends on the diameter of the fibers; thin fibers can easily be deposited in the lungs. Inhaled fibers remain in the alveoli, small hollow cavities at the end of the lungs. The immune system, through white blood cells, tries to break down and remove the fibers unsuccessfully, causing damage to the respiratory system.

2.3.1 Asbestosis

Exposure to inhalable asbestos fibers with diameter smaller than 3 μm may cause pulmonary fibrosis. This disease was called asbestosis by Cooke in 1927 (Weiss, 1999). It is a very serious degenerative and progressive lung disease that gradually destroys the lungs. It is caused by long-term exposure to asbestos, reduces the elasticity and function of the lungs and results in permanent respiratory disabilities and deficiencies requiring specialized medical assistance. Symptoms of the disease include dyspnea, cough, expectoration, and in the final stages pulmonary hypertension and hypoxia (Cookson et al., 1985).

Asbestosis is a chronic lung disease characterized by scarring in the lungs and leading to respiratory problems. The disease is not amenable to treatment. It is caused after exposure to asbestos, but it can be diagnosed decades later. Asbestosis is directly connected with thin straight fibers found in most of the known asbestos types. Excessive exposure to asbestos leads to accumulation of fibers in the lungs, laying the foundation for future fibrosis.

Direct link between asbestosis and lung cancer has been supported. Statistically, in a group of employees subjected to high exposure to asbestos, lung cancer occurs to those who had previously been diagnosed with asbestosis. In particular, exposure to asbestos is considered a prerequisite for the occurrence of asbestosis and, ultimately, lung cancer (Weiss, 1999). But this case has not been proven.

2.3.2 Mesothelioma

Mesothelioma is considered a type of occupational cancer that occurs in the mesothelium cells, and most often in the thin layer of tissue between the lungs, the chest wall (pleural) and the organs of the abdominal cavity (peritoneum). A high percentage of mesothelioma cases, in a

range of 70-80%, are related to asbestos exposure, rendering it as an asbestos-related signature cancer. It is considered both a rare and an aggressive type of cancer, which is not amenable to healing. The main cause of mesothelioma is the occupational exposure to asbestos. According to literature (Barone-Adesi et al., 2008) of epidemiological studies, it is noticed that the pleural mesothelioma develops 40 years after the first exposure. On average, diagnosis ensues 3 months after the beginning of symptoms, and prognosis a year later. It is responsible for 10.000 deaths per year worldwide (www.asbestos.com). In Asia, where asbestos is still mined and commercialized a large increase of cases is expected.

2.3.3 Lung cancer

Asbestos exposure increases the chances of lung cancer five times, and they are additionally multiplied in combination with smoking (Table 2.2).

Table 2.2: Risk of lung cancer

Factors	Risk of lung cancer (In comparison with general population)
Asbestos exposure	x 5
Smoking	x 11
Combination of asbestos exposure and smoking	x 53

Symptoms of the disease include respiratory failure, cough, chest pain, hoarseness, blood in sputum and weight loss. The main latency period of the disease (since the first asbestos exposure) ranges from 20 to 30 years. A growing incidence of lung cancer has been documented among workers involved in the extraction, grinding and manufacturing, and use of asbestos-containing products. All types of asbestos can cause lung cancer, including the commercial types of chrysotile, crocidolite and amosite. An estimation of the chance ratio of cancer due to exposure to chrysotile asbestos, amosite and crocidolite is 1:100:500, respectively. This ratio differs due to the chemical composition of amosite and crocidolite and mainly because of the form and the size of their fibers (Ding et al., 2002).

Chrysotile is generally more chemically unstable in the lung environment, and magnesium leaching leads to the dissolution of the fiber. Thus, chrysotile fibers are quickly broken into smaller fibrils that can easily be phagocytized and removed from the lung. Therefore, toxicologically, these smaller chrysotile fibers behave more like non-fibrous mineral powders. Even the curved chrysotile fibers have low flexural strength and when inhaled they do not reach the lung parenchyma but they are trapped in the wide branches of the airways.

2.4 Current situation and future perspectives

Asbestos extraction peak year is 1977, where the extracted quantity was recorded at 4.8 million tons (Park et al., 2012). From 1920 to 2003, 135 countries used ACM at least for short periods, and it is accounted that they consumed 181 million tons of asbestos (Virta, 2006). Asbestos was already related to negative effects on human health, thus, a long-term effort began for the imposition of prohibitive measures concerning asbestos extraction and ACM production. In

1983, the European Union (83/477/EEC) introduced a Directive on protection of workers exposed to asbestos and classified asbestos as hazard for human health. The following years a multitude of legal frameworks were proposed and implemented in order to ban extraction, manufacture and use of asbestos and ACM. However, it was only in 2005 that the ban was applied throughout the EU. Except for the 28 member states of the EU, there are only 38 more countries that have applied asbestos ban (IBAS, 2018), mostly developed countries, which respect environmental, health and safety legislation. Nowadays, the major consumers and producers of asbestos belong to developing countries. The leading countries on asbestos production during the last 5 years are illustrated in Figure 2.1 Up to 2015, more than 2 million tons were produced per year (Figure 2.2). Taking into consideration statistical data of the last 5 years it can be concluded (Figure 2.3) that Russia is responsible for 53% of the annual production, followed by China (20%), Brazil (15%) and Kazakhstan (12%) (www.statista.com).

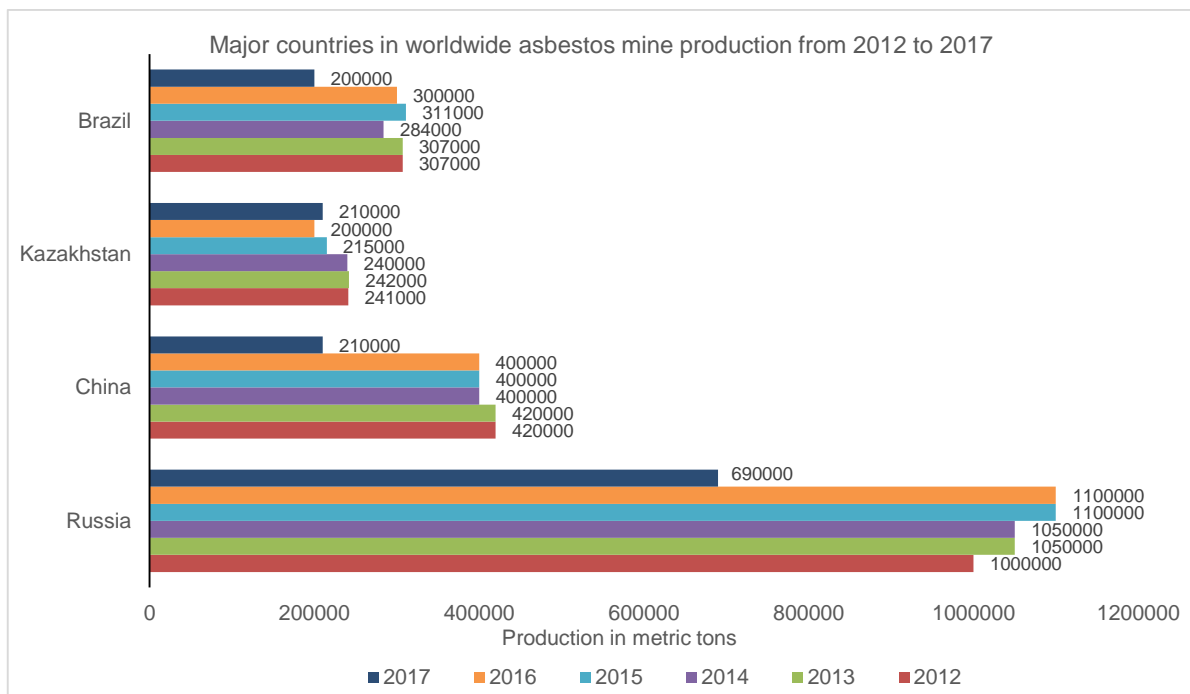


Figure 2.1: Major countries in worldwide asbestos mine production from 2012 to 2017 (production in metric tons) (www.statista.com)

These quantities are mainly distributed in the Asian market. According to literature (Li et al., 2014), in 2011 the annual production was 2.03 million tons of asbestos, 61.5% was consumed in the Asian-Pacific region, of which 30.5% regarded China and 15.4% regarded India. In general, according to Li et al. (2014), the Asian-Pacific region is the main market of asbestos and ACM. During the period 1998-2007, 9.76 million tons of asbestos were consumed by those countries. China, Vietnam, Thailand, India, Nepal and Pakistan, having active mines, are the main manufacturers of the Asian-Pacific market, while China, India and Thailand are the main consumers.

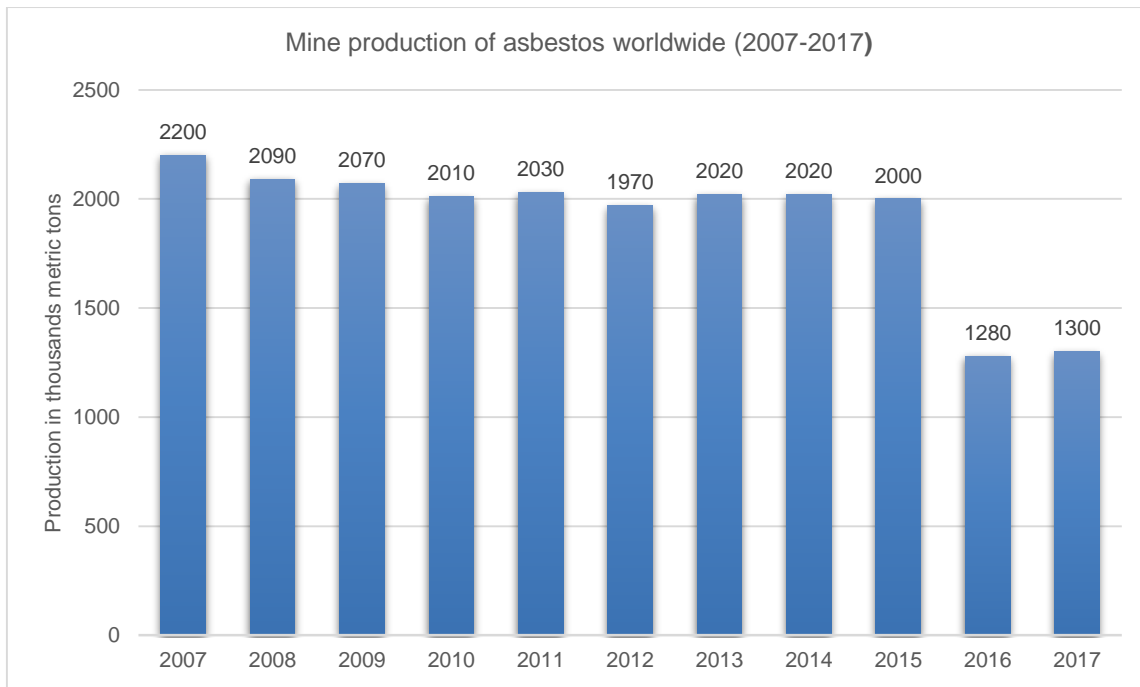


Figure 2.1: Mine production of asbestos worldwide (production in thousand metric tons) (www.statista.com)

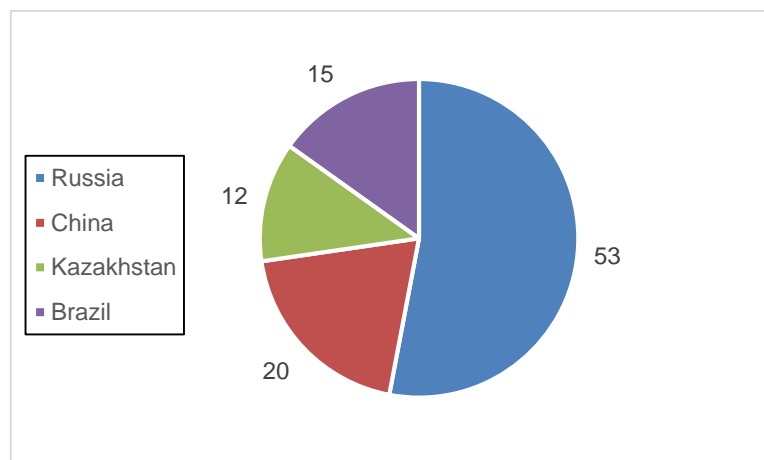


Figure 2.2: Distribution of asbestos production of major producers 2010-2017 (%) (www.statista.com)

2.5 Management of asbestos deposits and Asbestos Containing Materials (ACMs) in abandoned mining and public premises in Greece.

An asbestos mine was active in Greece, from 1982 since 2000. The region of asbestos mine, also known as MABE, is located in Western Macedonia, 40 km east of Kozani town and 1 km south of Aliakmonas river and the artificial lake Polyfytou. Aliakmonas is the longest river in Greece and constitutes the main source of drinking water for the city of Thessaloniki. Additionally, the water for irrigation for several regions of northern Greece is originated from Aliakmonas river and lake Polyfytou.

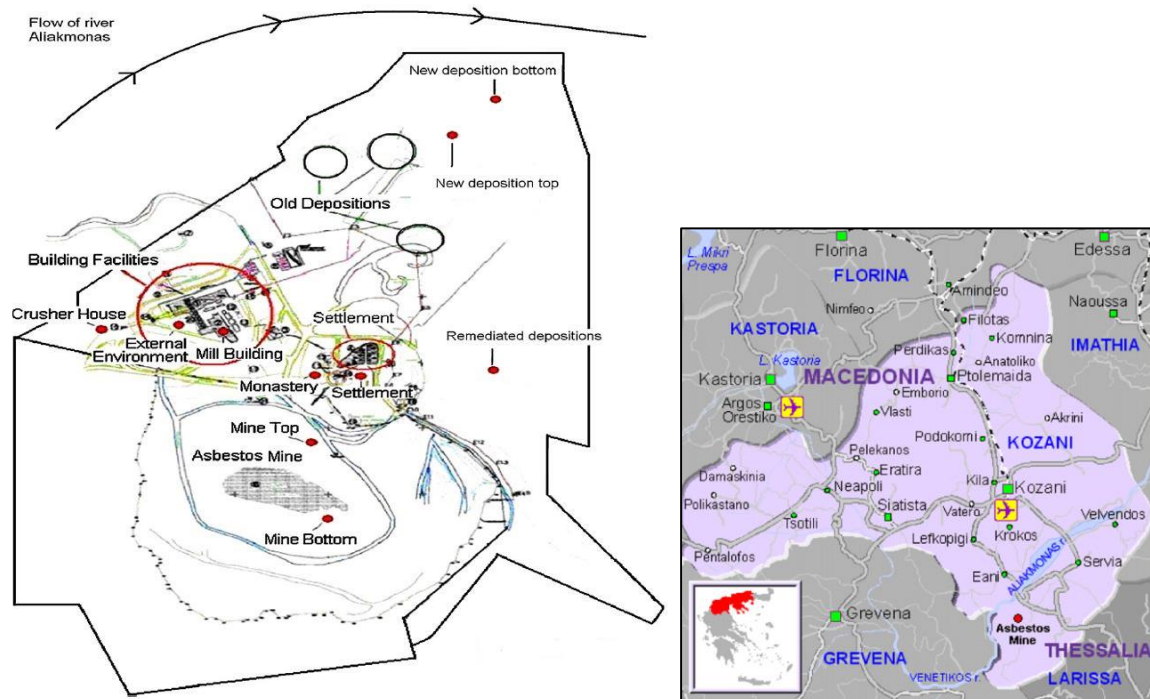


Figure 2.4: Maps of (a) MABE region and (b) asbestos mine location and in the Prefecture of Kozani

The presence of asbestos in this region was found in 1936 and some years later, in 1950s it was characterized as the most exploitable asbestos layer in Greece (Anastasiadou & Gidarakos, 2007). During mine operation, 18 years, the factory of MABE was produced about 100.000 tons of commercial chrysotile per year, rendering Greece the 7th largest producer of asbestos minerals worldwide. Vafeiadou (2003) has reported that from 1982 since 2000, it was excavated 70 million tons of serpentine, which led to the production of 881.000 tons of commercial chrysotile. Fibers of asbestos were extensively dispersed in the environment, since the excavation took place in an open mine and explosives were used (Koumantakis et al., 2009). Additionally, further contamination was determined due to natural erosion of the minerals. The contamination in the air that caused by the treatment procedures, loading and unloading of asbestos and barren material was characterized as immeasurable after extensive evaluation of environmental quality by measuring and monitoring the concentration of asbestos fibres in the air. Fibers in water samples were also found in high concentrations that varied from 8.000.000 to 35.910.000 fibers per liter. The deposits, after the closure of the mines were estimated to higher than 1.33 million tons, which considered a 10-fold increase since 1982 (Anastasiadou & Gidarakos, 2007).



Figure 2.5: The open pit of the mine and the site of depositions after asbestos mine closure

Taking under consideration the concentration of the fibers in the air, soil and water, it was considered mandatory a remediation procedure aiming to the production of the environment and human health. Gidakos et al., (2008) were proposed the use of MABE inactive asbestos mine for the construction of asbestos waste hazardous landfill. Based on successful case studies of European countries, where inactive mines have been used as disposal sites for municipal or hazardous waste, it was evaluated the sustainability of the use of the mine as disposal site for asbestos waste. The holistic investigation of suitability of the inactive mine was included the determination of topographic, geological, geotechnical and hydrological characteristics and climatic data. Additionally, it was determined the potential hazardous substances in soil, rock and water through sampling and analytic techniques. This study concluded that there were two suitable sites that satisfy the requirements for the construction of hazardous asbestos waste landfill, where the ACW derived from the restoration of the buildings facilities and the surrounding area of MABE were to be buried in the mine.

Two European projects were conducted by Toxic and Hazardous Waste Management Laboratory of Technical University of Crete. During these projects it were conducted in situ the removal of all asbestos materials from buildings and the external surfaces, the demolition of the buildings, while additionally it was performed the disposal of asbestos waste in the pilot asbestos landfill within the mine. Furthermore, planting of the area was carried out. A significant part of the depositions (40%) was rehabilitated while ensuring the necessary safety.



Figure 2.6: Procedure of asbestos mine rehabilitation

Since 2002 and for the next 30 years the MABE facilities will belong to the Region of Western Macedonia, with the intended purpose of remediation, improvement and exploitation of the area. Nowadays, the restoration of the inactive mine has been completed, following the proposal of Technical University of Crete.

The use of ACMs in Greece was very extensive in the construction sector up to 2000. Except MABE, in Greece there were also operated three factories of asbestos cement production. ACMs and mainly the asbestos cement corrugated roof sheets and asbestos-based insulating materials were found in many public premises, as schools, hospitals and building of public authorities. In 2014, it was determined that more than 250 School buildings were contained ACMs. The lack of statistics on the presence of asbestos in public and private buildings was an obstacle to the solution of the problem of ACMs dismantling in Greece.

The state, in the context of ensuring health and safety of the citizens, was launched a great campaign to remove every asbestos product and to restore every public building. The rehabilitation of the buildings and the management of asbestos containing waste were assigned by the Ministry of Labor to certified companies with properly trained workers. The ACW management was conducted in accordance with the existing legislation (2000/532/EC, 99/31/EC). These Directives classify ACMs as hazardous waste and determine the need for their disposal in hazardous wastes landfills. Since there is no special landfill in Greece, ACMs after their dismantling were properly bagged, classified (hazchem code) and transferred abroad in hazardous waste landfills.



Figure 2.7: Procedure of asbestos containing materials dismantling and packaging

2.6 Asbestos Containing Waste treatments

The existing legislation does not specify any method of treatment of asbestos waste. However, it indicates the disposal of waste in special hazardous waste landfills (Paglietti et al., 2016). It is worth noting that not all kinds of asbestos containing waste are able to be landfilled in their initial form. ACW is divided into brittle and non-brittle. If the specific weight is lower than 1000 kg/m^3 it is considered brittle, and it is obligatory to mix it with stabilizing materials in order to be transformed into non-brittle. The disposal process begins from the source, where asbestos containing waste is soaked with active surfactant and sealed airtight in suitable double polydiphenyl sacs (2 mm thick). The second coverage is preferred due to the hazardousness of waste in order to avoid fiber leakage. Additionally, since most of this waste is derived from demolition debris, the second coverage also protects from sharp edges which are likely to pierce the walls of the bags.

Waste disposal in landfills has some significant disadvantages. Firstly, it is not a permanent solution from an environmental and health perspective, because the waste is not subjected to degradation and the problem is postponed for future generations (Leonelli, 2006). Additionally, high costs of transportation, landfilling and unsustainable land use due to large volumes of waste are also drawbacks of this method. Moreover, even if waste is double sealed in sacks, earthmoving machines are likely to drift the sacks, resulting in fiber leakage in the air and raising a potential health risk. Specifically, around hazardous landfill areas, and despite protection measures, it is recorded that asbestos fibers' concentration is 10 to 1000 times higher than normal (0.01 fibers/cm³) (Cherry, 1988)

The European Parliament in order to effectively encounter the environmental and health issues associated with asbestos, heartened the EU members *“to work with the social partners and other stakeholders at European, national and regional levels to develop and share action plans for asbestos removal and management”* (Resolution EU-P7_TA, 2013). Moreover, the European Parliament *“points out that, as regards the management of asbestos waste, measures must also be taken e with the consensus of the populations concerned e to promote and support research into, and technologies using, eco-compatible alternatives, and to secure procedures, such as the inertisation of waste-containing asbestos, to deactivate active asbestos fibers and convert them into materials that do not pose public health risks”* (Resolution EU-P7_TA, 2013).

Several laboratory-scale treatment methods have been developed aiming at establishing a sustainable option for ACW treatment. Physical, chemical and biological methods are found in literature, in order to eliminate asbestos fibers and render the byproducts of treatments non-toxic for human health and the environment. The common purpose of the proposed treatments is the development of a sustainable solution that will contribute to the substantial cooperation between the research community and the industrial sector, and lead to a pilot plant and, eventually, the operation of a full-scale treatment plant.

2.6.1 Thermal treatments

Thermal stability of asbestos minerals is obvious due to their extensive use as thermal insulation materials in the industrial sector. Nonetheless, it is well documented in literature that asbestos fibers are unstable in temperatures higher than 500°C (Spasiano & Pirozzi, 2017). Dehydroxylation of asbestos fibers leads to mineral transformation and re-crystallization leads to non-asbestos forms. Each kind of asbestos degradation begins at a different temperature. Several studies have been conducted in order to identify the optimal conditions regarding thermal transformation of asbestos fibers. Moreover, despite asbestos hazard risk elimination, the research community tends to develop methods that create valuable byproducts. Different approaches have been developed concerning the minerals of pure asbestos, as well as asbestos containing materials such as asbestos cement corrugated sheets.

Zaremba et al. (2010) carried out a preliminary study on chrysotile asbestos thermal treatment. Since chrysotile is the most commonly found asbestos form, it is also the most studied. At temperatures between 600-800°C, chrysotile completely transforms into a harmless mineral.

During thermal treatment the mineral dehydroxylates and the stages of degradation are illustrated in Figure 2.8.

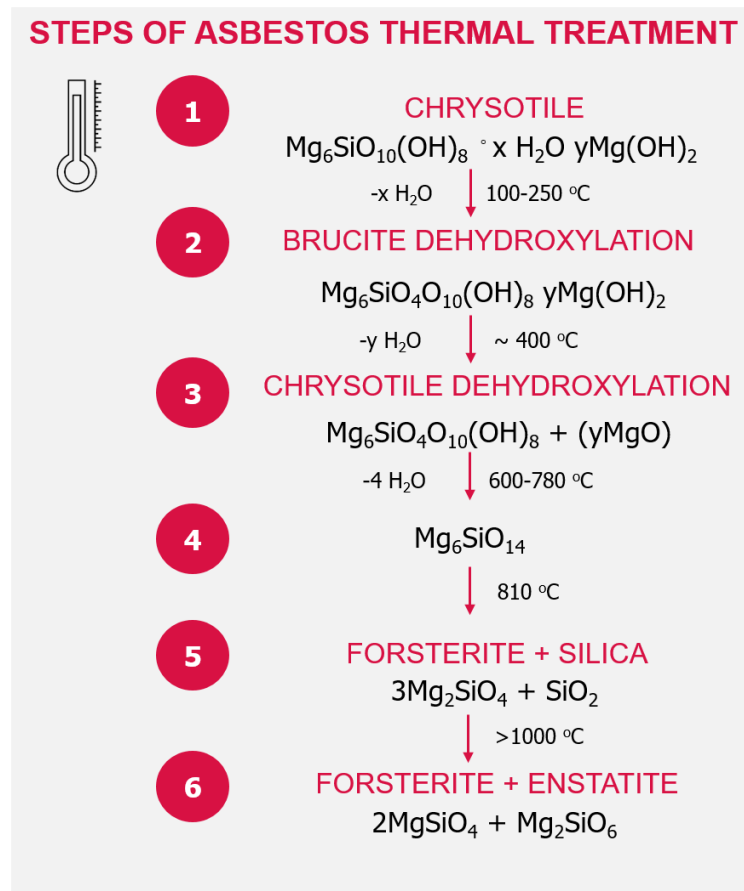


Figure 2.8: Steps of asbestos thermal degradation

Recently, Kusiorowski and co-authors (2013, 2015) have proposed a thermal treatment of asbestos resulting to asbestos detoxification and to possible reuses of raw material in clinker bricks manufacture and/or sintered ceramics (2016). Chrysotile dehydroxylation was achieved at temperatures from 400 to 650 °C, depending on asbestos origin and Mg content. Full decomposition was achieved at 800-880 °C. In the same study, crocidolite transformation to acmite, hematite, cristobalite and spinel is achieved via static heating at 600-950 °C. The authors noted that the content of magnesium in the initial sample was a significant parameter of the treatment. Higher magnesium content demands higher thermal energy to obtain a brittle harmless byproduct. In the context of a holistic approach the authors recycled the calcined ACM as secondary raw material in clinker bricks, at 5-10 %wt. substitution. Although the replacement of 10%wt results in a decrease of clinker quality, the replacement of material at 5%wt results in a similar to the initial product regarding standard parameters, such as water absorption, compressive strength and freeze resistance of clinker bricks.

Bloise et al. (2016) conducted a research investigation of the thermal behavior of different asbestos minerals. Specifically, they determined the decomposition temperature of the most predominant asbestos types in ACM: chrysotile, crocidolite, tremolite, anthophyllite and amosite. Asbestos decomposition and recrystallization take place at 660-1046 °C, depending

on mineral kind. The Table 2.3 presents the temperature and transformation of the recrystallization of minerals of each asbestos type.

Table 2.3: Temperature and recrystallization of thermal decomposition of asbestos minerals (Bloise et al. 2016).

Asbestos	Temperature (°C)	Transformation
Chrysotile	822	Forsterite
Crocidolite	850	Magnetite
		Crystobalite Acmite
Amosite	878	Enstatite
		Hematite
Anthophyllite	861	Enstatite Cristobalite
Tremolite	1046	Diospide

Aiming, both in treated pure asbestos and ACM, at the production of valuable and reusable byproducts through detoxification processes, the scientific community adopts the development of such methods. Ruiz et al. (2018) combined thermal energy with chemical reagents (Na_2CO_3), bentonite and sepiolite, in order to eliminate asbestos phases. Their method investigated the temperature and annealing time of the treatment and resulted in a variety of byproducts. The combination of ACM with sepiolite results in harmless Ca-Mg silicates and larnite, while with bentonite results in aluminum silicates. The obtained products contain clinker phases (C_2S , C_3S) and free MgO. The authors believe that these products are suitable for magnesium based cements for special applications such as contaminant immobilization due to low permeability (Ruiz et al., 2018).

The utilization of treated ACM in cement mortars constitutes an advantageous recycling method. Viani and Gualtieri (2014) proposed a treatment of a mixture of ACM and magnesium carbonate at 1100-1300 °C. The resulting product, contained MgO and was reactive with potassium dihydrogen phosphate which led to hydrated phases.

A combination of asbestos cement roof sheets with fly ash from industrial plants after thermal treatment at 1420-1440°C for 28 min in plasma reactor creates vitrified slag rich in SiO_2 , CaO, Al_2O_3 and MgO, rendering this glass matrix suitable for the production of insulation materials and ceramics (Lazar et al., 2016).

Another interesting treatment method arises through hydrothermal process, achieving the conversion of pure chrysotile. Anastasiadou et al. (2010), proposed asbestos treatment near supercritical conditions at temperatures ranging between 300-700 °C, pressure in 1.75-5.8 MPa and treatment duration 1-5 hours. Low concentration of acetic acid (1 % wt.) facilitates the whole procedure and chrysotile is transformed into forsterite.

2.6.2 Mechanical Treatments

Mechanical treatments aim at converting asbestos waste into amorphous material. In order to achieve this, it is necessary to develop high load, resulting in the crushing of the material in a short time, influencing the crystalline structure of asbestos. As a consequence of continuous grinding, transformation of asbestos crystal structure into new amorphous phases, similar to the ones of melting processes, is achieved (Plescia et al., 2003). Advantages of this method include treatment time and absence of emission through treatment. Apart from that, it is easy to install and carry over pilot plants *in-situ* (Gidarakos 2006).

Several researchers conducted different mechanical and/or mechano-chemical treatments, regarding mill types, milling time and possible reagents that facilitate the treatments or provide more valuable byproducts. Recently, Bloise et al. (2018) investigated treatment time using an eccentric vibration mill and its effect on chrysotile, amosite and crocidolite asbestos. The complete elimination of fibers was achieved after 10 minutes of milling. The mill type and the rotating speed are the most significant parameters of the mechanical treatment. A laboratory ring mill achieved amorphization of chrysotile (4 min), crocidolite and amosite (8-12 min) at 250 rpm (Plescia et al., 2003). ACM, the largest asbestos waste stream, was treated via high energy milling (HEM) for 120 min (Colangelo et al., 2011). This study constitutes a holistic proposal, because it investigated the hydraulic behavior of obtained powders in lime mortars. Pozzolan activity demonstrated recycling powders in building materials, which improved mortars in terms of compressive strength.

According to an AsbestEx company report regarding treatment costs, it is estimated that mechanical treatments are more expensive than thermal. However, possible mechano-chemical or mechano-thermal treatments are able to reduce this cost (Spasiano & Pirozzi, 2017). The addition of K_2HPO_4 in mechanical conversion of chrysotile was proposed (Borges et al., 2018), generating a new material of ditmarrite and/or potassium struvite, depending on milling conditions. This method achieved the synthesis of slow release fertilizers, useful materials for agriculture.

2.6.3 Chemical treatments and combined treatments.

Chemical treatment of chrysotile and amphibolite asbestos, as well as asbestos containing materials using strong acids is very well documented (Spasiano & Pirozzi, 2017). The degree and rate of dissolution of asbestos with acids depend on temperature, acid severity and concentration, and at a certain level from the origin of the raw mineral (Hyatt et al., 1982). Taking advantage of this knowledge, several studies have been conducted with acid solutions or combinational chemical and thermochemical methods leading to asbestos and ACM detoxification. Several chemical reagents were used in order to investigate asbestos denaturation treatments. For example, Yvon and Sharock (2011) proposed mixtures of asbestos cement with fluxes (Na_2CO_3 , NaH_2PO_4 and $Na_2B_2O_7$) aiming to decrease ACM melting point. They achieved asbestos melting at a temperature lower than 1200 °C, while the initial melting point was at 1450 °C. Additionally, the obtained byproduct was stabilized as a replacement in mortars up to 10 %wt. The addition of treated ACM affects the obtained compressive strength of the produced mortar. Spasiano et al. (2019), produced eco-friendly phosphorous based fertilizer. ACW subjected to dark fermentation pre-treatment and afterwards hydrothermal and

anaerobic digestion treatments. Sulfuric, lactic and malic acid were used as reagents at low temperatures. ACW transformation to struvite, an eco-friendly fertilizer, and methane recovery were achieved through the anaerobic digestion process. Sulfuric acid effect on pure chrysotile structure has been studied extensively (Rozalen & Huertas, 2013). Nam-Nam et al. (2014) proposed the use of waste sulfuric acid digestive destruction of asbestos cement roof sheets. That is a thermochemical treatment using 5N H₂SO₄ solution heated at 100 °C. It has been proven that the waste sulfuric acid is as strong as the commercial. This treatment achieved the conversion of AC to harmless calcium sulfate (CaSO₄). The effect of natural acids, such as oxalic, carbonic and hydrochloric acids on asbestos minerals has been studied by Lavkulich et al. (2014). Phosphoric acid in relatively high concentration (30 % wt.) eliminates ACW through a two-stage treatment process (Pawelczyk et al., 2017). Firstly, ACW is thermally treated at 800 °C in presence of sodium carbonate as a melting agent. Thereafter, chemical elimination of asbestos fibers is achieved using phosphoric acid and the final obtained byproduct consists of inert calcium and magnesium phosphate and silica.

Chapter III: Cement: composition and supplementary cementitious materials

Abstract

Hydraulic binders are the most common used type of binder in construction sector. Their name, in accordance with their properties, declares their need on water to react and harden. Portland cement is the most common type of hydraulic binder commercially used.

Supplementary cementitious materials are widely used in mortars either in blended cements or added separately in the mixing procedure. The term *Pozzolan* originated from the Pozzuoli region of Italy. Nowadays pozzolans are called the fine silicate (SiO_2) powders, with aluminum, iron, calcium oxides, etc. in smaller proportions. Such as these fractions are found in minerals at the surface of the Earth, it is most likely to be used as supplementary cementitious materials.

While they are characterized by relatively low hydraulicity, pozzolans are hydrated just like cements when mixed with a suitable binder (e.g. lime, gypsum, cement). During hydration - which takes place due to the pozzolanic reaction - they react chemically slowly, with calcium hydroxide forming hydrated calcium-silicate compounds similar to those of cement hydration.

Further separation of pozzolans is based on their origin in natural (e.g. volcanic ash) or artificial (e.g. silica fume). During the past decades, artificial pozzolans are used as cement admixtures aiming to develop mortars with advantageous characteristics and to reduce the environmental impact of the production of the dominant cement as binder. These alternative pozzolans, occasionally derived from waste (i.e. metallurgical or industrial plants) are able to improve the performance of cement mortars and concrete.

3. Cement: composition and supplementary cementitious materials

3.1 Binders

Binders are materials that, when mixed with a fluid substance (usually water), change into a paste with adhesive properties. This paste, after coagulation, in the early ages of hydration and curing, is the binder of mortars (e.g. cement or lime mortar). Coagulation is the phenomenon during which the paste is converted from a malleable mass into a material characterized by stability and mechanical strength. Curing is defined as the period following coagulation, where the paste obtains almost the final strength.

Depending on their behavior towards the water after coagulation, the binders are classified as non-hydraulic and hydraulic. Non-hydraulic binders (e.g. clay, lime, etc.) coagulate and cure in the presence of air and they remain in an atmospheric environment. However, they dissolve in water and in a strongly humid environment. Hydraulic binders (e.g. hydraulic lime, pozzolans, cement) remain in water after curing or in a periodically humid environment and they are insoluble in water. The hydraulicity of binders depends on their composition due to the presence of SiO_2 , Fe_2O_3 , Al_2O_3 . The curing of hydraulic binders is a physicochemical process during the course of which the hydrated phases are in a colloidal form, and are gradually converted into microcrystalline, as opposed to aerated cements which are initially crystalline. Further separation of binders is based on their natural (e.g. clay, pozzolans) or artificial (e.g. cement, lime) origin. During the past decades, new binders have been developed aiming to reduce the environmental impact of the production of the dominant cement as binder. These alternative binders, probably derived from waste (i.e. construction and demolition, industrial plants etc.), are able to improve the performance of mortars and concrete (Juenger et al., 2011)

3.1.1 Hydraulic binders

Hydraulic binders are the most commonly used type of binder in the construction sector. Their name, in accordance with their properties, declares their need for water to react. Additionally, hydraulic binders are able to harden in the presence of water, so they can be used for underwater constructions or in humid environments (Gartner et al., 2011).

3.1.2 Pozzolanic binders

The term *Pozzolan* originated from the Pozzuoli region of Italy, where the Romans used soil to produce mortars because they discovered that it presents hydraulic properties (Roman cement). Today pozzolans are the fine silicate (SiO_2) powders, with aluminum, iron, calcium oxides, etc. in smaller proportions. Since these fractions are found in minerals on the surface of the earth, it is more likely to be used as cementitious materials (Gartner et al., 2011). While they are characterized by relatively low hydraulicity, pozzolans are hydrated just like cement when mixed with a suitable binder (e.g. lime, gypsum, cement). During hydration, which takes place due to the pozzolanic reaction, they react chemically slowly, with calcium hydroxide forming hydrated calcium-silicate compounds similar to those of cement hydration.

They are divided into natural pozzolans, such as volcanic and sedimentary, and artificial pozzolans. Artificial pozzolans, usually derived from heat treatment of materials, containing CaO and hydraulic agents such as fly ash (obtained from lignite-fired power plants), blast-furnace slag (by-product of the iron and steel production process) and silica fume (by-product of silicon and ferrosilicon alloys industry). Such binders are often used as additives for cement or concrete.

3.1.3 Mortars

A mortar is any mixture of one or more binders with sand and water. Depending on their use, they are separated into mortars of load-bearing structural elements (e.g. masonry) or non-load bearing structural elements (e.g. coatings) (Wendehorst, 1975). Based on their properties, mortars are divided into hydraulic and aerated mortars. The water used in mixing should be clean and free of contaminants such as acids and salts (sulphates, chlorides). Sand, natural or artificial, should be derived from clean rocks, and contain less than 5-6 % wt. of impurities such as rust, mica, fossils, industrial waste and dust. The granulometry of the sand must have a fine (<0.25 mm) content of 10-25 % wt. The most important mortars are:

1. Ancient mortar
2. Ordinary Portland cement mortar
3. Polymer cement mortar
4. Lime mortar
5. Pozzolanic mortar

Cement paste is the product of the reaction of cement powder with water. Portland cement, widely used, is made of clinker with small amounts of impurities. The clinker consists mainly of 4 basic compounds in the following proportions and chemical composition:

- 40-80% C₃S (tricalcium silicate)
- 0-30% C₂S (dicalcium silicate)
- 7-15% C₃A (tricalcium aluminate)
- 4-15% C₃AF (tetracalcium aluminoferrite) (Lea, 1971).

After cement mixing with water, the needle crystals of hydrated calcium aluminum sulfate hydroxide (ettringite) form. At the same time, in early hydration stages, calcium hydroxide crystals also form, as well as very small fibrous form crystals of calcium silicates hydrate which occupy the voids developing by the reaction of water and cement grains. During the first days of curing, ettringite crystals are possible to dissolve. As a result, structural modification of the crystals from needle to plate-like sulfate hydrates will occur. This conversion takes place due to either a sulphate deficiency or a cement excess of C₃A.

3.2 Portland cement

Portland cement is the most common type of cement commercially used. It is produced from clinker milling, a product of heating of limestone and clay. It was named after the Portland stone quarried on Portland Island, UK, because of its color similarity.

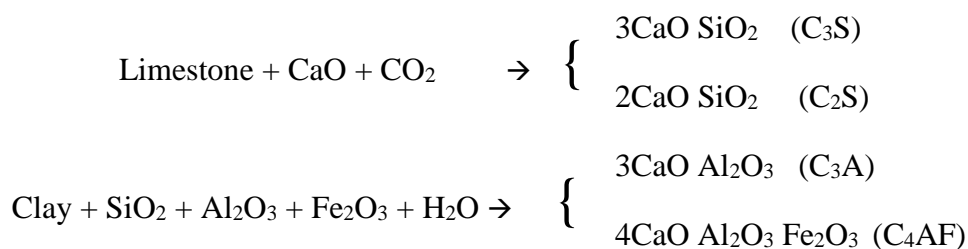
Portland cement is the result of processes including:

1. Mining of limestone rocks, clay soils and rocks that are crushed in grains in the size of centimeters.
2. Mixing of grains, pre-homogenization.
3. Milling to obtain mixture of fine granules (powder) in millimeter diameter.
4. The powder mixture is heated in a rotary cylindrical kiln. The temperature at the top of the kiln is about 600 °C, heated by coal or oil at the low part, where the temperature rises at 1500 °C. Export of grain product (clinker), in diameter of 5-25 mm.
5. Milling of the clinker, which, after cooling, is mixed with 2-3% gypsum to give Portland cement with a grain diameter of about 75 µm.

It is a common procedure to mix clinker with pozzolans in the last step of the Portland cement production process. Pozzolans are preferred due to their hydraulic properties, especially natural pozzolans (volcanic), fly ash and blast furnace slag. Furthermore, special natural or artificial inorganic minerals, the so-called fillers, are also commonly used, aiming at the improvement of Portland cement physical properties. Additionally, calcium sulphate is added (as gypsum) to adjust setting time. Gypsum addition in percentages up to 3 %wt. results in slower setting, while in higher percentages results in faster setting (Mc Arthur & Spalding, 2004)

3.2.1 Chemical synthesis

The chemical synthesis of cement depends both on the composition of raw materials and heating conditions (temperature and duration). The chemical reactions of its main components that take place during cement production are described as follows (Mc Arthur & Spalding, 2004):



Calcium silicates are the main components of cement as they determine the strength of the cement paste. C₃S and C₂S are found in ~55 %wt. and ~15 %wt., respectively. C₃S contributes to fast hydration of cement, high early and final strength, and the development of hydration temperature. C₂S contributes to slow hydration, final compressive strength, and low-temperature of hydration. It is worth noting that calcium silicates are in the form of oxides and significantly affect crystalline structure and hydraulic properties of cement.

Tricalcium aluminate is found in a percentage of ~12 %wt. and contributes to fast hydration of cement, development of: (i) high temperature of hydration, significantly in early compressive strength, (ii) shrinkage and sulphate resistance. C₃A is also responsible for ettringite formation resulting in mortars expansion.

Tetracalcium aluminoferrite is found in a percentage of ~9 %wt. and weakly affects the properties of cement paste. It contributes little to hydration and causes insignificant development of strength. It is characterized by average hydration temperature and offers strong color.

Table 3.4: Typical chemical composition of common Portland Cement (% wt)

Oxides	CaO	SiO ₂	Al ₂ O ₃	Fe ₂ O ₃	MgO	SO ₃	Na ₂ O	Other
	64	22	6	3	1.5	2	0.5	1

3.2.2 Types of Portland Cement

According to EN 197-1 cements are characterized by their type and a number that refers to compressive strength. Cement types are summarized as follows:

CEMI: Ordinary Portland Cement. It consists of clinker ground mixed with secondary materials, such as natural pozzolan, fly ash, furnace slag, fillers etc. up to 5 %wt.

CEMII: Portland-composite cement. It is produced by co-milling of clinker (65-94 %wt.) with other materials (6-34 %wt.) such as natural pozzolan, fly ash, furnace slag, powder of limestone. CEMII production is cheaper. CEMII is used in construction exposed to moderate sulfate attack.

CEMIII: Blast-furnace cement. It is produced by co-milling of clinker (5-64 %wt.) with furnace slag (36-95 %wt.) and secondary raw materials (0-5 %wt.). Its 3rd day early strength is equal with the strength of the 7th day of CEMI type.

CEMIV: Pozzolanic cement. It contains clinker (45-89 %wt.), natural pozzolan, or/and fly ash, or/and silica fume (11-55 %wt) and secondary raw materials (0-5 %wt.). Due to low content of C₃S and C₃A and higher pozzolanic content, it is characterized by low hydration reaction rate which renders the early compressive strength lower than the obtained of ordinary Portland cement. Although, long-term compressive strength is the highest of all cement types.

CEMV: Composite cement. It contains clinker (20-64 %wt.), blast furnace slag (18-50 %wt.), pozzolan and/or fly ash (18-50 %wt.) and secondary raw materials (0-5 %wt.). Due to its very low content of C₃A it is an advantageous option where high sulfate resistance is needed (Mc Arthur & Spalding, 2004).

3.3 Solids of hydrated cement binder

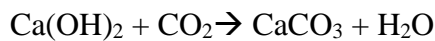
3.3.1 Calcium Silicate Hydrates (C-S-H)

It is considered to be the most important component of cement paste. It is the main product of hardened Portland cement due to hydration of C₃S and C₂S, and constitutes about 75 %wt. of solid phase (Lothenbach & Nonat 2015). Mechanical properties of concrete and cement mortars are attributed mainly in C-S-H (Hu et al., 2014). Morphology of C-S-H varies from low

crystallinity fibers to network. C/S ratio is 1.5-2, 1.7 on average, while H content is variable. C-S-H formation results from the anhydrous calcium silicates dissolution in the pore solution. Additionally, soluble siliceous materials used as additives in cement mortars, such as silica fume, fly ash, slag etc., contribute to C-S-H formation (Lothenbach & Nonat 2015). It is characterized by a large surface area (100-700 m²/kg) and its strength is the result of the van der Waals forces.

3.3.2 Calcium Hydroxide

Calcium hydroxide crystals constitute 20-25 % vol of cement paste solid phase. In contrast with C-S-H, calcium hydroxide has certain stoichiometry, Ca(OH)₂. It is responsible for the large hexagonal prism crystals formation, while its contribution to the van der Waals forces is limited compared to C-S-H. Additionally, Ca(OH)₂ presence in high percentage in the cement paste degrades cement resistance in acidic environment. Because CH reacts with atmospheric carbon dioxide, non-desirable carbonation of mature mortars takes place according to the equation:



Carbonation is responsible for mortar degradation since it leads to cracking, shrinkage and reduction of pH (Rostami et al., 2012).

3.3.3 Sulfuric salts

Their volume in cement paste is about 15-20%. Their contribution to structure and properties of cement paste is insignificant. Monosulfate hydrates are responsible for low resistance of the end-product to sulfur compounds.

3.4 Voids of hydrated cement binder

3.4.1 C-S-H internal layered structure voids.

Voids between C-S-H internal layers are characterized by extremely small dimensions and they do not affect the compressive strength and permeability of paste (Powers, 1958). However, it is possible for water to be encapsulated in these voids through hydrogen bonds, and it will contribute to phenomena like drying shrinkage and creep.

3.4.2 Capillary voids

Porosity depends on the initial distance of anhydrous cement grains (immediately after mixing cement powder with water), the water/cement ratio and hydration rate. The diameter of pores in hydrated cement paste, with low water to cement ratio is about 10-50 nm. In the early stages of hydration, the diameter ranges from 3-5 μm. It is noteworthy that the pores distribution is a more important parameter than total porosity, regarding the final quality of the mortars. Capillary voids, with pore diameter bigger than 50 nm, adversely affect the strength and water resistance of the mortars. On the other side, pores with diameter smaller than 50 nm, are responsible for drying shrinkage and creep of mortars (Triantafillou, 2017).

3.4.3 Air voids

Air voids have spherical shape. Such voids are either trapped during mixing of the mortar, or are deliberately inserted. These voids are much larger than the capillary; therefore, they negatively affect the final strength of the cement paste and its permeability (Triantafillou, 2017).

3.4.4 Structure-properties relationship of hydrated cement paste

The strength of the solid cement products is mainly developed due to the van der Waals forces. Any porous medium owes its compressive strength to its solid phase, and, thus, strength increases as the porosity decreases. It is noted that the voids of C-S-H internal layers as well as the micropores do not affect strength, which mainly depends on the capillary macropores and any microcracks. The hydration products occupy a much larger volume than the original cement, and thus it is concluded that the capillary porosity decreases with the increase of the hydration rate and lower w/c ratio (Bullard et al., 2011).

3.5 Compressive strength

The term of compressive strength refers to the maximum load that a material can carry until its failure. The compressive strength of the mortars is their most important property because it is directly related to almost all other properties, such as the modulus of elasticity, permeability, resistance to environmental effects etc.

3.3.1 Factors affecting compressive strength

The most determinant factor for compressive strength is water/cement ratio associated with porosity. Direct and accurate determination of porosity in the mortar phases is difficult for practical applications. There are individual factors that affect the compressive strength of mortars. These factors are related to the proportions of components, the conditions of hydration and maturation, and the way of experimental tests to determine strength. In the context of this dissertation, the factors related to characteristics and the proportions of the materials will be developed.

Water to cement ratio

The significant effect of the water to cement ratio on the compressive strength of the mortar is described by “Abrams law”,

$$F_c = \frac{k_1}{k_2^{w/c}}$$

Where: k_1 , k_2 are empirical constants. The typical curves described in this relation are given in Figure 3.1.

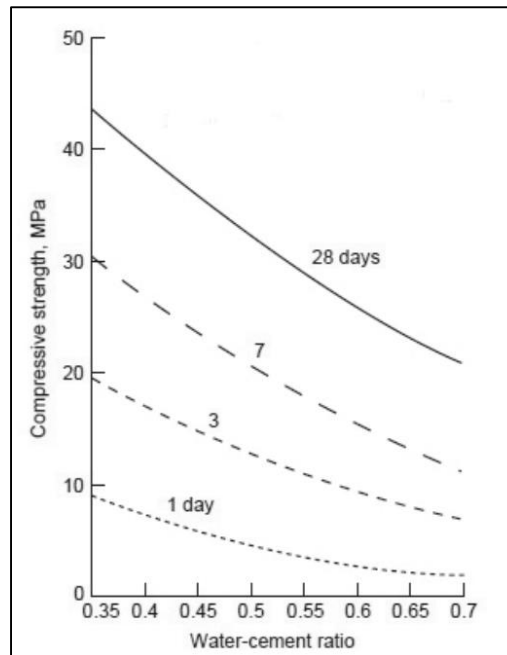


Figure 3.2: Effect of water to cement ratio on compressive strength (<http://www.omafra.gov.on.ca>)

The increase in the w/c ratio causes an increase in the porosity and consequently a reduction in the strength of the cement paste, while at the same time, reduces the resistance of the transition zone, mainly due to the increase of the size of $\text{Ca}(\text{OH})_2$ crystals.

Entrapped air

The presence of air voids in the mortar structure is due to either deficient condensation or the use of airborne additives that create bubbles in the paste. For a certain w/c, the trapped air generally reduces the strength of the mortar.

Aggregates

It is true that the type of aggregates used in the common mortars do not particularly affect the final strength, as the aggregates themselves are characterized by strengths clearly larger than the cement paste and the transition zone. However, some of the characteristics of aggregates, such as grain shape, surface texture, granulometric grading and their mineral composition may affect the strength of the mortar either indirectly by altering the water/cement requirements or directly by affecting the transition zone characteristics (Fic et al., 2018). For the same cement content and workability, mortars with larger aggregates have reduced water requirements but they are also characterized by weaker transition zones with intense microcracks. These two factors modify the final compressive strength according to the water/cement ratio. For small water/cement ratio, increasing the size of the grains has a great impact on the strength since the already reduced porosity of the transition zone plays an important role in the strength of the mortar. Also, for constant water/cement ratio and the maximum aggregate grain, the change in the granulometric gradient results in changes of mortars workability due to increased fluidity and, consequently, strength decreases (Braga et al., 2012).

Mixing water

The quality of mixing water considered of low significance for its durability. However, some harmful substances can adversely affect its strength. Water containing industrial or urban waste water should be avoided. Water with traces of sugars pauses the hydration, and water with acids binds the necessary CaO of setting process. Additionally, water with traces of oils prevents adhesion between aggregates and cement. Salty or brackish water contains chlorides or sulphates that bring about slightly higher early strengths, but reduce the final strength by 15-20% (Triantafillou, 2017).

Chemical admixtures and additives

The quality of mixing water is considered of low significance for its durability. However, some harmful substances can adversely affect its strength. Water containing industrial or urban waste water should be avoided. Water with traces of sugars stops hydration, and water with acids binds the necessary CaO of the setting process. Additionally, water with traces of oils prevents adhesion between aggregates and cement. Salty or brackish water contains chlorides or sulphates that bring about slightly higher early strengths, but reduce the final strength by 15-20% (Triantafillou, 2017).

3.6 Mineral additives

The use of admixtures aims to change specific properties, mechanical and physical, of mortars and concrete. The desired change is not possible to be obtained by modifying the composition or proportions of normal mix, so the use of inert or reactive material as admixture is proposed. Mineral additives are considered promising components in mortar and concrete production, since they can improve density, compressive strength and durability of the construction material (Nagroćkienė et al., 2017).

Mineral additives, such as silicate materials, zeolites, micro dust etc. in powder form, are often used either as admixtures for the cement production or as additives when mixing the components of the mortar or concrete. The main objective of their use is to reduce costs and improve certain properties of the mortar, developing new building materials (high performance concrete, special concrete etc.). Such materials may be natural, used after relatively simple processing of raw materials (e.g., pulverization), or industrial by-products which may be treated prior to use. One of the most common industrial by-products used as a cement additive is silica fume. Mineral additives that react with cement (i.e. fly ash, silica fume, blast furnace slag) modify Portland cement hydration kinetics, especially in early ages, in a complicated way because they affect both chemical and mineralogical composition of mortars (Deboucha et al., 2017).

3.6.1 Pore fillers

Several materials of powder form are suitable for application as pore fillers in cement mortars and concrete production. Pore fillers aim to improve cohesiveness of concrete, resulting in a material which has better resistance characteristics concerning concrete bleeding. Raw materials such as lime, calcium oxide, diatomaceous earth, kaolin etc., are traditionally used as

pore fillers. Additionally, more reactive materials such as fly ash and blast furnace slag may also be used as pore fillers, since they also provide advantageous properties in cement hydration process (Murdock et al., 1979).

Pore fillers related to filler effect are classified mainly according to their particle size. The density of cement with filler mixture depends on fillers granulometry. If the particle size of pore filler is lower than the one of Portland cement, the desirable incorporation of materials is achieved in order to fill the voids between cement particles (Wang et al., 2018). The improvement of particle size distribution in the paste decreases porosity and water requirement, and leads to the increase of compressive strength and mortar durability (Cyr et al., 2006). In spite of the fact that pore fillers offer advantageous characteristics in void filling and compressive strength, it should be noted that they also reduce paste flowability if the specific surface area of the particles is high.

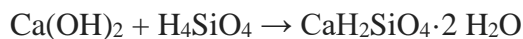
3.6.2 Pozzolan

Pozzolan is defined as “*a siliceous and aluminous material which, in itself, possesses little or no cementitious value but which will, in finely divided form in the presence of moisture, react chemically with calcium hydroxide at ordinary temperature to form compounds possessing cementitious properties*” (ASTM C125, 2007). The name pozzolan declares its use by the Romans since antiquity as a raw material. Pozzolan was applied in concrete as part of the binder even earlier. It is believed that one of the primal constructions with pozzolanic concrete can be found in Mesoamerica over the period 1100-850 BC (Rivera Villarreal & Krayner, 1996) and in Kameiros, the ancient city of Rhodes Island, Greece, in ca. 500 BC (Davidovits, 1987).

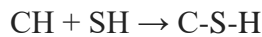
Pozzolans as raw materials can be natural, artificial or industrial by-products. Natural pozzolans should only be pulverized before use. Artificial pozzolans derive from chemical or industrial processes, and initially, they are characterized by low or no pozzolanic properties (Hewlett, 2003). Their reactivity and compatibility with cement depends on their particle size distribution, mineralogical structure and composition. When effective use of the pozzolans is achieved, the produced mortar or concrete has advantageous characteristics concerning compressive strength, durability, shrinkage and cracking.

Natural pozzolans are mainly natural minerals or materials of volcanic origin. Natural pozzolans either occur naturally (i.e. zeolite, volcanic ashes) in pure form or are obtained after calcination (i.e. metakaolin, expanded shale). The criteria of natural pozzolan reactivity are mainly the alkali content and silica to alumina ratio (Barger et al., 2001). Even in natural pozzolans, pre-treatment such as pulverization, is required in order to obtain the optimal surface area of the material particles. Pozzolanic properties of clay minerals are achieved after calcination at high temperatures (600-900 °C), and their use in the construction sector is established in hydraulic mortars. Calcination of these hydrous minerals leads to their structural amorphization, because of the loss of water molecules, while anhydrous minerals (i.e. quartz) are not subjected to any transformation due to thermal treatment. The former crystalline network of clay minerals is destroyed and replaced by silica and alumina of high reactivity.

The use of pozzolanic materials, both natural and artificial, as a replacement for Portland cement is extensive in mortars and concrete production. These fine powders, which are compositionally characterized as amorphous silica rich materials, react with calcium hydroxide ($\text{Ca}(\text{OH})_2$), in the presence of water. Hydration of pozzolanic materials is accelerated in a basic environment, $\text{pH} > 12$ when containing calcium and/or alkali ions. Products of solid hydration are incorporated with calcium and alkalis forming strong bonds of C-A-S-H hydrates (Gartner et al., 2011) responsible for cement strength. Furthermore, amorphous alumina is often found in pozzolanic materials composition, which is characterized by high reactivity and it is responsible for aluminosilicates formation in cement paste (Paiva et al., 2017). This is the result of the pozzolanic reaction. Considering a silicate material to be pozzolan, the chemical reaction occurs between calcium hydroxide and silicates as following:



Which abbreviated as:



Pozzolanic materials due to their fineness act as fillers between the voids of cement and capillary voids, achieving decrease of paste porosity. Additionally, they offer advantageous characteristics since they decrease the voids of interfacial transition zone between cement particles and aggregates. This reduction of porosity and increase of cohesion lead to increase of the van der Waals forces between the particles and, consequently, they positively affect compressive strength.

3.6.3 Silica Fume

Silica fume, also known as microsilica, is a fine powder of amorphous silicon dioxide. It is a by-product of silicon metal and ferrosilicon alloy production. This process takes place in electric arc furnace at temperatures up to 2000 °C. The fumes generated contain spherical microparticles of amorphous silicon dioxide, and are condensed into microspheres of amorphous silica in the upper parts of furnace. It is called silica fume due to its form and chemical composition (Hewlett, 2003). The fumes are selected from the furnace by fans, separated from larger fractions (i.e. wood, carbon etc.) and then collected after filtration (Figure 3.2). During cooling, the fumes are condensed in small particles of microsilica and are about 50 to 100 times finer than cement particles. It is estimated that microsilica production worldwide is up to 1.5 million tons per year (Sakulich 2011; Sanjuan et al., 2015).

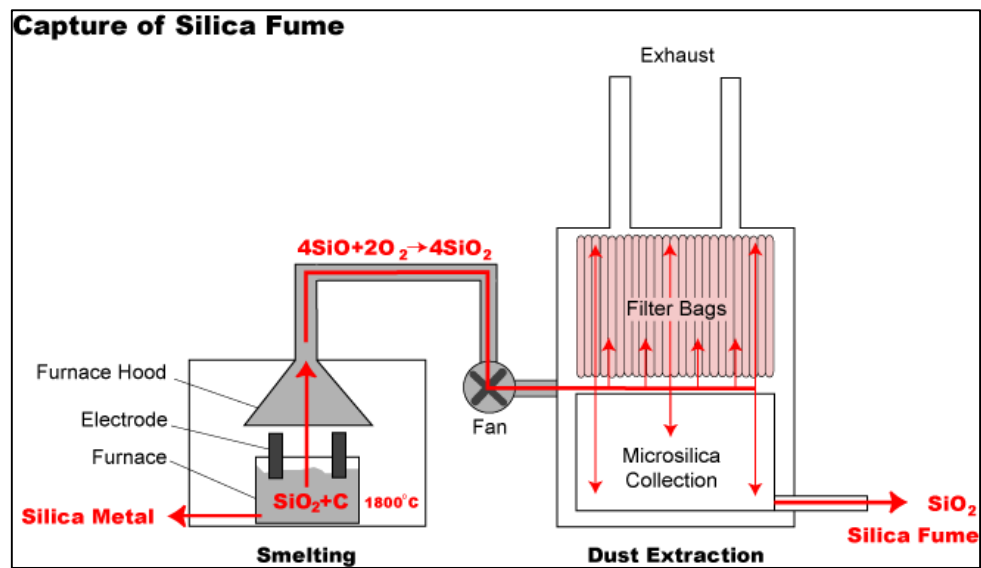


Figure 3.3: Diagram of silica fume production process (www.bulkmaterialsinternational.net)

Microsilica composition and morphology are characterized by high silica content ($\text{SiO}_2 > 85\%$ wt.), fine particle size, high specific area ($15000\text{--}25000\text{ m}^2/\text{kg}$) and amorphous structure. Microsilica addition to Portland cement has proved to be advantageous in microstructure, physical and chemical characteristics of hardened pastes, improving:

1. mechanical strength: compressive, tensile and flexural strength and modulus of elasticity,
2. durability: weathering resistance, low permeability, sulphate resistance, resistance to chemical attack, lower shrinkage, seawater resistance etc.,

when added in optimal amounts (Sanjuan et al., 2015). Besides additive proportions in cement paste, other important factors that determine the properties of mortars are the fineness of the material and the solubility of SiO_2 . Probably, the effect of soluble SiO_2 is more important than particle fineness, since it is responsible for the formation of C-S-H gel. Silica fume acts both as micro-filler between cement particles and as pozzolanic material (Liu & Wang, 2017). High solubility of silica fume renders it capable of consuming a considerable amount of calcium hydroxide, improving pore structure and interfacial transition zone of hardened cement paste (Zhang et al., 2016). Nevertheless, microsilica is likely to form agglomerates during cement mixing. These larger particles cannot act as fillers anymore and their pozzolanic reactivity is extremely lower, provoking negative effects on the final cement product (Yajun et al., 2003).

Chapter IV: Materials and methods

Abstract

This section presents the materials used in the thesis and describes their preparation. Thereafter, the experimental setups that performed, the analytic techniques, the methods and procedures that followed are presented in detailed.

4. Materials and methods

4.1 Experimental setup of Asbestos Containing Waste treatment

4.1.1 Materials

4.1.1.1 Asbestos cement

Asbestos cement waste (ACW) was collected from demolition waste from the building of “Old General Hospital of Chania”, built in 1905 and demolished in 2013. The samples were corrugated sheets of roof that had been exposed to weathering for more than a century. The “Toxic and Hazardous Waste Management Laboratory” supplied the ACW samples in the course of national project entitled: “Dismantling of asbestos containing materials in the building of Old General Hospital of Chania – Performing measurements”, funded by municipality of Chania.

Prior to treatment, samples were dried at 105 °C for 24 hours in laboratory oven (INNOVENS - Thermo Fisher Scientific). Then, ACW was pulverized using a high-speed cutting mill of solid samples (Universal Cutting Mill Pulverisette 19, FRITSCH), which was connected to a cyclone, using protective equipment. The particle size of ACW after grinding was < 0.5 mm. The samples were pulverized using acetone and industrial vacuum to prevent fibers diffusion. The whole experimental procedure was conducted into a glove box in order to ensure the health protection of researchers.

4.1.1.2 Reagents

In this current dissertation it was studied the effect of acidic and alkaline reagents in the structure of ACW. The experimental procedure was conducted using oxalic acid dihydrate ($\text{H}_2\text{C}_2\text{O}_4 \cdot 2\text{H}_2\text{O}$), tetraethoxysilane (TEOS) ($\text{SiH}_2\text{O}_2\text{C}_2\text{H}_5$), isopropanol (ISP) ($\text{C}_3\text{H}_8\text{O}$) and potassium silicate (WG) (K_2SiO_3). The reagents were purchased by Sigma–Aldrich (Germany). Distilled H_2O was used in all experimental parts.

4.1.2 Experimental design: Chemical treatment process

4.1.2.1 Treatment with oxalic acid

Aqueous solutions of different oxalic acid concentrations (Table 4.1) were mixed with ACW in order to be investigated the effect of oxalic acid in asbestos fibers in the presence of cement, and to be determined the required efficient concentration to transform ACW.

Table 4.5: Syntheses of the treatments with oxalic acid

Sample	Concentration (M)	ACW/Ox (w/w)	Temperature (°C)
OxL	0.1	1/0.3	27
OxM	0.15	1/0.5	27
OxH	0.3	1/1	27

4.1.2.2 Treatment with oxalic acid-TEOS

This treatment was conducted in two steps. Firstly, ACW was dispersed in a solution of oxalic acid 0.3 M, and afterwards it was added in the mixture a solution of TEOS in ISP (Table 4.2). The selection of this procedure was intended the embodiment of treated ACW into a silica

polymer. The pH value of the solution was measured equal to 1.9. The molar ratio was ACW/Oxac/TEOS = 1/6/47. The experiment was carried out at room temperature ($T = 27\text{ }^{\circ}\text{C}$).

4.1.2.3 Treatment with oxalic acid-sodium silicate

The experimental procedure of this treatment was similar to the previous one. Firstly, it was prepared a solution of oxalic acid 0.3 M with ACW under stirring. Then aquatic solution of WG 6% w/w was added. The pH value of the solution was 1.78.



Figure 4. 4: Chemical treatment of ACW

4.1.2.4 Treatment under microwave irradiation

Microwave treatment consisted of irradiation at 2.45 GHz in a MARS 6 Microwave Reactor System by CEM Corporation. Briefly 100 mg of ACW were diluted in 10 ml of mixed solution of oxalic acid 0.3 M and TEOS (solution ratio of 9 to 1, respectively), and then heated at $150\text{ }^{\circ}\text{C}$. The sample was exposure to microwave radiation at this temperature for 20 min. Temperature detection was performed real time via a fiber optic temperature sensor (MTS 300 High Temperature Probe, CEM).

Table 4.6: Syntheses of combined treatments

Samples	Oxalic acid concentration (M)	Mass ratio (w/w)	pH
STG/ STF	0.3	AC/Ox/TEOS/ISP 1/1.5/20/17	1.9
SWG	0.3	ACW/Ox/WG 1/1.6/1.6	1.78
MW	0.1	ACW/Ox/TEOS 1/0.3/10	1.4

4.1.3 Characterization of materials- Analytical techniques

Treated and untreated materials were characterized through analytical techniques such as X-Ray Fluorescence (XRF), Fourier Transform Infrared Spectroscopy (FTIR), X-ray Diffraction (XRD), Thermogravimetric analysis (TG), stereo zoom microscopy.

4.1.3.1 X-Ray Fluorescence (XRF)

Chemical composition of samples in the form of oxides was determined using an X-ray fluorescence energy dispersive spectrometer (XRF-EDS) Bruker-AXS S2Range type. Loss on ignition (LOI) was determined by heating the material at 1050 °C for 4 h. Glass beads preparation were carried out by mixing 3 g of each sample with 8 g of flux (Li-tetraborate) and fused at 1100 °C.

4.1.3.2 X-Ray Diffraction (XRD)

Identification of mineralogical composition of AC samples was recorded with Ni-filtered CuK α radiation (35 kV 35 mA) and a Bruker Lynx Eye strip silicon detector while the generator was operated at 35 kV and 35 mA. Data were collected from 4° to 70° 2 θ with a step size of 0.05° and a time of 200 s per strip step. These specific conditions were chosen to obtain more accurate results in quantitative amorphous and the calculation of crystalline phases. In order to include the Roentgen-amorphous in the quantitative phase analysis a crystalline internal standard (corundum) was added (16 %wt.) to the samples. The homogenization was performed manually in the presence of acetone as a milling agent. The X-ray powder data was used for quantitative estimation of the minerals phases. Firstly, phases were determined with the DiffracPlus EVA software (Bruker), and subsequently quantitative phase analysis was carried out by the Rietveld method, using the RayflexAutoquan software (Thomaidis & Kostakis, 2015).

4.1.3.3 Fourier transform infrared spectroscopy (FTIR)

FTIR analysis was carried out on KBr pellets with a PerkinElmer 1000 spectrometer, in the spectra range of 400-4000 cm⁻¹. Prior to FTIR analysis samples were dried at 105 °C for 24 h. For the production of the pellets each sample was mixed with KBr at a ratio 1:100 w/w. The mixture was grinded for 2 min. The samples pressurized in 10–14 tones for 3 min, in a sample holder with diameter of 1.2 cm. Spectra were obtained at different stages, during the experimental procedure. Measurements consisted of 20 scans and each sample was mixed and measured 3 times.

4.1.3.4 Thermogravimetric analysis (TG)

Thermal behavior of samples was investigated using a Setaram LabSysEvo 1600 at a heating rate of 10 °C/min under nitrogen atmosphere from 27 to 650 °C. The measurements were carried out in alumina cubicles in an inert N₂ gas flow of 60 ml/min. TG/DTG analysis was used to determine the phases of raw asbestos cement waste and the obtained byproducts of proposed treatments.

4.2 Investigation of pozzolanic activity of treated materials

4.2.1 Materials

Physical and chemical properties of the materials that used to investigate pozzolanic activity are given below. The choice of the materials is based on European standards requirements and local market availability.

4.2.1.1 Cement

Two types of cement were used for the production of specimens, Ordinary Portland cement CEMI (42.5N, Finomix) and Portland-limestone cement CEMII/A-LL (42.5N, TITAN) according EN 197-1. Chemical composition and physical properties of the cements are listed in Table 4.3 and in Table 4.4 is presented the composition of cement compounds that were estimated according to Bogue's calculation.

According EN 197-1 the CEMI 42.5N is a cement that consist of clinker content equal or higher than 95% and around 5% of minor additional constituents. CEMII/A-LL 42.5N consists of approximately 85% of clinker, 10% of limestone and 5% of minor additional components. Mineralogical composition of clinker phase of CEMI and CEMII/A-LL determined by Bogue calculation (Table 4.4). Bogue calculation is used to calculate an estimation of the four main clinker minerals of Portland cement: alite (C_3S), belite (C_2S), aluminate phase (C_3A) and ferrite phase (C_4AF). According ASTM C150, mineral components are calculated through a set of equations based on the chemical compositions in form of oxides (%), establishing the relationship between oxides and crystalline phases of cement clinker. Minor components of cement are not included in this calculation. The equations that provide mineralogical composition are (Bogue, 1929):

- $C_3S = (4.071 \cdot \%CaO) - (7.6024 \cdot \%SiO_2) - (1.4297 \cdot \%Fe_2O_3) - (6.7187 \cdot \%Al_2O_3)$
- $C_2S = (8.6024 \cdot \%SiO_2) + (1.0785 \cdot \%Fe_2O_3) + (5.0683 \cdot \%Al_2O_3) - (3.0710 \cdot \%CaO)$
- $C_3A = (2.6504 \cdot \%Al_2O_3) - (1.6920 \cdot \%Fe_2O_3)$
- $C_4AF = (3.043 \cdot \%Fe_2O_3)$

4.2.1.2 Silica Fume

Densified silica fume (SF) is classified as pozzolanic material, according American Concrete Institute (Committee 226). Commercial SF (SF 920D, Topkon), from ferrosilicon alloy production line is certified according ASTM C1240. Its high content of silicon dioxide (SiO_2 86.8%) and specific surface area ($18.800 \text{ m}^2/\text{kg}$) are responsible for pozzolanic reactivity of the material. Chemical composition and some physical properties are illustrated in Table 4.3. SF is employed as reference pozzolanic material.

4.2.1.3 Sand

Standard sand (standardized by SNL according EN 196-1) is used as aggregate. Particle size distribution is varied in accordance with EN 196-1 (grain size 0.08-2 mm). The physical characteristics are as follows: relative specific density 2617 kg/m^3 and water absorption 0.67%.

Table 4.7: Chemical composition and physical properties of the co-binders

Oxides	CEMI	CEMII/A-LL	SF (densified)
SiO ₂	21.2	18.7	86.8
CaO	61.3	66.7	-
MgO	1.8	1.9	-
Na ₂ O	0.2	0.1	1.2
Fe ₂ O ₃	2.4	1.1	-
Al ₂ O ₃	5.1	4.2	-
LOI	6.9	7.1	3.1
Total	98.9	99.8	91.1
Particle size (µm)	35	42	200
Bulk density(g/m ³)	-	-	654
Specific surface area(m ² /g)	-	-	18.8
Blaine (cm ² /g)	3454	-	-

Table 4.8: Mineralogical composition determined by Bogue calculation (%)

Clinker minerals	CEMI	CEMII/A-LL
C ₃ S	50.68	58.86
C ₂ S	22.55	9.21
C ₃ A	9.45	9.27
C ₄ AF	7.30	3.34

4.2.2 Pozzolanic reactivity determination

Pozzolanic reaction is the interaction of the vitreous phase of pozzolanic materials with calcium ions in a strong alkaline solution, in presence of cement. Pozzolans are characterized by their degree of reactivity, that it is expressed through calcium consumption. Parameters that affect reactivity of the pozzolanic materials investigated in this dissertation. Specifically, they are the composition of Portland cement, the composition of pozzolan itself, the particle size distribution and specific surface area of the grains, and the ratio cement/pozzolan of mortars mixtures.

4.2.2.1 Direct determination of calcium consumption (Chapelle test)

The pozzolanic activity of AP and SF is investigated based on an accelerated method that determines lime-pozzolan reaction. Considering lime consumption as indicator of pozzolanic reactivity, it is followed Chapelle test (NF P 18-513) that quantifies the pozzolanic reaction measuring Ca(OH)₂ reduction in presence of pozzolans. Solutions of CaO (blank) and CaO with studied material mixed in 250 ml of distilled water and are placed in bath at 90 °C for 16 hours. After bath, a saccharose solution (240 g/L) of same volume is added in each mixture in order to dissolve the remain Ca(OH)₂. It is followed filtration of the solution and then it was titrated with 0.1M HCl. Titration result is referred in mg of CaO that is reacted per gram of pozzolan (Table 4.5). For solutions of 2 g CaO and 1 g of pozzolan, CaO consumption is calculated according the equation (Quarcioni et al, 2015):

$$mgCaO = \frac{28x(v_2 \times m_2 - v_1) \times F_c \times 2 \times 2}{m_3 \times m_2 \times m_1},$$

m_1 = grams of pozzolanic material;
 m_2 = grams of CaO mixed with pozzolanic material;
 m_3 = grams of CaO in the blank test;
 v_1 = milliliters of HCl 0.1 M consumed by the sample solution;
 v_2 = milliliters of HCl 0.1 M consumed by the blank solution;
 F_c = correction factor of HCl 0.1 M standard solution.

Table 4.9: Sequential procedure of Chapelle test

Step	Fraction	Reagents	Mixing time and temperature
1 st	Pozzolan reaction	2 g CaO, 1 g Pozzolan	16 h at 90 °C
2 nd	Dissolution of remain Ca(OH) ₂	Sacharrose solution (240g/L)	15 min at 27 °C
3 rd	Filtration	-	-
4 th	Titration	HCl 0.1M, Phenolphthalein indicator	-

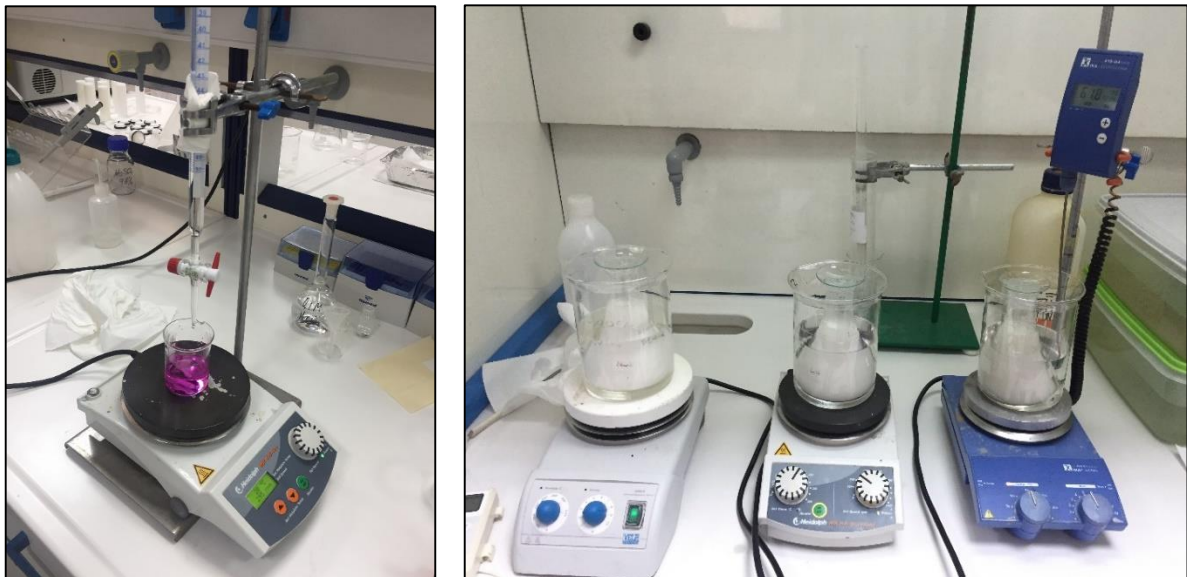


Figure 4.5: Apparatus of Chapelle test

4.2.2.2 Particle size distribution and specific surface area

Particle size distribution and grain size of the materials were determined in an aqueous suspension by a laser particle size analyzer (Malvern Instruments, Mastersize-S).

Specific surface area of the samples was determined via Brunauer – Emmet- Teller (BET) method. The samples, firstly, were heated for 12 hours at 250 °C, heating rate at 5 °C/minute under continuous N₂ gas flow. Measurements were carried out using N₂ as an adsorbate.

4.2.2.3 Effect of treated material as admixture in cement mortars

Preparation of the pastes

The preparation of cement pastes is very important to obtain comparable results of different syntheses. The mixing procedure of all cement mortars was conducted using a mortar mixer (Alfa C-050). The mixer has a 5 L blender and two mixing speeds: 140 and 285 rpm. The cement mortars were prepared according the demands of EN 196-1.

- Dry cement and admixture were mixed manually for 10 sec.
- Water and powders were mixed for 30 sec at 14 rpm.
- The sand was added in the paste over a 30 sec period at slow mixing speed.
- The paste was mixed for 30 sec at high speed 285 rpm.
- The mixing procedure was paused for 90 sec.
- The mixture was mixed for another 60 sec at high speed.

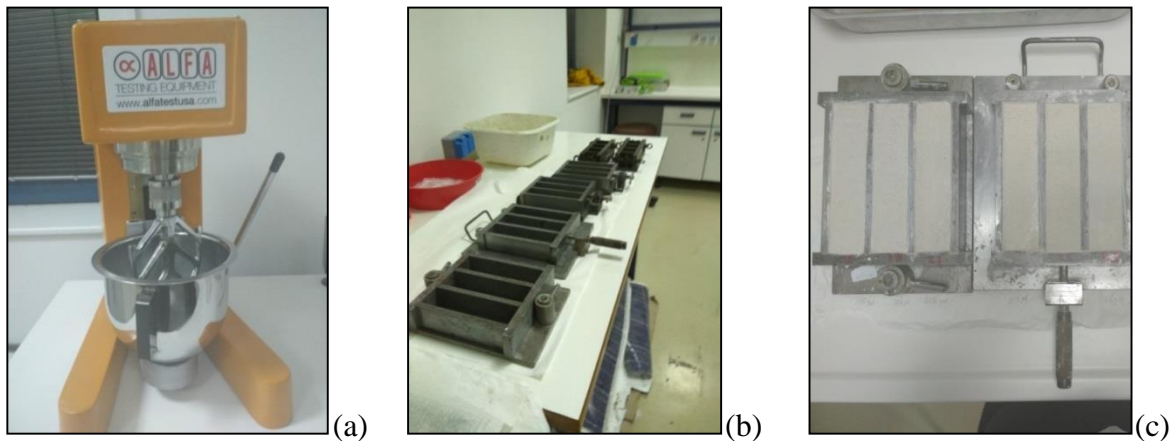


Figure 4.6: (a) mortar mixer, (b) steels moulds and (c) cast of mortars

Two cement types were studied. For each one of them (CEMI, CEMII/A-LL) it was prepared a control paste with no pozzolan addition. All specimens were produced at constant water to cement ratio (w/c) 0.48 and sand to cement ratio (s/c) at 2.75. The mixtures proportions are presented in Table 4.6.

Table 4.10: Mixture proportions of studied specimens

Mix name	Amount by weight in mix (g)			
	Cement	Admixture	Water	Sand
Control	333	-	161	916
1.5%	328	5	161	916
2.5%	325	8.3	161	916
4%	320	13.3	161	916
5%	316	16	161	916

4.2.2.4 $\text{Ca}(\text{OH})_2$ consumption in hydrated pastes – TG

The rate of reacted $\text{Ca}(\text{OH})_2$ indicates the reactivity of pozzolans in cement pastes. The mortars were investigated at 90 days of curing using thermogravimetric analysis in a nitrogen atmosphere with heating rate of 10 °C/min from 27 to 900 °C and N_2 gas flow of 60 ml/min.

These measurements were carried out in order to investigate the Ca(OH)_2 consumption in time and to determine the pozzolanic reaction products. Ca(OH)_2 content was determined according to the method developed by Kim & Olek (2012). Calcium silicate hydrate (CSH) and Ca(OH)_2 and decompositions were calculated by weight loss at temperature range 27-400 °C and 400-500 °C respectively.

4.2.3 Properties of the mortars

The ultrasound pulse velocity, the compressive strength and water absorption of hardened mortar samples were determined according to BS 1881-203, EN 196-1 and BS 1881-122 respectively. Additionally, porosity of the materials via both vacuum saturation porosity and mercury intrusion porosimetry was calculated.

4.2.3.1 Non-destructive evaluation of mortars using Ultrasonic Pulse Velocity

Ultrasonic pulse velocity (UPV) is one of the most popular non-destructive methods used in the evaluation of quality and properties of mortars and concrete specimens. When a surface of a solid is excited by a mechanical force varied with time, energy is given by the source as three types of elastic waves. The wave that crosses first the solid is called compression or P-wave. P-wave is the one that has particle displacements in the direction of travel, and its velocity (V_p) is a function of the dynamic of Young's modulus (E), Poisson's ratio (ν) and density (ρ) (Lawson et al., 2011), as presented in the following equation:

$$V_p = \sqrt{\frac{E(1-\nu)}{\rho(1+\nu)(1-2\nu)}} \quad (\text{m/s})$$

According to the equation, it is obvious that velocity depends on elastic properties of the studied specimens, and the geometry of the material is irrelevant parameter. Thus, higher velocity of the pulse derives from higher quality of the mortar specimen in terms of density, homogeneity and uniformity (Lawson et al., 2011).

According to the principles of standard method BS 1881: Part 203 (BS 1881, 1986) the velocity was calculated as

$$V = \frac{L}{T} \quad (\text{m/s}),$$

L= length of specimen (m) and T= time of wave travel (s). UPV measurements were conducted in all mortar specimens at an age of 2, 7, 14, and 28 days. Pulse velocity detects flaws on mortars, due to experimental errors, and facilitates the discard of certain measurements. The quality of mortars is classified as listed in Table 4.7.

Table 4.11: Quality of mortars as a function of UPV (BS 1881, 1983)

UPV (m/sec)	Mortar quality
Above 4500	Excellent
3500-4500	Good
3000-3500	Medium
Below 3000	Doubtful

4.2.3.2 Strength activity index

Strength activity index (SAI) is an indicator of long-term pozzolanic activity of a material, according to EN 450-1 (2012). Specimens of cement mortar were produced according to EN 196 - 1 (2005). The specimens were casted in prismatic moulds (40x40x160 mm), demoulded after 24 hours and kept in a curing chamber (E139, MATEST) with stable conditions at 27-30 °C and relative humidity of 90%, for 28 days. For each mixture three specimens were tested for compressive strength, and the mean value was used for the calculation of SAI, according to the equation:

$$SAI = \frac{A}{B} \times 100,$$

Where, A is the compressive strength (MPa) of pozzolan mortar and B the compressive strength (MPa) of control mortar.

4.2.3.3 Compressive strength

The pastes were casted in prismatic steel moulds 4x4x16 cm³. Moulds were vibrated for a few minutes to reduce the presence of air voids within the paste and then were remained at room temperature for 24 hours (Figure 4.2). Specimens were then demoulded and kept in curing chamber (E139, MATEST) with stable conditions at 27-30 °C and humidity 90%. The specimens were remained under these conditions for an ageing period up to 90 days. The compressive and flexural strength of specimens were measured using a Matest type compression and flexural machine with dual range 500/15 kN. Measurements were carried out in triplicate.

4.2.3.4 Water absorption

Water absorption was measured in accordance with standard method BS 1881-122 (2011). Specimens were dried in laboratory oven at 105 °C ± 5 °C for 72 hours. Specimens were removed from the oven and were remained in room temperature for 24 hours. After cooling the specimens were weighted (dry mass). Then, they were immersed in a water tank and when removed, the excess water of the surface was wiped. Water absorption was calculated as the increase of the specimen's mass after immersion as percentage of the dry mass.

4.2.3.5 Vacuum saturation porosity

Vacuum saturation method was used to calculate the total porosity of the specimens. Vacuum saturation apparatus was used after drying the sample at 105 °C ± 5 °C up to a constant mass. The samples, after cooling were placed in the apparatus of a tank connected with a vacuum

pump. The tank was evacuated for 2 hours by pumping and afterwards it was filled with water up to cover the specimens. The specimens were remained to soak for 24 hours. Porosity was calculated as follows:

$$\text{Porosity} = \frac{m_{sat} - m_{dry}}{m_{sat} - m_{soak}} \times 100$$

4.2.3.6 Mercury Intrusion Porosimetry (MIP)

Mercury intrusion porosimetry is a validate technique measuring the porosity (%) and pore size distribution of cement mortars. Selected specimens were measured using a Micromeritics AutoPore 9400 porosimeter (Mercury Intrusion Porosimetry (MIP)).

Chapter V: Effect of the reagents on raw asbestos fibers

Abstract

The present chapter investigates potential detoxification of raw chrysotile asbestos by following an acid leaching treatment with oxalic acid dihydrate ($\text{H}_2\text{C}_2\text{O}_4 \cdot 2\text{H}_2\text{O}$). Oxalic acid was chosen due to its low environmental impact (or toxicity) and cost. It is demonstrated the effectiveness of different concentrations of oxalic acid as proposed formulations. Therefore, it is studied a combined treatment of oxalic acid dihydrate with silicates, tetraethoxysilane (TEOS) ($\text{SiH}_2\text{O}_8\text{C}_8\text{O}_4$) and potassium silicate (K_2SiO_3). These reagents used in the experimental procedure, do not cause adverse effects on the environment and are cost effective.

The results of FTIR, XRD and scanning microscopy coupled with EDS analyses indicated that the reagents are able to destruct chrysotile structure and it is yielded silica of amorphous phase and the biomaterial glushinskite from the oxalic acid reacted with brucite [$\text{Mg}(\text{OH})_2$] layer.

Oxalic acid with the external brucite (Brc) ($\text{Mg}(\text{OH})_2$) layer surface of Chrysotile. Oxalic acid 0.05 M was selected as the optimal concentration for an eight-day treatment for the detoxification. Each of the proposed combined formulations can be applied for the detoxification of asbestos, according to priorities related to the specific products of the recovery treatment. Therefore, oxalic acid leaching followed by the TEOS addition is preferred in cases of glushinskite recovery; TEOS treatment of asbestos with subsequent oxalic acid addition produced amorphous silica production; finally, oxalic acid leaching followed by potassium silicate encapsulated the asbestos fibers.

5. Effect of the reagents on raw asbestos fibers.

5.1 Selection of the materials

An earlier research has reported the use of sulfuric acid with a direct attack on asbestos to convert the latter into a non-toxic material (Rozalen & Huertas, 2013). This research revealed the decomposition of asbestos when reacting with acids, such as sulphuric acid or in the aqueous solution of ammonium sulfate. Asbestos is usually treated by heating, mixing, cutting and stirring in acid conditions. Although since strong acids can be used to detoxify the asbestos fibers, they are still considered even more hazardous than chrysotile asbestos (Anastasiadou et al., 2010).

On the other hand, weak organic acids, such as acetic and lactic acid, have also been used to convert asbestos-containing materials into non-toxic (Koshi & Sakabe, 1972). Rozalen and Huertas (2013) investigated the mechanism of chrysotile modification using different acids at pH 1. Furthermore, the use of polycarboxylic acids, such as oxalic acid, is considered advantageous due to its capability of converting asbestos into non-toxic materials, with or without adding alkali (Turci et al., 2008). The oxalic acid leaching of chrysotile can be achieved by a reaction between brucite and oxalic acid. As a result, the magnesium hydroxide of brucite sheet is decomposed. Oxalic acid is a moderate organic acid, in terms of acidity and toxicity. It is a cost efficient choice of a reagent since it is a byproduct of chemical industry. Additionally, it is found in soils and lichens. Therefore, in accordance to environmental requirements both reuse of waste and cost effective detoxification treatment are achieved. It has been demonstrated in literature that when lichens contact with chrysotile, the detoxification of fibers is achieved (Favero-Longo et al., 2005, Kapridaki et al., 2014).

In the present study, weak organic acid, the oxalic acid, was used in order to detoxify chrysotile. The main objective was to identify the optimal conditions of chrysotile transformation. Experiments conducted in laboratory scale investigated the Oxalic acid's effect on different concentrations of chrysotile, and the required time of optimum treatment. Based on this study, the optimum composition and time of treatment were selected.

Afterwards, acid treatment using oxalic acid combined with reagents promoted a silylation process, such as pure water glass (WG) and TEOS, has been investigated. The oxalic acid-leaching can transform the natural polymer of chrysotile, by removing the Mg sheet, to an excellent source of SiO₂. The silylation of chrysotile is a simple process and once implemented correctly, a silicon polymer is obtained (Habaue et al., 2008). Its properties are enhanced compared to the corresponding synthetic silica gel (Habaue et al., 2008, Fonseca et al., 2001). The addition of TEOS in an acid solution of oxalic acid leads, through the silylation process, to a sol-gel material. The WG addition in the same solution leads to the encapsulation and transformation of fibers into a resinous coating. Therefore, in this combined treatment method, where the oxalic acid assisted in the transformation of fibers, which were subsequently embedded into the silica network created either by TEOS or pure WG through the silylation process. Furthermore, WG creates a type of vitrification on the top of the material which prevents the diffusion of the fibers.

5.2 Results of preliminary experimental investigation

5.2.1 The effect of different concentrations oxalic acid aquatic solution on fibers of chrysotile

Figure 5.1 illustrates the XRD diffractograms of chrysotile samples after 10 days of treatment with oxalic acid in different concentrations. For comparisons reasons an untreated chrysotile sample was also analyzed by XRD. As shown in Figure 5.1a, the diffractogram of the untreated sample exhibited two peaks which are characteristics of chrysotile. In the diffractograms of chrysotile samples treated with 0.1 M and 0.05 M oxalic acid solution, these two reflections almost disappeared after 10 days of treatment, while at the same time, new reflections were observed. More specifically, the two neo-formed peaks correspond to magnesium oxalate which was produced by the reaction of the external sheet of chrysotile with the oxalic acid (Lakshmi et al., 2014). Despite the formation of magnesium oxalate, one more new-formed material was also identified. The peak noticed at 2θ 38.5° corresponds to forsterite (Mg_2SiO_4), a product mainly formed upon recrystallization of the heat treated chrysotile (Gulumian, 2005).

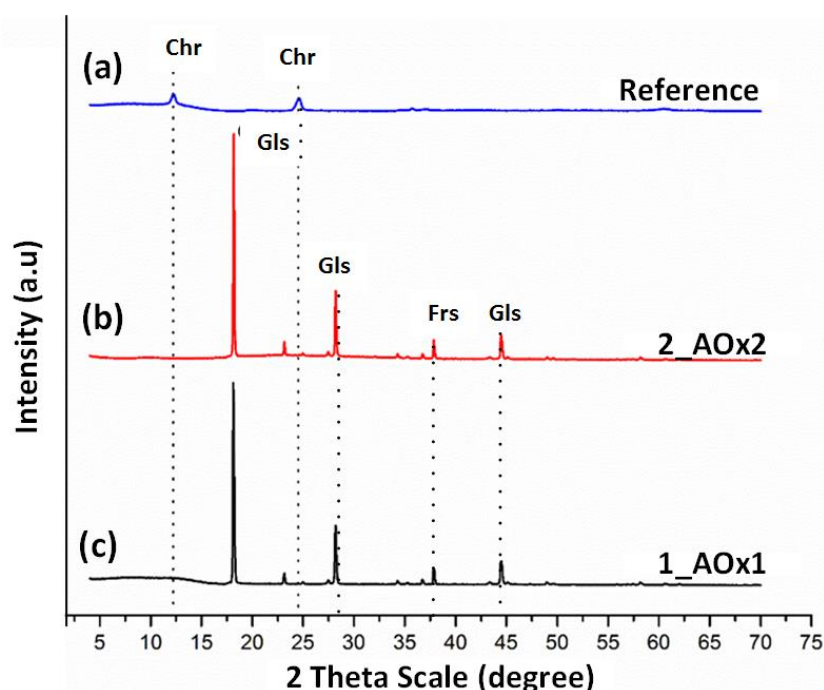


Figure 5. 1: XRD diffractograms of (a) untreated chrysotile sample, (b) 2_AOx2, (c) 1_AOx1 after 10 days of treatment. (Gls: Glushinskite, Chr: Chrysotile, Frs: Forsterite)

FTIR spectra of the effect of oxalic acid on different concentrations of chrysotile after 10 days of treatment and the required time of optimum treatment are illustrated in Figure 5.2. The infrared spectrum of pure chrysotile was used as reference in order to better characterize the changes induced by the treatment. Absorption at 3845 cm^{-1} indicates Mg-OH stretching vibration, while those at 3446 and 1630 cm^{-1} are attributed to absorbed water. The peaks at 1085 and 955 cm^{-1} correspond to Si-O-Si and Si-O-Mg stretching vibrations, respectively (Finley et al., 2012), while the band at 611 cm^{-1} is attributed to Mg-O vibration (Habaue et al., 2008). As can be clearly seen, the intensity of the main peaks that correspond to Chrysotile at 3845 , 3684 , 955 , 611 and 434 cm^{-1} were remarkably decreased after 10 days of treatment with oxalic acid (Favero-Longo et al., 2005). More specifically the double peak at 3878 and

3684 cm^{-1} attributed to Mg-OH stretching vibration of chrysotile, while the peaks at 611 and 434 cm^{-1} belong to inner Mg-OH vibrations, and to Mg-OH translation or Si-O bending, respectively. The peak at 955 cm^{-1} refers to both Si-O-Mg and Si-OH bonds.

The presence of two double peaks in the range of 1660 - 1635 and 1370 - 1324 cm^{-1} corroborated the results of the XRD analysis related to the formation of Glushinskite. Similar results have also been reported by Rozalen & Huertas (2013). According to their study, glushinskite was produced as a byproduct during detoxification of asbestos by using oxalic acid.

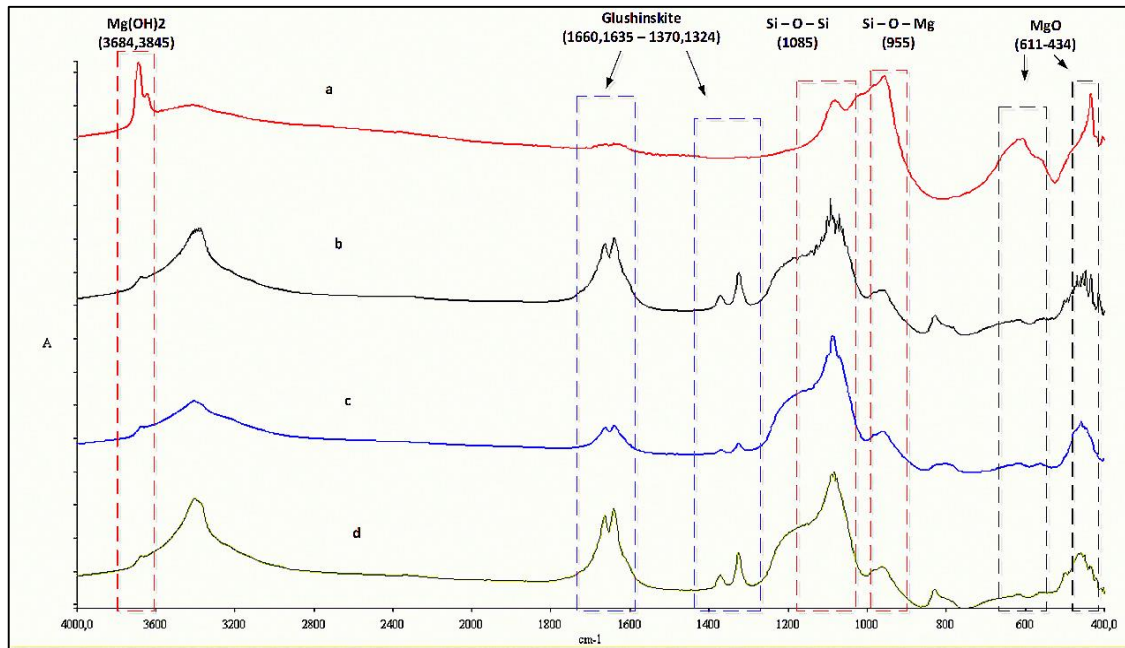


Figure 5.2: FTIR spectra of (a) untreated Chr sample, (b) 1 AOx1, (c) 2 AOx2 and (d) 3 AOx4 samples after 10 days of treatment.

Selection of the optimum synthesis

As the results of examined samples have already been determined, subsequently, an optimal synthesis of treatment was selected. According to the abovementioned results, sample 1_AOx1 presented optimal behavior. Sample's 1_AOx1 concentration of oxalic acid was 0.05 M , which led to satisfying results after 10 days of treatment. FTIR plots (Figure 5.2) demonstrate that Mg-O peaks, which constitute an indicator of chrysotile's toxicity, are remarkably minimized. Increase of Si-O-Si bonds as opposed to the decrease of Si-O-Mg demonstrate dissolution of chrysotile's fiber external structure and its conversion to amorphous silicate mineral. Through XRD analysis (Figure 5.1) peaks representing chrysotile have been reduced significantly.

This composition has been selected as optimal in terms of exploitation of byproducts. In the abovementioned analyses a large concentration of magnesium oxalate was detected in the supernatant solution. Preliminary tests established that the most considerable quantity of magnesium oxalate, responsible for MgO production, was detected after 8 days of treatment. Therefore, the eight-day treatment was suggested due to the optimum reaction rate; an

increasing time treatment reduced the magnesium oxalate production rate as a consequence of the dissolution/precipitation processes governed the Mg^{2+} and COO_2^{2-} ions present in the solutions under study. Besides the cost-effectiveness due to the absence of heating and catalyzing agents, further economic and environmental efficiency is achieved, from minimizing the Oxalic acid quantity (Valouma et al., 2017).

5.2.2 The effect of combined treatment with oxalic acid aquatic solution and silicates

The XRD diffractograms of Chrysotile samples treated a combined treatment of oxalic acid and silicates are illustrated in Figure 5.3 it is obvious that the main characteristic reflections of pure chrysotile disappear after 30 days of treatment. The decrease of these main reflections of chrysotile is accompanied by newly formed reflections, which are attributed to the formation of magnesium oxalate, glushinskite (diffractograms b and d).

The mineral lansfordite ($MgCO_3 \cdot 5H_2O$) with a main reflection at 2θ 14.5° is identified in the 15th day of treatment with ATOx (diffractogram c₁). This is an extremely unstable mineral that, at temperatures higher than 10 °C, is formed during exposure to ambient air by absorbing atmospheric CO₂ (Ming & Franklin, 1985). In the AOxWG treatment, after 30 days, a new mineral appeared; the minguzzite (Mgz) [$K_3Fe^{3+}(CO_2O_4)_3 \cdot 3H_2O$]. This was quite expected since the chrysotile asbestos used in these experiments has been collected from Asbestos Mines of Northern Greece, which include iron compounds (Anastasiadou et al., 2010). Therefore, minguzzite's formation was caused by a reaction between iron ions, water glass and oxalic acid. In the ATOx and AOWG treatments the absence of chrysotile and the formation of an amorphous phase is evident indicating the destruction of the chrysotile structure upon these treatment conditions.

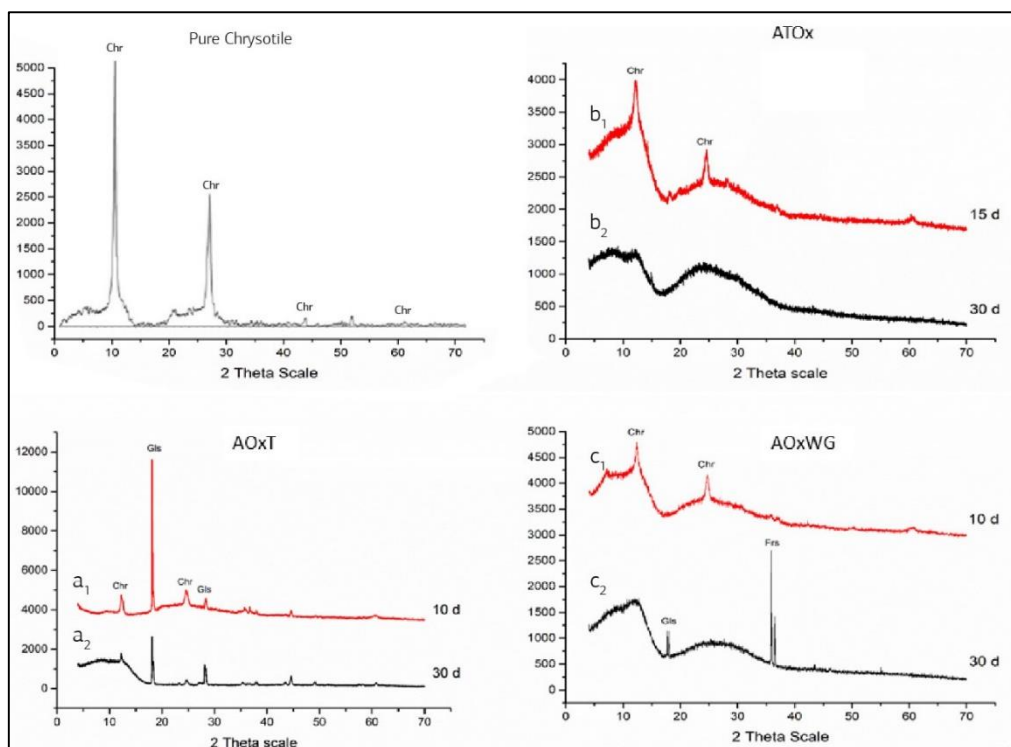


Figure 5.3: XRD spectrum of chrysotile after 5, 15 and 30 days of treatment.

Within 10 days in all of the applied treatment methods the main absorptions of chrysotile at 3878 , 962 and 612 cm^{-1} were remarkably decreased and disappeared after 20 days of treatment (Stănescu-Dumitru 2008). In all of the treatments the neo-formed doublets at 1663 - 1668 and 1373 - 1326 cm^{-1} are attributed to the magnesium oxalate, as a result of the reaction between the brucite and oxalic acid. Furthermore, in the present study from the 1st day of treatment the intensity of the peaks at 1083 and 962 cm^{-1} showed an opposite appearance comparing to that observed in the studies of Rozalen and Huertas (2013) and in the reference sample, indicating that an advanced formation of amorphous phase has taken place.

The similarities of AOxT and AOxWG are entirely related to the prior action of oxalic acid, before the addition of TEOS and pure WG, respectively (Figure 5.4_a and 5.4_c). The oxalic acid functions as an acid leaching agent of Chrysotile yielding amorphous silica and glushinskite. The disappearance of brucite characteristic peaks at 3878 , 962 and 612 cm^{-1} prove the depletion of Mg from the chrysotile structure followed by the glushinskite formation, as indicated by its characteristic peaks at 3379 cm^{-1} and the doublets at 1663 - 1668 and 1373 - 1326 cm^{-1} . Oxalic acid plays also a catalytic role in the hydrolysis of TEOS and the subsequent condensation that occurred, as evidenced by the decrease in the glushinskite formation in the 5th day of AOxT treatment (spectrum a₂) and the simultaneous increasing intensity at 1083 cm^{-1} of the amorphous silica network.

However, during the treatment with ATOx, the FTIR analysis showed that the Mg-OH is remarkably decreased after 15 days and is finally decomposed within 20 days of treatment (Figure 5.4_b). The peak at 962 cm^{-1} refers to both the bonds Si-O-Mg and the neo-formed Si-

OH ones after the hydrolysis of TEOS. Indeed, in the ATOx and after 5 days of treatment with TEOS only, a decrease in the intensity of this peak is observed due to the destruction of the Si-O-Mg bond. Taking into account the remarkable decrease of the Mg-OH intensity at 3878 cm^{-1} a possible explanation could be the contribution of the OH ions of brucite in the basic hydrolysis of TEOS and the subsequent condensation, since alkaline conditions condensation may occur prior to complete hydrolysis (Jiang et al., 2006). Indeed, after the oxalic acid addition the intensity of the peak at 962 cm^{-1} has increased again as it is evident in spectrum b₃, since in acid conditions the hydrolysis prevailed of the condensation, leads to the formation of Si-OH. However, this peak decreases from the 15th day and thereafter, suggesting that both the hydrolysis is completed and a condensation process is taken place leading to the formation of the silica network, as expressed by the increasing intensity of the Si-O-Si bond at 1083 cm^{-1} (spectrum b₄). Furthermore, the formation of the biomaterial glushinskite was also noticed after the addition of oxalic acid in the spectra b₃ and b₄ (Fonseca et al., 2001).

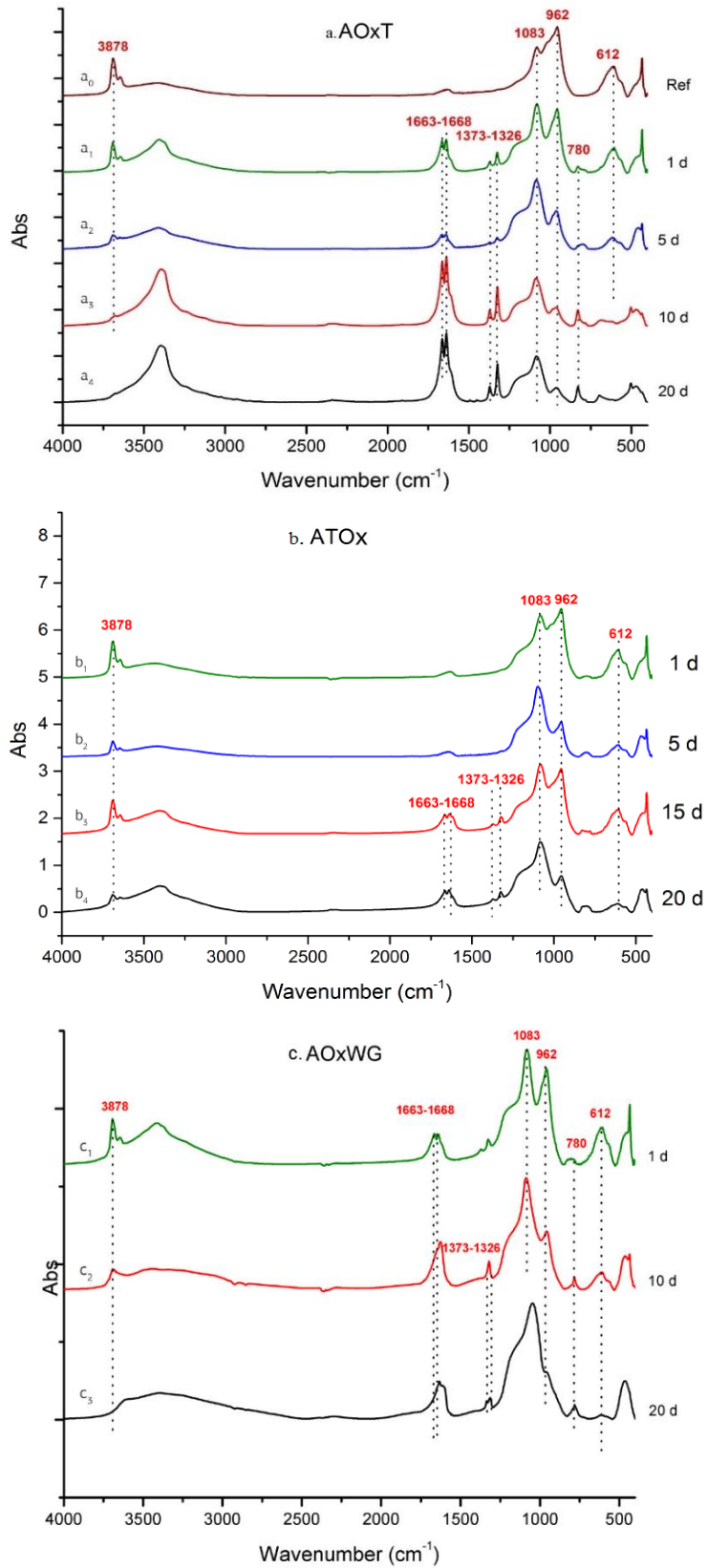


Figure 5.4: FTIR spectra of chrysotile asbestos samples during the 1st, 5th, 10th and 20th day of treatment

The last characterization method, SEM, applied to each sample to confirm the initial assumption about morphological characteristics of the samples. The SEM micrographs of AOxT (Figure 5.5_b) indicate that in the original fibrous material the outer brucite's layer has been broken (Figure 5.5_a), achieving the detoxification of the material. At the same time the silylation process was accomplished, as indicated by the EDS elemental analysis, showing the reduction of Mg, which is a result of the removal of the Mg compounds from the fibers. The bonds Si-O-Mg were cleaved and new Si-O-Si bonds were created, as indicated from the analysis of FTIR.

The ATOx treatment was also studied via SEM microscopy. From the analysis carried out it was found that in the 15th day of the ATOx treatment an amorphous phase was produced; the fibrous form had broken and TEOS coated the external layer of the fibers, transforming the material into an amorphous silica phase (Figure 5.5_c). This result was also confirmed by elemental analysis according to which the Mg had been noticeably reduced. The low quantity of the Mg identified can be justified by the existence of magnesium oxalates, as it is indicated by the FTIR analysis.

AOxWG related micrographs indicate the transformation of chrysotile into an amorphous material. A kind of coating was created in the fibers operating as encapsulation mean even preventing dispersion both in air and liquid solutions. The elemental analysis proves the successful action of the coating, as it does not appear in the obtained results Mg, but only Si due to the outer layer of fiber. The micrographs of AOxWG illustrated in Figure 5.5_d prove that vitrification and coverage are achieved due to the influence of pure WG. The fibers are no longer visible. The EDS analyses carried out in the entire surface of AOxWG evidenced the chrysotile's fibers encapsulation, since magnesium could not be detected, whereas only Si and K were identified.

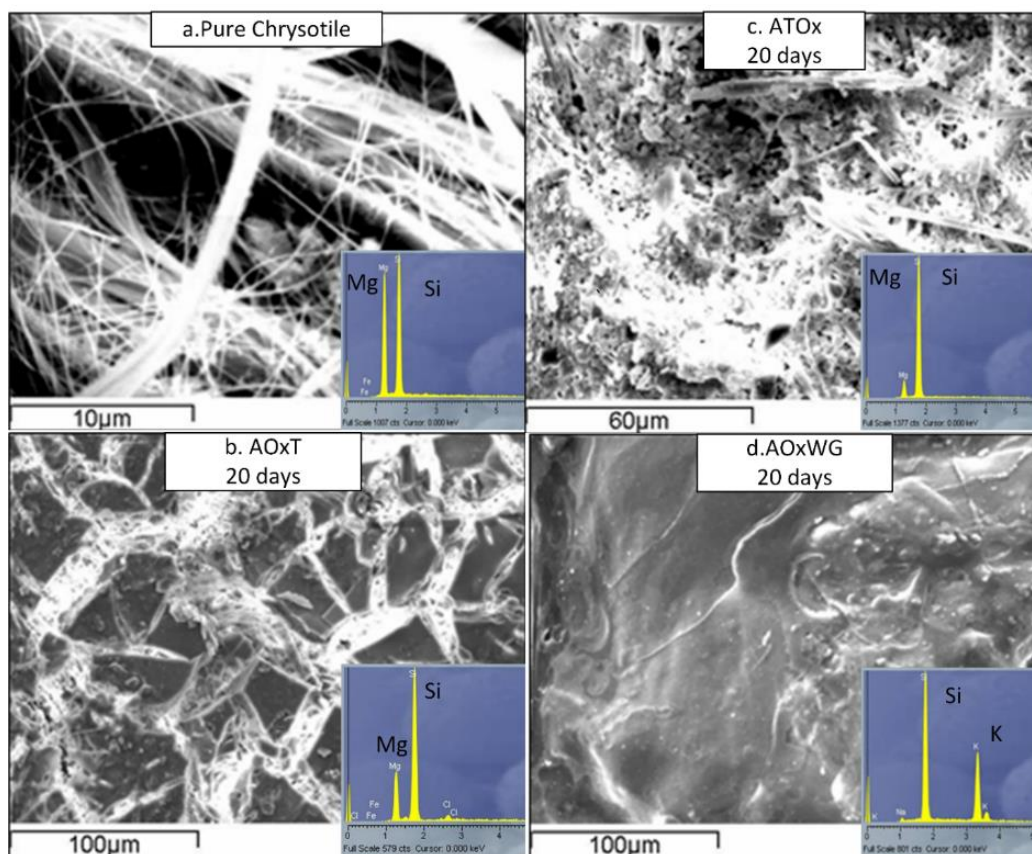


Figure 5.5: SEM and EDS micrographs of chrysotile samples after 20 days of treatment.

Selection of the optimum treatment

Comparing the results obtained for AOxT and ATOx treatments, it is observed that in the case of AOxT, the magnesium oxalate is formed faster and in larger quantity compared to the ATOx's magnesium oxalate. The difference between the two experiments was the order in which the ingredients were mixed. In ATOx, chrysotile was mixed with the TEOS and distilled H₂O and oxalic acid was added after 5 days (pH = 2.65), while in the AOxT chrysotile asbestos was first mixed with oxalic acid and then TEOS and ISP mixture was added to the solution (pH = 1.1). So evidently, oxalic acid is able to induce amorphous chrysotile fibers caused by the transformation of Mg-OH into magnesium oxalate. Furthermore, oxalic acid plays a catalytic role in the hydrolysis of TEOS and the subsequent formation of an amorphous silica network. The XRD and FTIR results prove that the silylation processes occurred with the initial addition of TEOS in the ATOx experiments, which have led to the destruction of chrysotile and its conversion into amorphous silicate mineral. In this treatment the OH ions of brucite played an important role, since they have assisted in the basic hydrolysis of TEOS and the formation of the amorphous silica network after the cleavage of the Mg-OH and Si-O-Mg bonds, as indicated by the FTIR analysis.

After the completion of the experimental procedure and the analysis of the obtained results for the treatment of chrysotile asbestos, the most effective mixture was chosen. The optimum experimental synthesis for the treatment of chrysotile was the ATOx. Both in ATOx and AOxWG experiments, equally decomposition of asbestos fibers was achieved. However, the

advantage of the ATOx experiment was the co-production of the biomaterial glushinskite, while the AOxWG experiment was advantageous in the coverage of the material and encapsulation of the fibers at the same time of their inactivation. Detoxification of fibers in both experiments was achieved, but the XRD analysis indicated the full transformation of chrysotile into an amorphous material occurred only during the ATOx experiment.

Chapter VI: Asbestos Containing Waste detoxification processes

Abstract

This chapter includes the results of asbestos containing waste detoxification procedures that carried out. Firstly, a circumstantial characterization of the initial untreated samples is conducted, under chemical and mineralogical perspective. The ACW is investigated in order to fully understand the composition of the material after years of degradation due to weathering.

Thereafter, the results of an experimental investigation concerning the effect of the concentration of oxalic acid, which is the reagent responsible for asbestos fibers detoxification, are presented.

Finally, the proposed combined treatments achieve the detoxification of asbestos containing waste and its transformation to a harmless material, while in the same time it is formatted a non-toxic amorphous silica network aiming by the treated asbestos containing waste.

Characterization analysis of asbestos minerals, cementitious and amorphous phases of asbestos containing waste, as well as new-formed phases of treated samples, are performed with XRPD, FTIR, XRF and TG-DTG analyses and stereoscope microscopy.

6. Results of Asbestos Containing Waste detoxification processes

6.1 Characterization of raw asbestos cement waste

Foremost, a circumstantial characterization of the initial untreated samples was conducted, under chemical and mineralogical perspective. The ACW were investigated in order to fully understand the material composition after years of weathering degradation.

6.1.1 Chemical composition

Chemical components of ACW are reported in Table 6.1, where the percentages of main chemical components values are CaO 43.9%, SiO₂ 15.3% and LOI 29.5%. CaO and SiO₂ are predominant due to both cementitious phases and asbestos fibers. Specifically, high percentage of CaO is anticipated due to predominant cementitious phases. Furthermore, SiO₂ considerably high presence is originated from both asbestos fibers and cement. MgO as chrysotile fibers external layer (brucite: Mg(OH)₂), is present at a low proportion around 2.4%. The relatively high content of Fe₂O₃ in the sample could be explained due to presence of crocidolite asbestos [(Na₂Fe²⁺₃Fe³⁺₂)Si₈O₂₂(OH)₂].

Table 6.1: Chemical composition of asbestos cement waste (% wt.)

Oxides	% wt.
SiO ₂	15.3
CaO	43.9
MgO	2.4
Na ₂ O	1.2
K ₂ O	0.3
TiO ₂	0.1
MnO	0.1
Fe ₂ O ₃	2.9
Al ₂ O ₃	1.3
SO ₃	1.4
LOI	29.5
Total	98.4

6.1.2 FTIR analysis

The infrared spectrum of raw ACW is used as reference in order to better understand the material, and afterwards to characterize the changes that may be induced by the treatment. The spectrum of the untreated ACW is illustrated in Figure 6.1. Absorptions at the range 3500 – 2600 cm⁻¹ are attributed to water molecules. The peaks at 3690, 3640 and 610 cm⁻¹ denote to Mg-OH and Mg-O stretching vibration of asbestos fibers external layer, brucite (Mg(OH)₂). Cementitious phases of ACW cement matrix, probably of calcite or vaterite (CO₃²⁻), are represented via C-O bonds at 1446, 1080 and 874 cm⁻¹. Band at 966 cm⁻¹ is denoted to calcium silicate hydrates (C-S-H) due to

hydrated cementitious phases. Si-O-Si network of asbestos silica matrix is attributed at peaks at 1024 and 454 cm^{-1} .

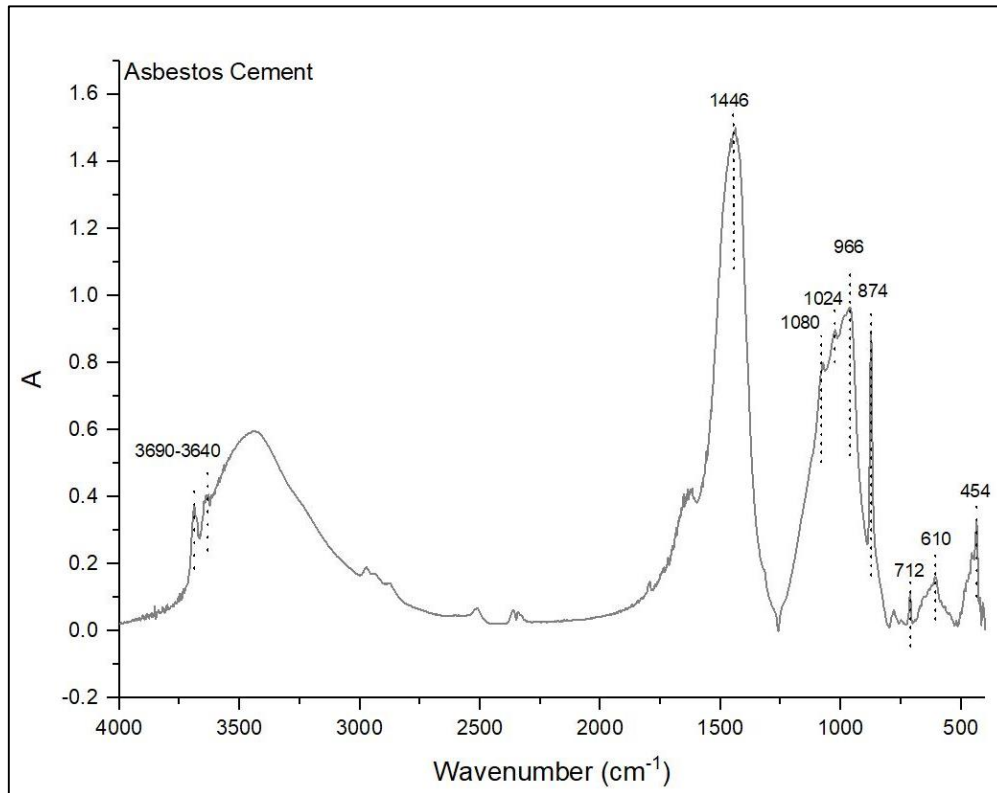


Figure 6.7: FTIR spectra of untreated asbestos cement

6.1.3 Mineralogical composition

XRD pattern of raw material is presented in Figure 6.2. Cement binder of ACW is highly heterogeneous and as a result several crystalline phases are detected. Quantitative estimation of crystalline phases (Table 6.2) was determined by Rietveld method, including Roentgen-amorphous phase (Thomaidis & Kostakis, 2015).

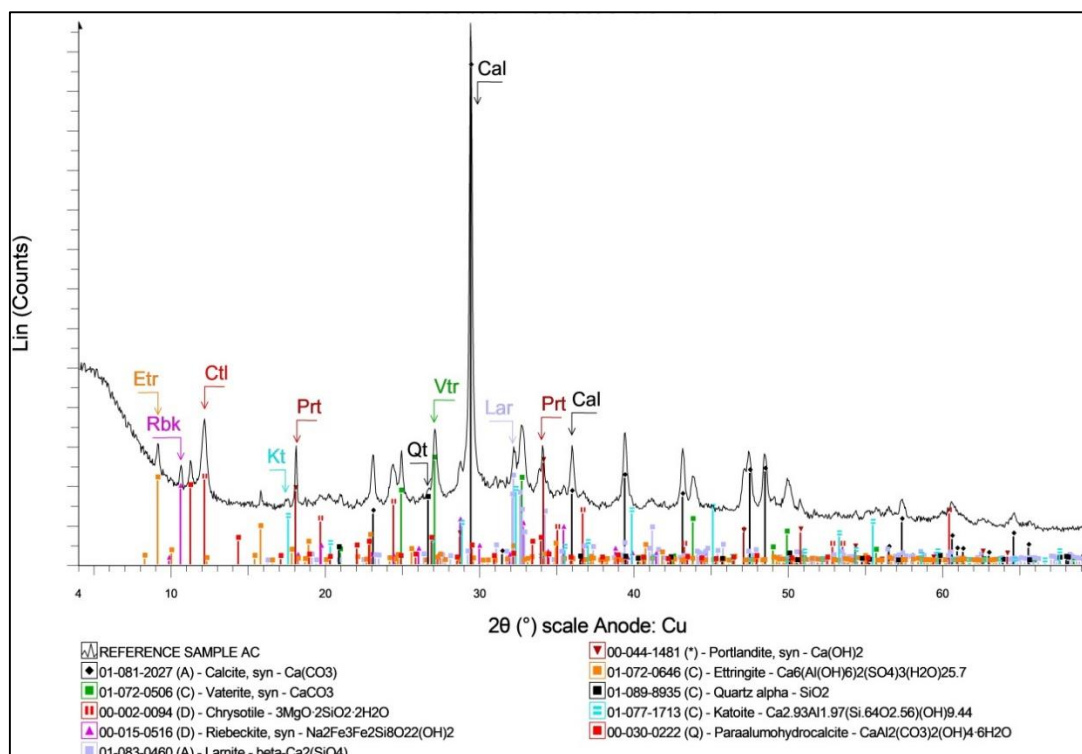


Figure 6.2: Mineralogical composition of untreated asbestos cement (Etr: ettringite, Rbk: magnesianriebeckite, Ctl: chrysotile, Prt: portlandite, Qt: quartz, Vtr: vaterite, Cal: calcite, Lar: larnite)

The preponderant crystalline phase is the one of calcite (22 %wt.) and subsequently vaterite (19 %wt.), contained most of the calcium detected in them (Table 6.1). These minerals pertaining to calcium carbonate (CaCO_3) phases, which consist the main products of cement weathering. Portlandite (Ca(OH)_2) and ettringite ($\text{Ca}_6\text{Al}_2(\text{SO}_4)_3(\text{OH})_{12}\cdot 26\text{H}_2\text{O}$) recorded such as they are main products of cement hydration process (~3 %wt.). Larnite (Ca_2SiO_4) is the natural mineral used for the industrial mineral belite, which is very important on Portland cement manufacture. The main constituent of these phases, dicalcium silicate (~9 %wt.), is an impurity of Portland cement clinker production (Lea, 1971). Such as calcium is the main component of the ACW (CaO 49.9%), following by silicon (SiO_2 15.3%), it is understandable that the most crystalline phases are denoted to products of their reaction, fact that explains the presence of katoite and paraalumohydrocalcite in smaller proportions. Quartz (SiO_2) presence is attributed either to aggregates that were used in the production of cement mortar of ACW, or it is occurred as additive of cement binder.

Asbestos phases of chrysotile and magnesianriebeckite (mineral phase of the commercially used crocidolite asbestos) identified at proportions of 8 and 2 %wt., respectively.

The sample, besides the crystalline phases, is also synthesized by 37 %wt. of amorphous phase. The hydration process is responsible for the formation of calcium silicate hydrates (CSH phase), which however it is characterized of low degree of crystallinity, and as a result X-Ray perceive CSH as amorphous phase (Kusiorowski et

al., 2015). CSH identification is consistent with the high percentage of amorphous in XRPD and the CSH bonds of FTIR diagram (Figure 6.1).

Table 6.2 Results of the quantitative phase analyses of the raw ACW (values in % wt.). JCPDS: 01-081-2027 (calcite), 01-072-0506 (vaterite), 01-089-8935 (quartz), 00-044-1481 (portlandite), 01-077-1717 (katoite), 01-072-0646 (ettringite), 00-002-0094 (chrysotile), 00-015-0516 (magnesioriebeckite), 01-083-0460 (larnite), 01-077-0409 (belite).

Minerals	(% wt.)
Calcite	22
Vaterite	19
Quartz	<1
Portlandite	2
Katoite	<1
Ettringite	<1
Chrysotile	8
Magnesioriebeckite	2
Larnite	<1
Belite (C2S betta Mumme)	8
Amorphous	37

6.1.4 Stereoscopy

Macroscopical observations of raw ACW are illustrated in Figure 6.3 Asbestos fibers are clearly visible in the samples. Long fiber of Figure 6.3a is probably a crocidolite fiber, such as it is known that these fibers are characterized by needle-like form that their length ranges from 0.5 to 2.5 cm, in their initial form (Gualtieri et a., 2004). Additionally, in the same image it is detected the cement matrix of ACW. Interpreting these images, it can be clearly argued that in both images the heterogeneous cement matrix and fibrous structure of asbestos are easily detectable.

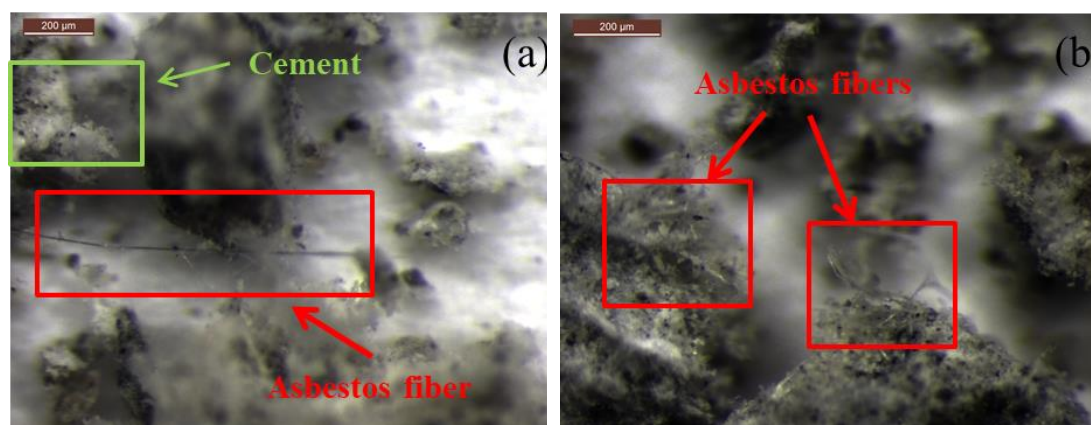


Figure 6.8: Macroscopical observations of raw asbestos containing waste

6.2 Characterization of treatment with oxalic acid

6.2.1 FTIR analysis

The infrared spectrum of raw ACW was used as reference (Figure 6.4_a) in order to better characterize the changes induced by the treatment. Comparing the results of treated ACW (Figure 6.4_{b-d}) with the initial spectra of untreated ACW, it is observed that the main absorptions of asbestos at 3690 cm^{-1} , 3640 and 610 cm^{-1} , denoted to Mg-OH and Mg-O stretching vibration of brucite respectively, are decreased. In all the examined samples neo-formed peaks are appeared, at 1622 and 1316 cm^{-1} , and doublets at $3490\text{-}3432\text{ cm}^{-1}$, that are attributed to calcium oxalate as a result of the reaction between the calcium of ACW and oxalic acid. Specifically, peaks at 1622 and 1316 cm^{-1} belong to C=O and C-O respectively (Sekkoum et al., 2016), and the doublets at $3490\text{-}3432\text{ cm}^{-1}$ represent the H-O of the water molecules of calcium oxalate ($\text{Ca}(\text{C}_2\text{O}_4)\cdot\text{H}_2\text{O}$) (Verganelaki et al., 2014). The bands at 1446 and 874 cm^{-1} are denoted the C=O vibrations due to CaCO_3 presence. The band at 966 cm^{-1} is corresponded to Si-O-Mg stretching vibration (Sugama, 1998), and its reduction indicates the dissolution of chrysotile's fibers Mg-octahedral sheet bonded to Si-tetrahedral sheet. The peaks of treated samples at 782 and 518 cm^{-1} are attributed to C-H and C=O bonds, also characteristic peaks of whewellite (Sekkoum et al., 2016).

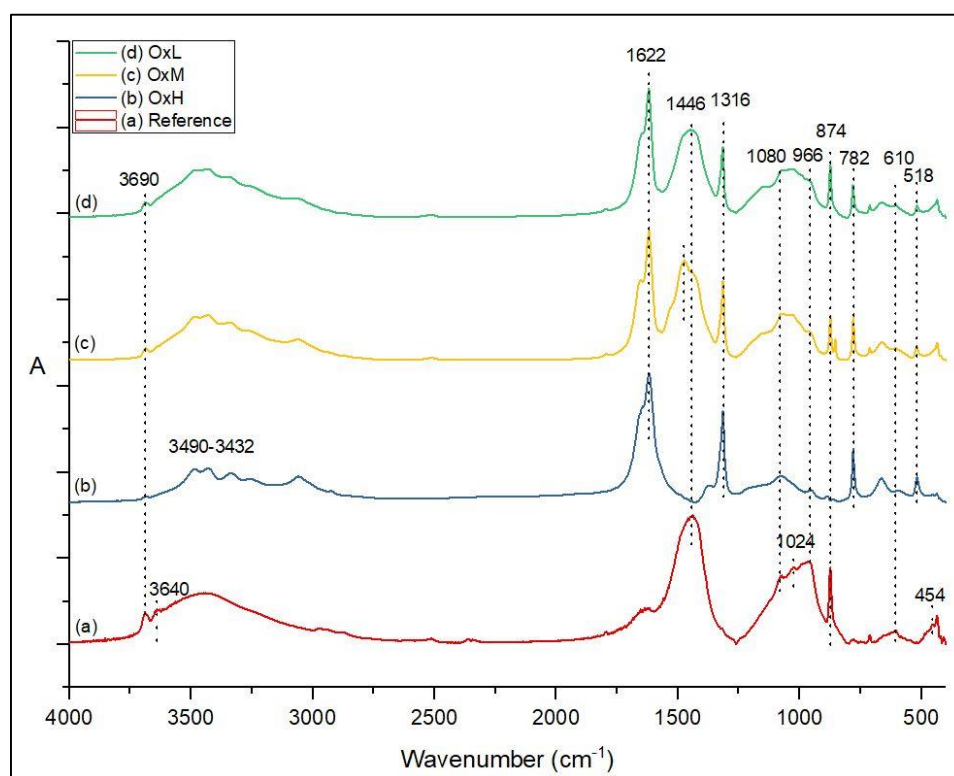


Figure 6.4: FTIR spectra of (a) untreated asbestos cement and treated samples with oxalic acid in (b) high (OxH), (c) medium (OxM) and (d) low (OxL) concentration.

6.2.2 Mineralogical composition

Figure 6.5 illustrates the results of mineralogical analysis of the different oxalic acid concentrations (0.3, 0.15, 0.1M) that are examined as proposed treatments. The

mineralogical analysis of the samples confirms the results of FTIR spectra. It is observed that in all the examined syntheses (OxH, OxM and OxL) asbestos related diffraction reflections are still visible but to a lesser extent. It is notable that the higher is the concentration of the oxalic acid, the intensities of asbestos reflections are decreased, and they are wider. This indicates that this acid is capable to cause structural amorphization of asbestos in presence of cement.

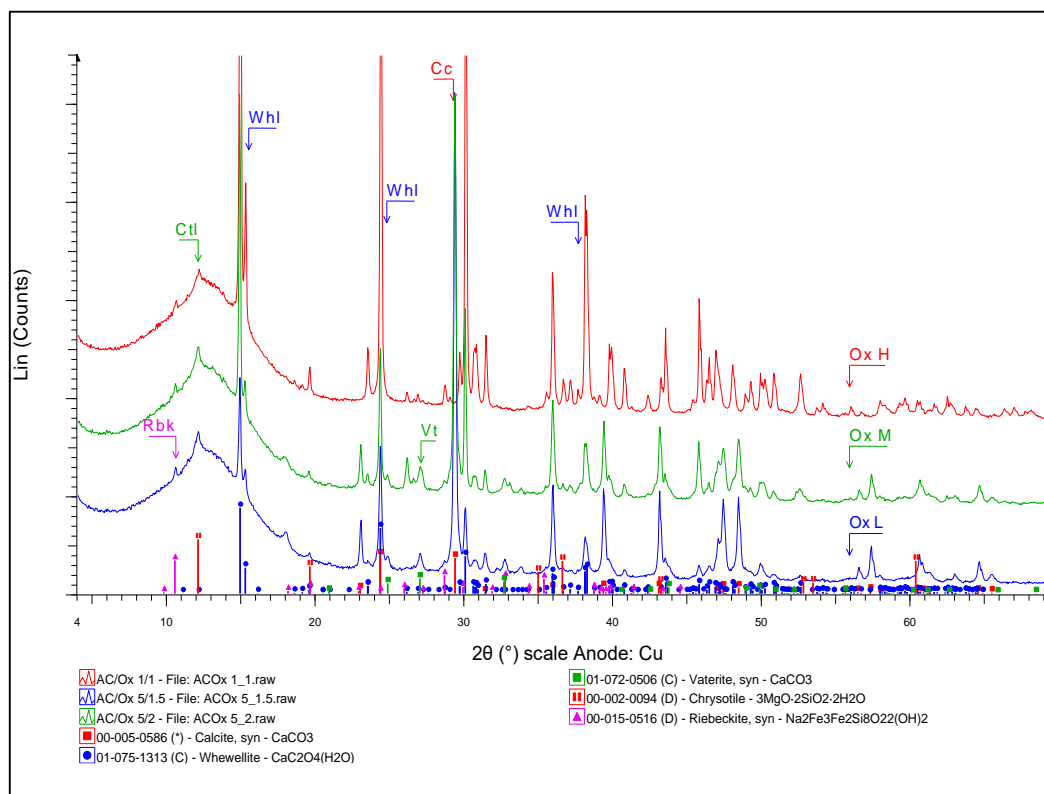


Figure 6.5: Mineralogical composition of treated asbestos cement samples with oxalic acid in high (OxH, medium (OxM) and low (OxL) concentration.

The composition of treated samples varied essentially in the examined concentrations. The OxH sample, with higher oxalic acid concentration, is composed mainly of whewellite (74 % wt.), following the amorphous phase in percentage of 19 %wt. Chrysotile is reduced from 8 to 4 % wt. at all the examined treatments, while crocidolite quantity is under detection limit. It is observed that oxalic acid excess tends to react with calcium carbonates and create calcium oxalate (whewellite) as byproduct.

Table 6.3: Results of the quantitative phase analyses of the treated samples studied (values in % wt.). JCPDS: 01-081-2027 (calcite), 01-072-0506 (vaterite), 00-002-0094 (chrysotile), 00-015-0516 (magnesioriebeckite), 01-075-1313 (whewellite).

Minerals	OxH	OxM	OxL
Calcite	2	21	24
Vaterite	-	8	7
Chrysotile	4	4	4
Magnesioriebeckite	<1	<1	<1
Whewellite	74	20	11
Amorphous	19	47	55

6.2.3 Stereoscopy

The stereo-zoom microscopic observations of oxalic acid treatments (Figure 6.6_{a-c}) at different concentrations illustrate the presence of asbestos fibrous structure but in lesser extent than the untreated sample (Figure 6.3). Furthermore, there are distinguished salt-like crystals due to the presence of calcium oxalate.

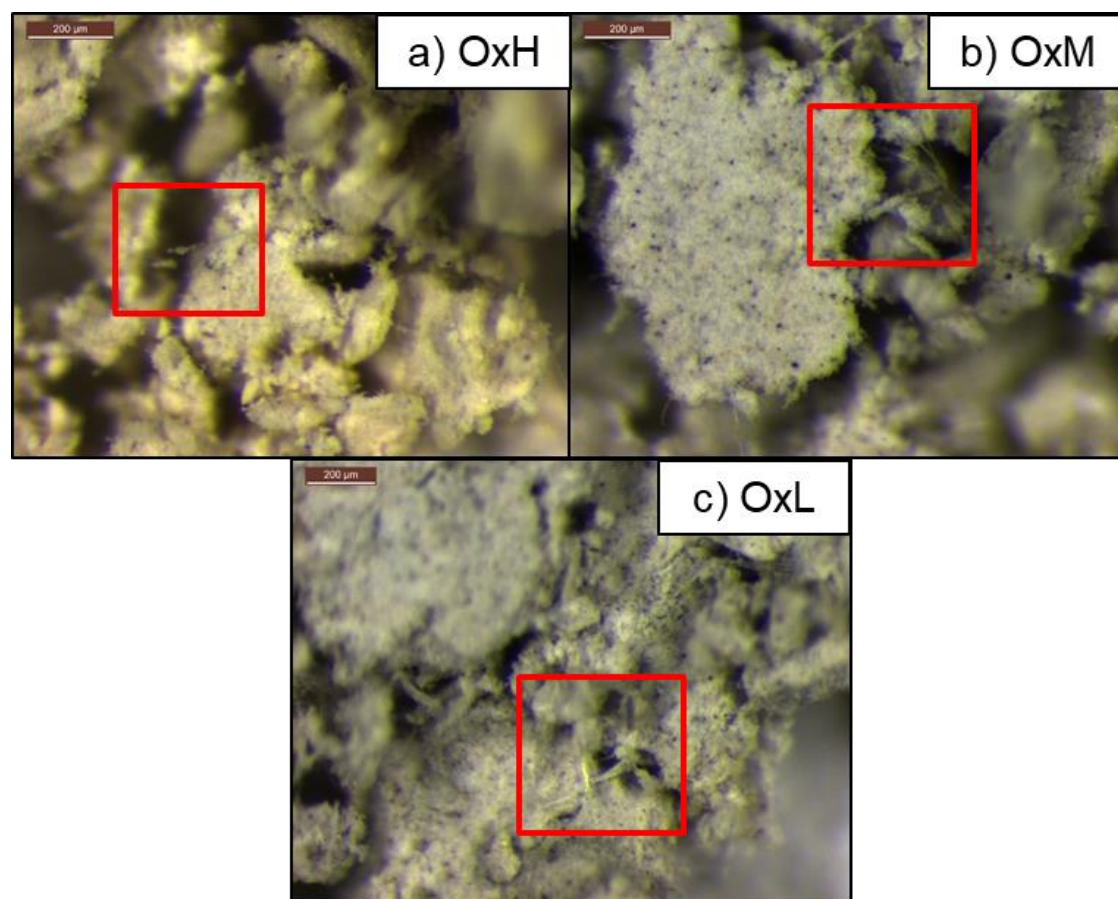


Figure 6.6: Macroscopical observations of ACW treated in oxalic acid solutions with high (a) OxH, medium (b) OxM and low (c) OxL concentration

6.3 Combined treatments: Oxalic acid combined with tetraethyl orthosilicate

6.3.1 Selection of the materials

Oxalic acid is deemed capable of ensuring asbestos fibers transformation. The combined treatment of ACW with oxalic acid and TEOS/ISP mixture is studied. ISP addition to this transformation system is selected to increase TEOS hydrolysis rate. ISP as a solvent preserves a complex role in sol-gel systems. The following treatments have as main objective the transformation of asbestos fibers, and the encapsulation of the treated ACW in TEOS silica network.

The selection of the reagents of the combined treatments is based primarily to the oxalic acid ability to destruct the fibers of chrysotile (Valouma et al., 2017, Rozalen & Huertas, 2013). Additionally, oxalic acid is used as acid catalyst in sol-gel processes. Sol-gel processes are consisted research area aiming the production of silica glasses, ceramic and composites, characterized by homogeneity, large surface area and low density (Rao & Bhagat, 2004). Such characteristics are considered advantageous in various applications, rendering sol-gel processes a promising and attractive research field.

The morphology and the properties of the final products are depended highly on the reactions that are took place during sol-gel processes (Boonstra & Baken, 1990). The two most important reactions of the procedure are the hydrolysis and the condensation. These reactions are able to be affected by several intermediates which may facilitate or impede the process. TEOS transformation to silica gel occurs in water-ethanol medium, according the equations presented schematically in Figure 6.7 These reactions illustrate the water and the alcohol condensation that follows TEOS hydrolysis.

According to Ro & Chung (1989), hydrolysis rate increases as the acid concentration increases. Additionally, the same study noticed that there is an upper limit of acid concentration that facilitates the hydrolysis. Further increase of acid concentration leads at the increase of esterification, the reverse reaction of the desired hydrolysis.

Taking under consideration these studies, it was chosen the oxalic acid concentration (0.3 M) that ensures the destruction of asbestos fibers, while the pH of the medium was 1.49 ensuring that the esterification would not be facilitated. TEOS/ISP mixture addition to the oxalic acid – ACW solution resulted increase of pH at 1.91.

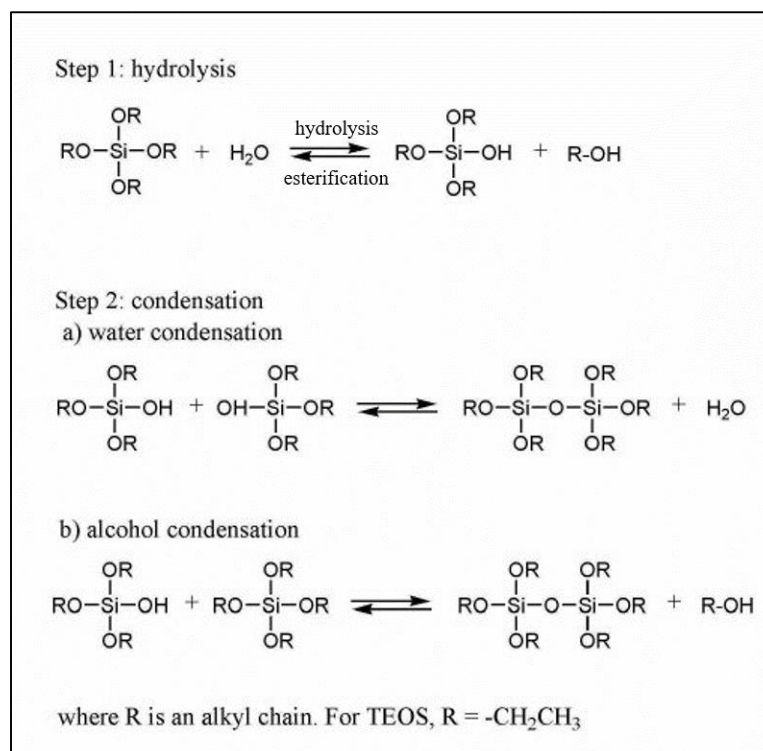


Figure 6.9: Reaction scheme of the sol-gel process (Colleoni et al., 2016)

6.3.2 Chemical composition

Two solutions were prepared (STF, STG samples) and the treatments were conducted under the same conditions, and they only were differed on their duration. STF was treated for 30 days while STG until was fully transformed to sol-gel (45 days).

According to the chemical composition of these samples (Table 6.4) in both STG and STF samples high silica content prevails (73.3 and 47.8 %wt. respectively), followed by the CaO content. It is important to note that CaO presence in STG sample is significantly lower than in STF, presuming that the reaction between oxalic acid and ACW continued after 30 days of treatment.

Table 6.4: Chemical composition of STF and STG samples (% wt.)

Oxides	STG	STF
SiO ₂	73.3	47.8
CaO	2.3	10.2
MgO	0.1	1
Na ₂ O	0.3	0.6
K ₂ O	0	0
TiO ₂	0	0
MnO	0	0
Fe ₂ O ₃	0.1	0.8
Al ₂ O ₃	1	2.7
SO ₃	0	0
LOI	22.6	36.9
Total	99.7	100

6.3.3 FTIR analysis

Reagents' combinations were selected in order to be achieved both detoxification of ACW and co-production of non-hazardous valuable materials. The effect of the variation in treatment time under the same reagent concentration is illustrated in FTIR spectra (Figure 6.8). According to literature (Barbarena-Fernandez et al., 2015), TEOS hydrolysis is considered complete after three weeks, while consolidation continues thenceforward.

The disappearance of Mg-OH and Mg-O characteristic peaks at 3690, 3640 and 610 cm^{-1} proves the dissolution of Mg from asbestos fibers and the destruction of brucite ($\text{Mg}(\text{OH})_2$) external layer of chrysotile fibers. Oxalic acid is the most significant reagent of fibers destruction, while simultaneously it plays a catalytic role in the hydrolysis of TEOS and the subsequent condensation that occurred, as it is indicating by the increasing intensity of 1084 cm^{-1} , which represents the amorphous silica network (Valouma et al., 2016).

The band at 782 cm^{-1} , which is denoted to ethoxyl groups, is higher in STF sample, indicating that polymerization is not completed. The spectra of the samples present bands at 3490 and 3432 cm^{-1} that is interpreted to be primarily due to O-H stretching vibrations of calcium oxalate. Additionally, main peaks of calcium oxalate are considered these at 1622 and 1318 cm^{-1} , found in both treated samples and they are attributed to C=O bonds. Such as in oxalic acid as in combined treatments, peaks at 1412 and 874 cm^{-1} are denoted to the C-O vibrations due to CaCO_3 presence. These bands are eliminated during time, and in STG sample are completely absent.

Absorption at 1084 cm^{-1} is corresponded to Si-O-Si stretching vibrations of silica network, and it is the most intense peak of these samples. It is noteworthy the decrease of 962 cm^{-1} peak in all treated samples, that is attributed to Si-O-Mg bond. This differentiation indicates the dissolution of the matrix of asbestos fibers, where Mg is leached at supernatant and Si-O embedded in sol-gel. Vibration at 468 cm^{-1} is related to O-Si-O. Bands at 518 cm^{-1} are also attributed to whewellite, representing O-C=O. Peak at 668 cm^{-1} is owing to small amounts of Fe^{2+} , possibly due to dissolution of crocidolite asbestos (Theodosoglou et al., 2007).

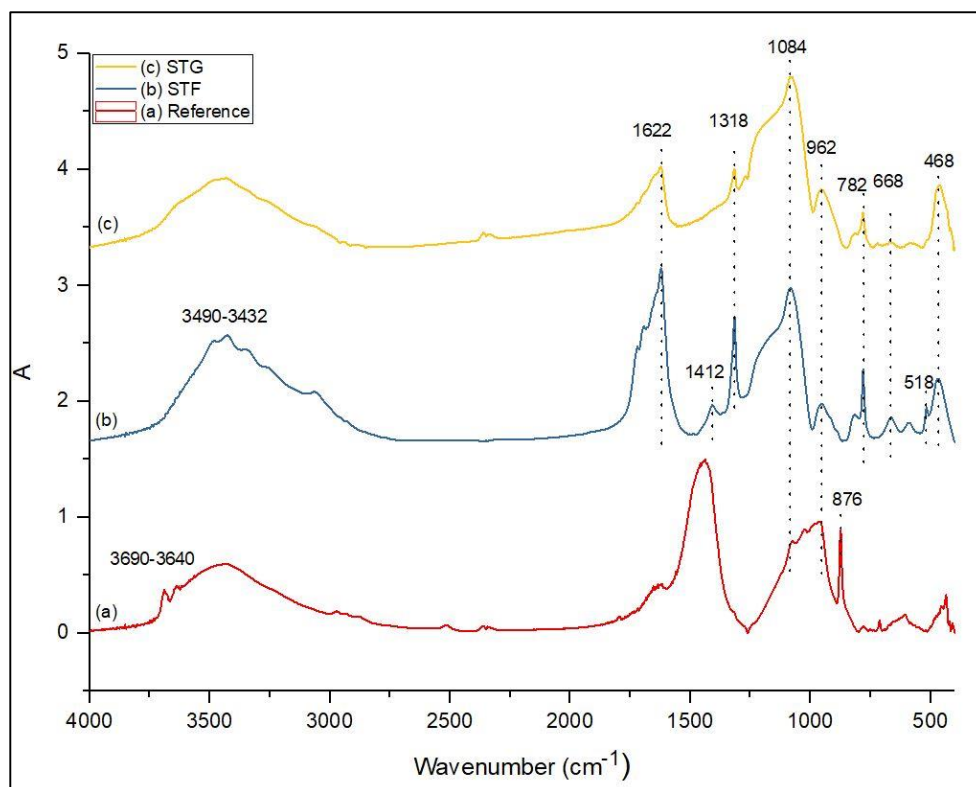


Figure 6.10: FTIR spectra of (a) untreated asbestos cement and treated samples (b) STF and (c) STG

6.3.4 Mineralogical composition

Morphological transformation of ACW is identified as one where none of the asbestos characteristic peaks are detected in STF and STG samples. XRD patterns (Figure 6.9, 6.10) show reflections of the predominant crystalline phase of whewellite (calcium oxalate) and amorphous halo. The amorphous halo demonstrates the increased amount of amorphous material present, compared to the untreated reference sample. Asbestos minerals are not detected on XRD diagram or in quantitative mineralogical data obtained via Rietveld method (Table 6.5). The addition of TEOS in treatment process has as a result the production of a great quantity of a non-toxic amorphous material. Amorphous phase of STG and STF amounts to 90 and 74 % wt., followed by whewellite at 9 and 26 % wt., respectively. Traces of calcite are also detected. Taking under consideration the results of chemical and mineralogical analyses, amorphous phase is created due to TEOS in combination with silica matrix of treated asbestos and CSH phase. Minor quantity of glushinskite, mineral phase of magnesium oxalate ($C_2MgO_4 \cdot 2H_2O$), is reported in both XRD diffractograms (Figure 6.9, 6.10). The magnesium hydroxide of brucite sheet is decomposed due to oxalic acid presence and thereafter it resulted in the production of magnesium oxalate (glushinskite) (Valouma et al., 2016).

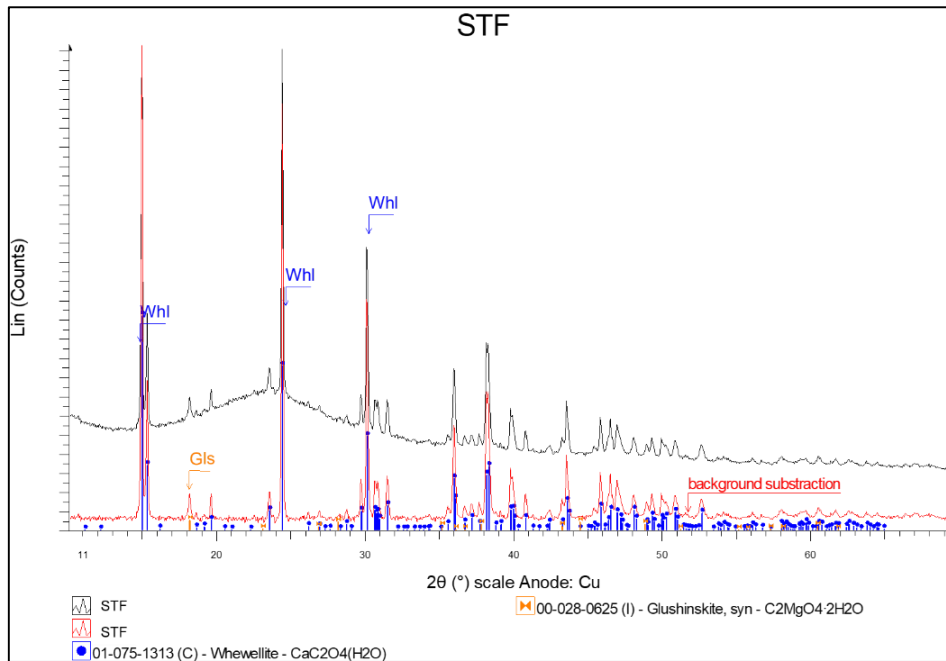


Figure 6.911: Mineralogical composition of STF sample

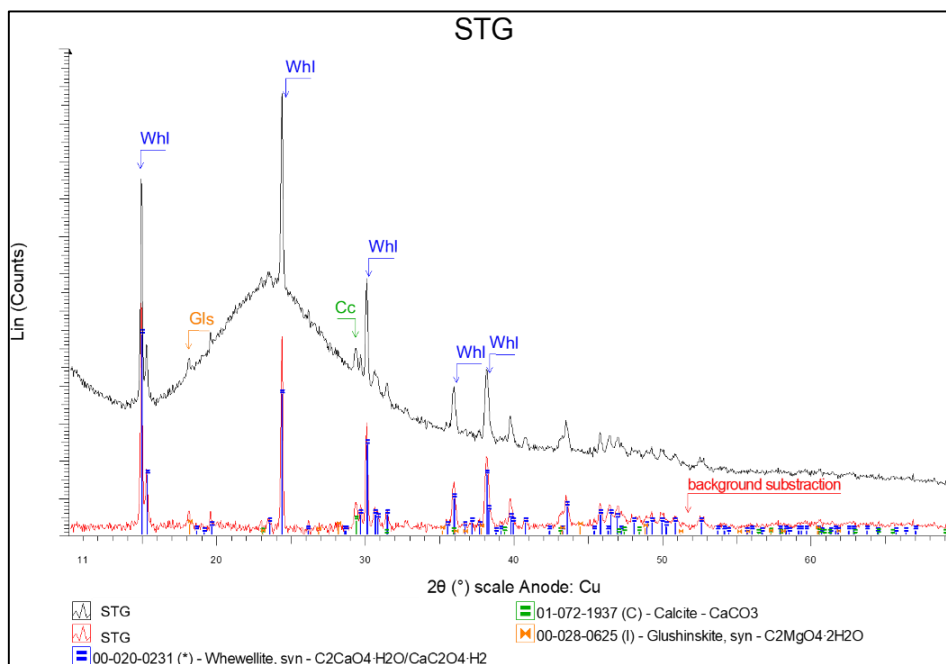


Figure 6.10 Mineralogical composition of STG sample

Table 6.5: Results of the quantitative phase analyses of the treated samples STG and STF (values in %wt.). JCPDS: 01-081-2027 (calcite), 01-075-1313 (Whewellite).

Samples	STG	STF
Calcite	<1	-
Whewellite	9	26
Amorphous	90	74

6.3.5 Stereoscopy

Macroscopical observations of STF and STG samples are illustrated in Figure 6.11. These samples differ only to treatment time. Both of them are considered asbestos-free according FTIR and XRD analyses, while stereo-zoom microscopic observations verify these results since there was not detected any fibers in the samples. Interpreting these images, it can be clearly argued that in both samples the heterogeneous cement matrix has transformed to homogenous amorphous-like structure. Salt-like crystals due to calcium oxalate presence are detected in both samples.

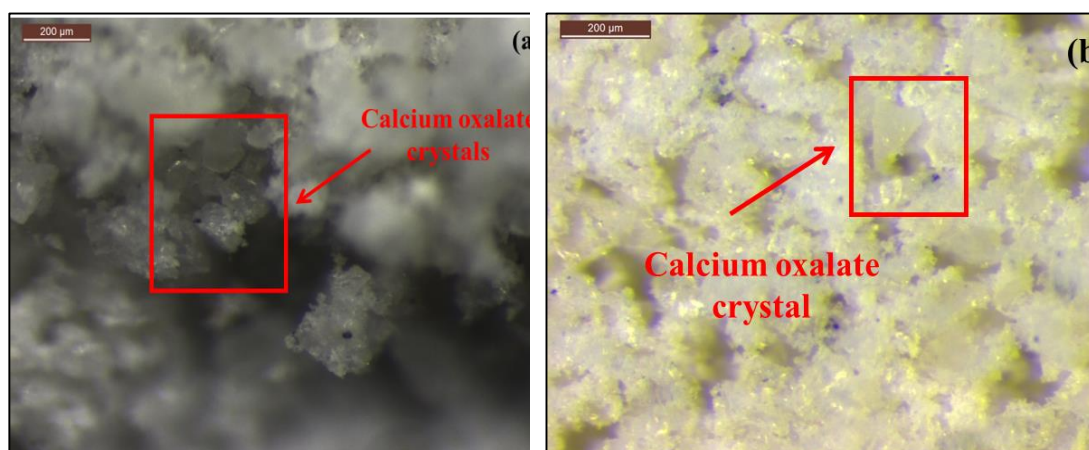


Figure 6.12: Macroscopical observations of treated asbestos cement samples a) STF, b) STG

6.4 Combined treatments: Oxalic acid combined with potassium silicate

6.4.1 FTIR analysis

The FTIR spectra of treated ACW in aquatic solution of oxalic acid (0.3 M) and potassium silicate in comparison with raw ACW are illustrated in Figure 6.12. It is observed at spectra of treated sample (Figure 6.12_b) that the asbestos characteristic absorptions at 3690, 3640 and 610 cm^{-1} denoted to Mg-OH and Mg-O stretching vibrations of asbestos fibers external layer, brucite ($\text{Mg}(\text{OH})_2$), are completely eliminated, indicating that asbestos fibers destruction is achieved.

The cementitious phases of ACW, are represented by bands at 1448, 1080 and 874 cm^{-1} are either remarkably decreased (1080, 874 cm^{-1}) or disappeared (1446 cm^{-1}). This alteration is attributed to oxalic acid reaction with calcium carbonates, calcite and vaterite, of the initial sample, resulting in the new-formed peaks at 1622, 1318 and 518 cm^{-1} . The bands at 3490 and 3432 cm^{-1} are referred to O-H stretching vibrations of calcium oxalate ($\text{Ca}(\text{C}_2\text{O}_4)\cdot\text{H}_2\text{O}$). The formation of absorption at 1084 cm^{-1} is denoted to Si-O-Si stretching vibrations of silica network that is created due to sodium silicate and silica matrix of asbestos fibers.

These increasing intensities point out the structural rearrangement of ACW due to oxalic acid which functions as acid leaching agent of asbestos yielding calcium oxalate and amorphous silica.

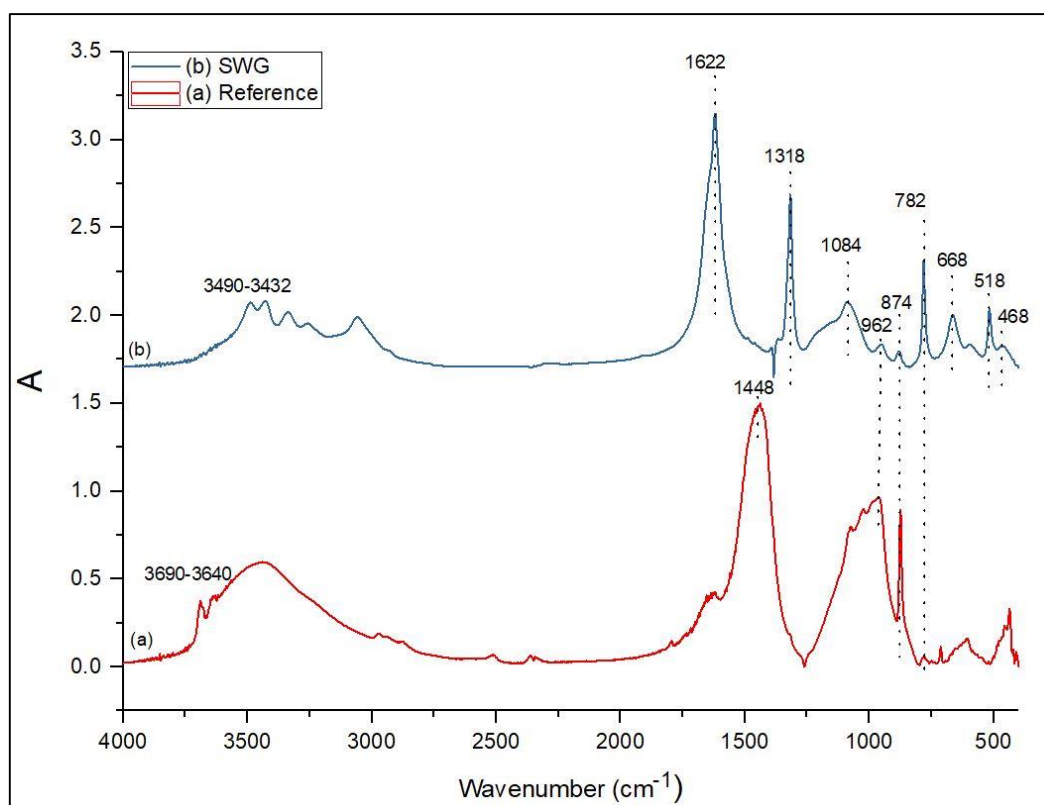


Figure 6.12: FTIR spectra of (a) untreated asbestos cement and (b) treated sample with oxalic acid and sodium silicate (SWG)

6.4.2 Mineralogical analysis

In the XRD diffractogram of treated sample shown in Figure 6.13, it is obvious that the characteristic reflections of chrysotile asbestos at 2θ are completely disappeared. The reflection of riebeckite (crocidolite) is still identified but as a minor peak. In quantitative mineralogical analysis riebeckite phases are not detected and it is considered that after treatment the mineral is destructed partial, and the remaining quantity is lower than 0.5 %wt. in the sample. Additionally, the decrease of asbestos phases is accompanied by decrease of all cementitious phases of ACW, while in parallel new-formed peaks are detected, which are attributed to the formation of calcium oxalate, whewellite ($\text{Ca}(\text{C}_2\text{O}_4)\cdot\text{H}_2\text{O}$). This mineral formation is caused by the reaction of oxalic acid with calcium ions of ACW. According Table 6.6 this reaction leads to the formation of a substantial quantity (50 %wt.) of whewellite. Calcite is detected at percentage of 3 %wt., minor quantity which comply with FTIR results (significant decrease of CO_3^{2-} peaks at 1080 and 874 cm^{-1}). The amorphous phase of this sample was calculated at 47 %wt.

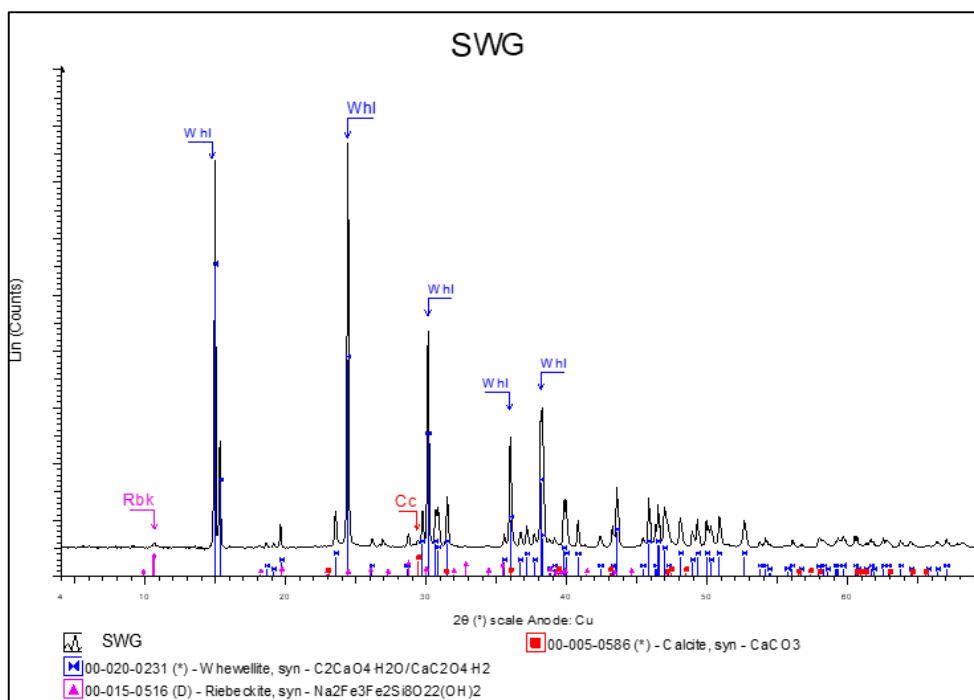


Figure 6.13: Mineralogical analysis of SWG sample

Table 6.6: Results of the quantitative phase analyses of the treated sample SWG (values in % wt.). JCPDS: 01-081-2027 (calcite), 01-075-1313 (Whewellite).

Samples	SWG
Calcite	3
Whewellite	50
Amorphous	47

6.5 Microwave treatment

6.5.1 FTIR analysis

The FTIR spectra of treated ACW in aquatic solution of oxalic acid (0.1 M) and TEOS (Ox/TEOS: 9/1 v/v) under microwave irradiation in comparison with raw ACW are illustrated in Figure 6.14. It is observed at spectra of treated sample (Figure 6.14_b) that the asbestos characteristic absorptions at 3690, 3640 and 610 cm^{-1} that represent Mg-OH and Mg-O stretching vibration of asbestos fibers are not detected, indicating asbestos fibers dissolution.

There are detected the calcium oxalate characteristic peaks represented by O-H stretching vibrations at 3490 and 3432 cm^{-1} and by calcium bonds at 1622, 1318 and 518 cm^{-1} . This is result of the reaction between cementitious phases of the raw sample with oxalic acid solution. The greater peak is observed at 1084 cm^{-1} which is attributed to the formation of Si-O-Si silica network.

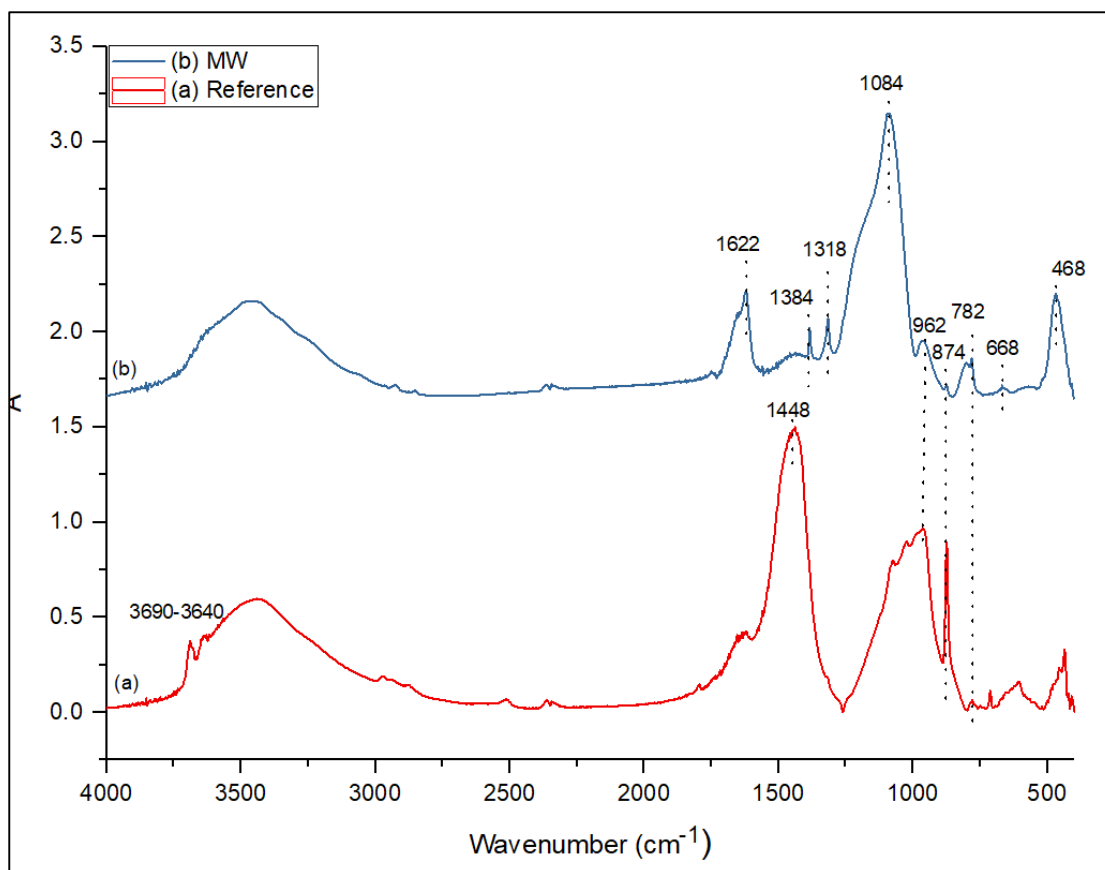


Figure 6.1414: FTIR spectra of (a) untreated asbestos cement and (b) treated sample under microwave irradiation (MW)

6.5.2 Mineralogical analysis

Figure 6.15 illustrates the results of mineralogical analysis of MW sample after the proposed treatment. It is observed that chrysotile asbestos main diffraction reflection is still visible but to a lesser extent and it is wider indicating partially destruction of its crystalline phase.

Microwave treatment induced decrease of crocidolite and chrysotile asbestos peaks. It is clearly observed the main reflection of chrysotile, that according Rietveld method results is corresponded to 4 % wt. (Table 6.7), while crocidolite quantity in the sample is reduced under detection limit. Additionally, whewellite composition is detected lower in comparison with the previous treatments at 8 % wt. Other cementitious phases are remained detectable (vaterite 3 % wt. and belite 4 % wt.) which indicates that the reaction between cementitious phases and oxalic acid is uncompleted.

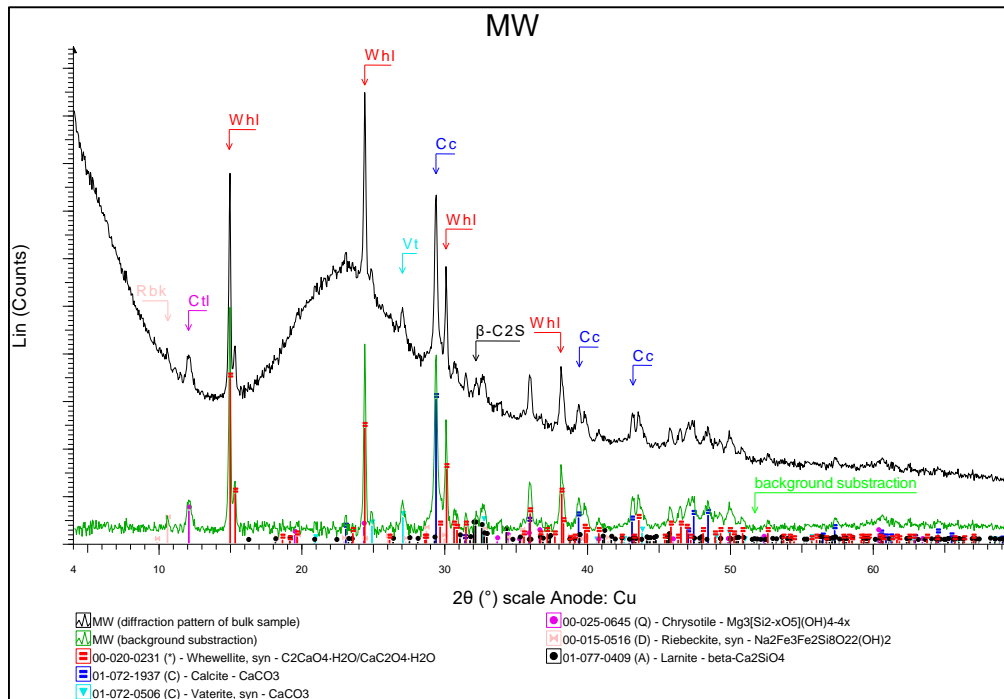


Figure 6.15: Mineralogical analysis of MW sample

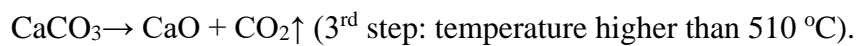
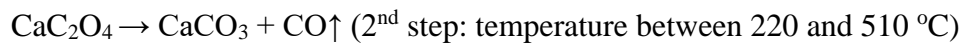
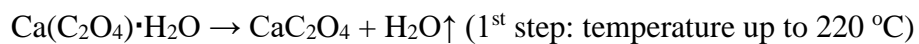
Table 6.7: Results of the quantitative phase analyses of the MW sample (values in %wt.). JCPDS: 01-081-2027 (calcite), 01-072-0506 (vaterite), 00-002-0094 (chrysotile), 01-083-01-077-0409 (belite), 01-075-1313 (whewellite).

Samples	MW
Calcite	<1
Vaterite	3
Chrysotile	4
Belite (C ₂ S betta Mumme)	4
Whewellite	8
Amorphous	80

6.6 Thermal analysis of selective specimens

Weight loss rate, and endothermic peaks as they ensue from differential thermogravimetry measurements, are illustrated in Figure 6.16. Pyrolysis behavior of the optimal treated samples (STF, STG, SWG) present similarities, in accordance with mineralogical and chemical analyses. The samples show a three-step degradation process which is interpreted to be primarily due to with calcium oxalate presence. As referred in the literature (Echigo et al., 2005, Verganelaki et al., 2014) the weight loss (TG curve) and the peaks (DTG curve) up to 220 °C are relative to dehydration of calcium oxalates and water molecules from C-S-H bonds (Vedalakshmi et al., 2003). The second step is observed at temperature up to 510 °C, where carbon monoxide is released, and thereafter the remaining product is calcite. This step also includes the dihydroxylation of potential remaining calcium hydroxide (Dheilly et al., 2002). At temperatures higher than 510 °C the weight loss continues for each sample and it is

related to calcite transformation to lime (CaO) due to carbon dioxide release. The steps that take place during the thermal decomposition of calcium oxalate included in the samples are presented as follows (Echigo et al., 2005):



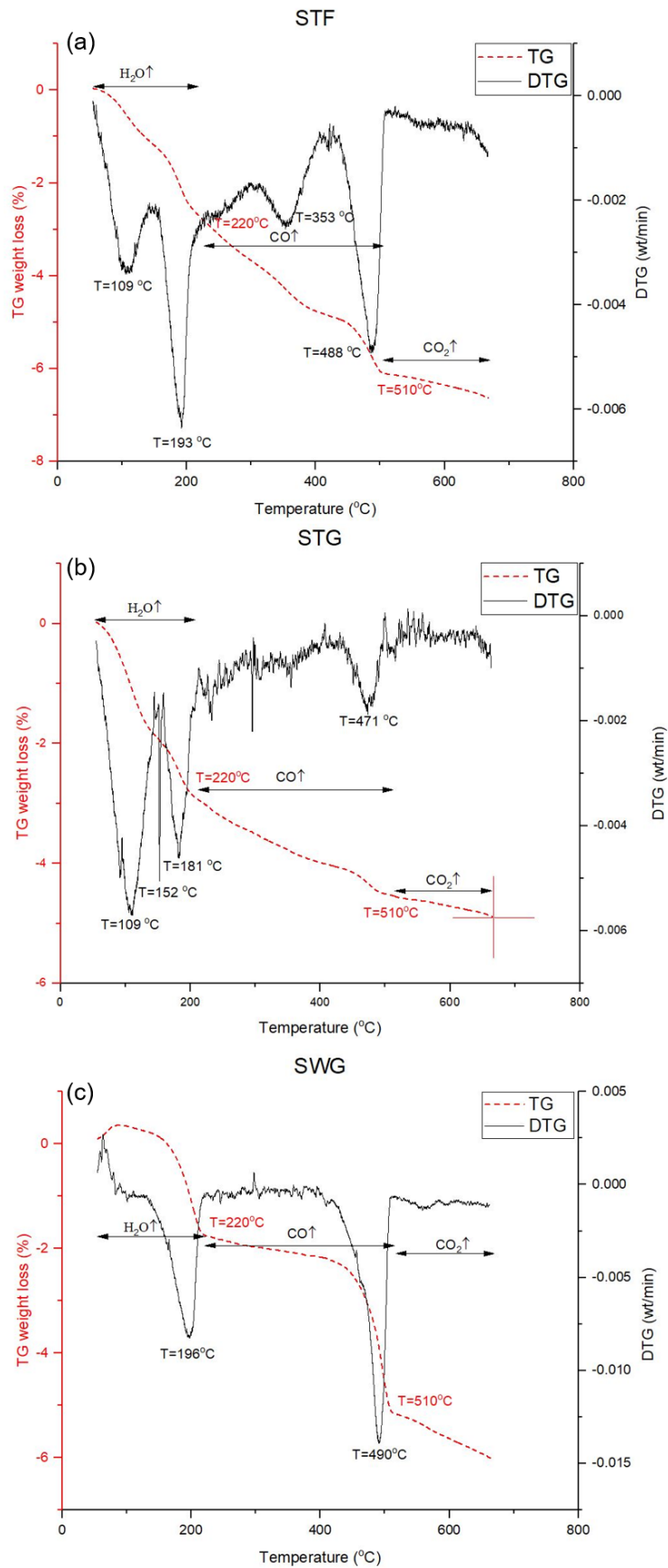


Figure 6.15: TG-DTG thermograms of (a) STF, (b) STG, (c) SWG treated samples

6.7 Discussion - Selection of the optimum treatment

As it has already been mentioned, this study aimed to the detoxification of ACW and their transformation into a harmless and potentially valuable material. The main objective was initially the destruction of asbestos and then the selection of the optimal synthesis in terms of economic and environmental efficiency.

The complicated composition of ACW, due to the initial raw materials and their subsequent degradation of the cement matrix through the years, is responsible for the complex mineralogical phases, reported in Table 6.2. The preponderant crystalline phase is the one of calcite, followed by the vaterite. These minerals pertaining to calcium carbonate phases, which consist the main products of cement weathering. Ettringite, quartz, katoite, paraalumohydrocalcite are also identified. Portlandite is recorded since it is one of the main products of cement hydration process. The hydration process is responsible for the formation of calcium silicate hydrates (CSH phase), which, however, is characterized of low degree of crystallinity, and as a result X-Ray perceive it as amorphous phase (Kusiorowski et al., 2015). CSH identification is consistent with the high percentage of amorphous in XRPD and the CSH bonds of FTIR diagram. Asbestos presence is classified as chrysotile and magnesioriebeckite (crocidolite) in percentages of 8 and 2 %wt., respectively.

Treatments that are occurred using oxalic acid as reagent, varying its concentration (0.05-0.3 M), demonstrated that Mg-O peaks of FTIR analysis, which constitute an indicator of asbestos fibers presence, are remarkably minimized but not completely eliminated. Results of XRD mineralogical analysis are verified these results, identifying peaks that represent chrysotile mineral and estimating its quantity in treated samples at a percentage of 4 %wt. Similar results are obtained also by treatment under microwave irradiation.

Comparing the results obtained for STF and STG treatments, it is observed that in the case of STF calcium oxalate is formed, in larger quantity (26 %wt.) compared to the STG sample (9 %wt.). On the other hand, amorphous phase of STG sample is higher and amounts 90 %wt., while amorphous phase of STF is 74 %wt. The difference between the two experiments is the treatment time, while each sample is treated in room temperature. Polymerization is completed faster at high temperature (Burgos-Cara et al., 2017). Even if TEOS hydrolysis is considered complete, according to Barbarena-Fernandez et al. (2015), it could be ascertained that consolidation remains ongoing for a period more than a month. In this stage, the chemical reaction of silanol groups is in progress due to the addition of TEOS solution and the simultaneous dissolution of asbestos silica matrix. Calcium carbonates that are originated from ACW, are responsible for the necessary additional time in order to the consolidation be accomplished. The particles of carbonated minerals are difficult to effectively undergo interfacial bonding with siloxanes (Barbarena-Fernandez et al. 2015).

Thus, it is evident that oxalic acid is able to induce asbestos fibers dissolution, while in parallel plays a catalytic role in the hydrolysis of TEOS and the subsequent formation

of an amorphous silica network (Rozalen & Huertas, 2013). Calcium cations contained in ACW are diffused in the solutions and they are responsible for calcium oxalate formation. According to Burgos-Cara et al. (2017), calcium interaction with oxalic acid is resulted the formation of calcium oxalate. The acidic pH (1.9) and the presence of water in the procedure is the reason for monohydrated calcium oxalates formation, whewellite, while calcium oxalates dehydrated (whedellite) are crystallized in basic pH and high humidity environment. Additionally, oxalic acid interaction with asbestos fibers is the reason of neo-formed magnesium oxalate (Valouma et al., 2016), found as traces in STF sample (Figure 6.9).

The XRD and FTIR results prove that these treatments occurred with TEOS/ISP mixture addition have led to asbestos minerals destruction and conversion of ACW mainly in amorphous silicate mineral. In this treatment the OH ions of brucite assisted the basic hydrolysis of TEOS and the formation of the silanol network after the dissolution of Mg-OH bonds (Valouma et al., 2016).

The combined experiments STF, STG, and SWG were achieved the decomposition of asbestos fibers. Although, the advantage of STG treatment was the production of amorphous silicate mineral. These results are coming to superinduce a valuable material derived from AC transformation. The high percentage of amorphous silica in the secondary raw material STG (90 %wt.) renders it suitable for reuse as partial replacement or additive in binders (cement, lime etc.) for hydraulic mortars production and as raw material for the production of alkali activated materials, contributing to the protection of the environment, human health and the conservation of natural resources.

Chapter VII: Pozzolanic reactivity

Abstract

Pozzolanic reactivity of materials is investigated by measuring the reaction rate between the relevant material and calcium hydroxide. The characteristics of treated asbestos containing waste as the chemical composition and the high content of amorphous silica consist the main reason of the investigation of potential pozzolanic reactivity.

Pozzolanic reactivity determination is evaluated based on an accelerated method (NF P 18 - 513) that determines lime-pozzolan reaction and quantifies the pozzolanic reaction measuring Ca(OH)_2 reduction in presence of pozzolans. This method is a fast and accurate way to determine the pozzolanic reactivity of a material.

The long-term pozzolanic reactivity of the material, as supplementary cementitious material in mortar specimens is evaluated via Strength Activity Index (EN 450-1). Thermogravimetric analysis is also conducted in the specimens in order to understand the pozzolanic reaction through the consumption of Ca(OH)_2 and the formation of calcium silicate hydrates.

7. Pozzolanic reactivity determination

7.1 Direct determination of calcium consumption (Chapelle test)

The pozzolanic reactivity of studied materials has been evaluated through direct determination of calcium consumption. The proposed ACW treatments produced several by-products. Due to relatively high silica content of these materials, all of them were investigated over pozzolanic properties. Additionally, a sample of SF was also tested in terms of pozzolanic reactivity as control sample. SF is considered one of the most common contemporary used pozzolanic materials in the construction sector. Its pozzolanic properties and advantageous characteristics are very well documented (Siddique, 2011, Massazza 1998).

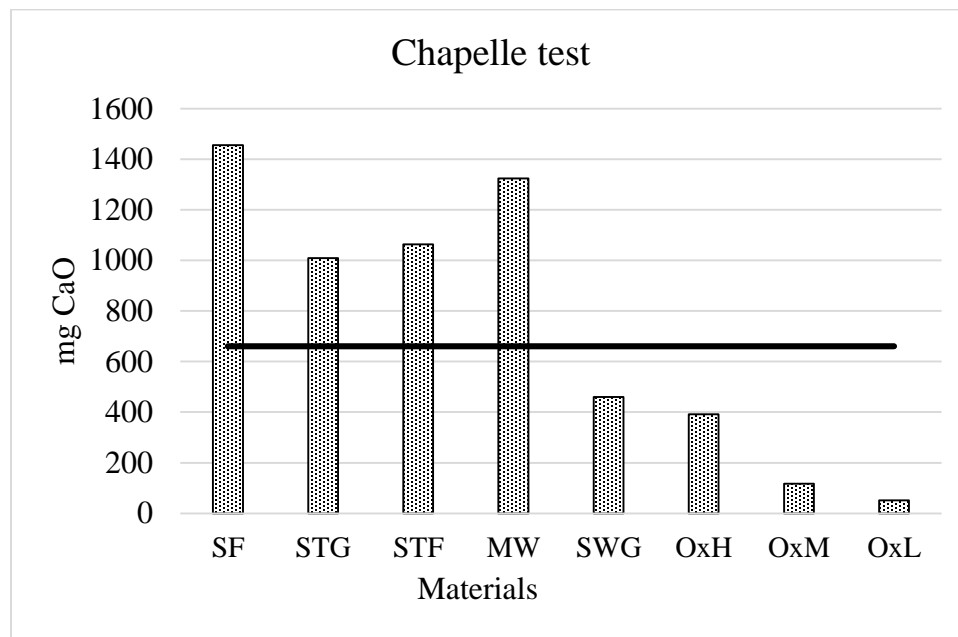


Figure 7.1: Calcium consumption of tested materials. The reference line corresponds to the threshold value indicated in NF P 18 -513

The results are reported in Figure 7.1. A mixture of CaO and the by-product of each treatment were tested as described in Chapter 4. According to NF P 18-513, the amount of CaO consumed by each material should be higher than 660 mg per 1 g of studied material (Table 7.1) in order for a material to be considered as a pozzolan. The solubility of CaO varies with temperature, so the whole procedure took place in triplicates and constant temperature to ensure its accuracy. The obtained results demonstrated in Figure 7.1 establish the pozzolanic reactivity of SF, STG, STF and MW samples. On the other hand, SWG, OxH, OxM and OxL reacted with CaO but in a lesser extent, as expected due to chemical composition of these materials ($\text{SiO}_2 + \text{Al}_2\text{O}_3 + \text{Fe}_2\text{O}_3 < 70\%$) and relatively low amorphous content. Even if the silica content is high, the amorphousness is also necessary. High crystallinity of a material renders the containing silica less reactive. Active silica is

considered the part of silica that is able to react with calcium hydroxide which leads to the formation of calcium silicate hydrates (CSH).

Table 7.1: Calcium consumption of tested materials

Material	SF	STG	STF	MW	SWG	OxH	OxM	OxL
CaO (mg/g)	1455	1009	1064	1324	460	392	116	51

This method is a fast and accurate way to determine the pozzolanic reactivity of a material. However, reactivity rate depends on a set of parameters related to the use of materials for the production of mortars, such as fineness, specific surface area, binder composition (cement, lime, etc.), pozzolan percentage in the binder, water/binder ratio (Sanjuan et al, 2015). Therefore, the degree of activity in cement mortars is studied for selective materials.

7.2 Strength activity index

A material is considered pozzolanic if $SAI \geq 75\%$ (EN 450-1). The results are calculated as mean values of triplicates. The compressive strength of the control mortar at 28 days was 48 MPa. Figure 7.2 illustrates the results of the mortars, produced by replacing 10 %wt. of the Portland cement with each studied material. Even if pozzolanic materials react slowly with calcium hydroxide, the results of SAI obtained at 28 days of curing, confirm the results of Chapelle test of pozzolanic activity, as SAI is higher than 75% for all the examined samples.

Specifically, it is observed that the addition of SF, STG, STF to the produced mortars as cement replacement cause decrease of obtained compressive strength. On the other hand, MW addition in the mortars results increase of the compressive strength at 28 days of curing. That effect is attributed primary to the pozzolanic reaction due to high content of amorphous phase (80 %wt.) and fine particles of the material ($d_{90} = 60 \mu\text{m}$), but also due to the presence of chrysotile asbestos fibers at percentage 4 %wt. (PDF 00-025-0645) in the initial material, according to quantitative mineralogical analysis (Section 6.5). Even if MW promises high pozzolanic reactivity and improvement on Portland cement mortars, it was chosen that this is not going to be investigated further. Asbestos presence, even in low proportions, renders the produced mortars hazardous, and this is in contrast with the overall approach of this dissertation.

It is noticed that the SAI value of STG sample is higher than the one of SF (94% and 86% respectively), in contrast with Chapelle test results (Table 7.1) This is probably attributed to the slightly finer particles of STG (STG $d_{90} = 170 \mu\text{m}$, SF $d_{90} = 200 \mu\text{m}$) in association with CaO content (Table 6.4). An increase of the specific area or a decrease of particle size is responsible for higher reactivity such as there is greater surface area to be conducted the chemical reaction. The effect of particle size and specific surface area on pozzolanic

reaction and mechanical properties will be discussed further in Section 7.3. Additionally, a limited excess of CaO content may enhance the reactivity of the pozzolanic material with cement composites. Strength is related with a set of parameters. Permeability, porosity, chemical composition of cement and additives, particle size distribution, curing period affect, among others, the strength development (Donatello et al., 2010). For the purpose of this study the control samples used for SAI calculation were produced according to EN 196-1, without cement replacement.

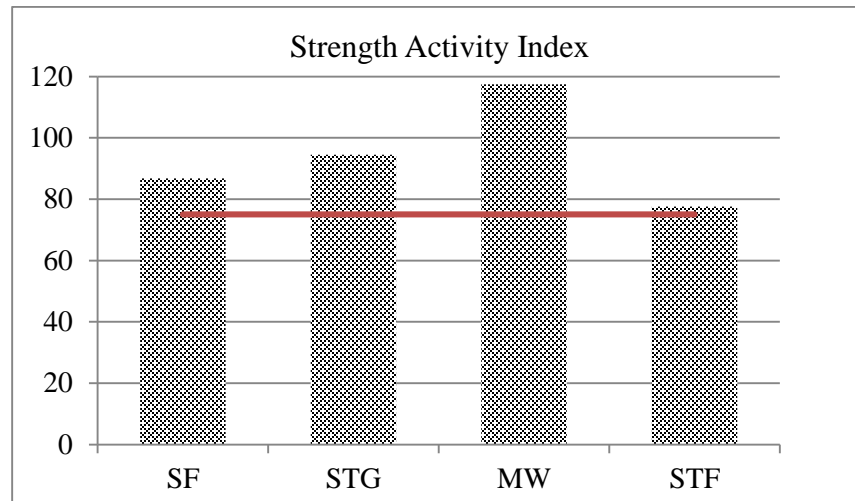


Figure 7.16: SAI results at 28 days. The reference line corresponds to the threshold value indicated in the EN 450-1

7.3 Fineness and diffraction particle size

The physical properties of the studied pozzolanic materials (SF and STG) are shown in Table 7.2. The estimated values are compared with typical values of silica fume according to the American Concrete Institute (ACI 363R-92). It is observed that STG sample, produced during this thesis, is finer than commercial SF (SF 920D, Topkon).

SF consists of fine spherical particles, and more than 90% of these are finer than 200 μm , while 50% are finer than 61 μm . SF is a highly active commercial pozzolanic material due to its fineness and high silica content of amorphous form (~87%). Additionally, its fineness leads to high specific surface area (20694 m^2/kg).

STG is an even finer material. More than 90% of its particles are finer than 170 μm while 50% are finer than 48 μm . The specific surface area of this material was measured at 376244 m^2/kg , significantly higher than SF value. These extremely high values are in accordance with typical literature values of specific surface area concerning sol-gels produced using TEOS (Parale et al., 2018, Feng et al., 2016).

Table 7.2: Physical characteristics of SF, and STG compared to typical properties of silica fume according American Concrete Institute (ACI 363R-92)

Sample	Particle size		Specific surface area (m ² /kg)	Bulk density (kg/m ³)	Amorphous content (% wt.)
	d ₉₀ (μm)	d ₅₀ (μm)			
SF (densified)	200	61	20694	654	99
STG	170	48	376244		90
SF (typical values)	<1 - 300	0.1-70	13000-30000	480-720	-

Reactive silica is found in amorphous and vitreous part of silica. Its non-crystalline structure renders it appropriate for reinforcement of cement mortars, as supplementary cementitious material, such as it reacts with calcium to the formation of the desired CSH gel. This pozzolanic effect is highly affected by fineness of the pozzolanic material. Therefore, higher strength might be obtained by mortars produced with the finer admixture. Fine materials of these particle size distribution act beneficially at cement mortars such as they act both as fillers and reinforcements.

On the other hand, STG with smaller particles could result to a reduction of mortar workability, since the water demand of mortars containing smaller particles is increased. Particle size distribution also affects the workability of the binders. The particle size distribution of SF is narrower than STG. A wider particle size distribution would result to better workability and lower water demand (Sanjuan et al., 2015).

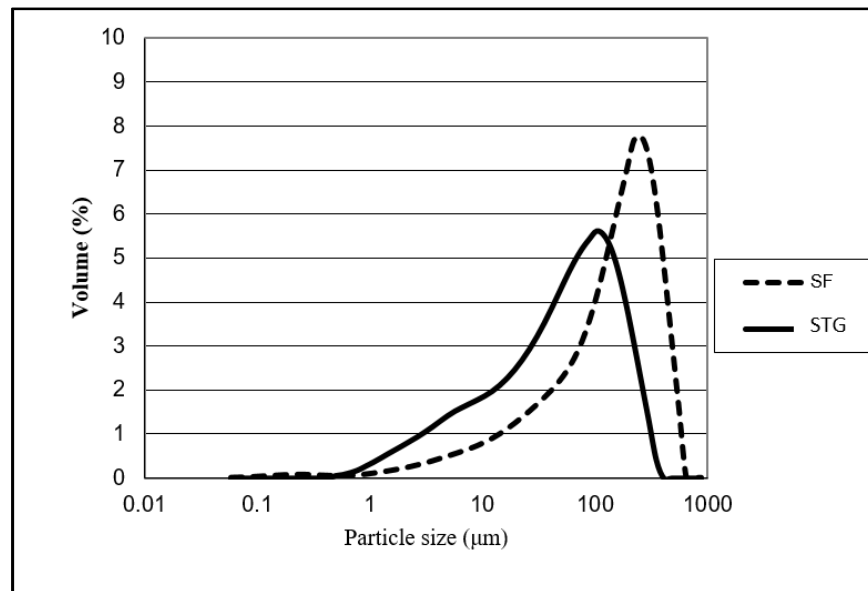


Figure 7.3: Particle size distribution of SF and STG samples

7.4 Evaluation of pozzolanic activity by thermal analysis

Several studies have been conducted demonstrating the relationship between the consumption of $\text{Ca}(\text{OH})_2$ into the mortars and the pozzolanic reactivity. (Deboucha et al., 2017, Kim & Olek, 2012, Moropoulou et al., 2003, Roszczynialski, 2002). Pozzolanic activity of materials depends on various parameters, as their chemical composition, crystallinity of their phases, particle size distribution, specific surface area etc. Both chemical composition and crystal phases are responsible for active silica content, whose presence in cement paste leads to the formation of calcium silicate hydrates (CSH phase), responsible for the increase of compressive strength (Roszczynialski, 2002). In order for the reaction that leads to CSH formation to be conducted, calcium ions are consumed by silica and as a result calcium hydroxide content is reduced. Therefore, the reduction of calcium hydroxide and the increase of CSH in cement pastes containing mineral admixtures is considered to be a reliable indicator of pozzolanic reactivity of the materials.

TG-DTA curves of the control mortars, produced with CEMI and CEMII/A-LL, and the reinforced mortars are plotted in Figures 7.4-7.5. DTG thermograms present three major endothermic peaks. The first one indicates the dehydration of CSH and ettringite at about 100 °C (Hewlett & Liska, 2019). A slight temperature variation of this peak, denoted by $\text{CaO}:\text{SiO}_2$ ratio of hydrated cement pastes, is observed. The second peak illustrated at about 450 °C is attributed to $\text{Ca}(\text{OH})_2$ decomposition, where carbon monoxide is released, and thereafter the remaining product is calcium carbonate of which the decomposition is represented by the third peak at around 730 °C. This step is related to calcium carbonate transformation to lime (CaO) due to carbon dioxide release. The total weight loss corresponds to water loss of hydrates up to 900 °C.

7.4.1 $\text{Ca}(\text{OH})_2$ content

The weight loss due to $\text{Ca}(\text{OH})_2$ decomposition estimated from the TG curves for the temperature range is indicated by the corresponding peaks of derivative curves. $\text{Ca}(\text{OH})_2$ content was determined according the equation:

$$\text{Ca}(\text{OH})_2 = \frac{74.1}{18} \frac{M_s - M_e}{M_c}$$

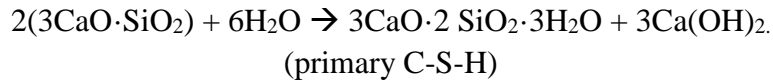
Where, M_s and M_e are the corresponding mass of the start and end points of the temperature range, and M_c is the total mass of the studied sample (Kim & Olek, 2012). Since this equation refers to anhydrous cement paste, the factor 74.1:18 is attributed to the molar weight ratio of $\text{Ca}(\text{OH})_2$ to H_2O (Vedalakshmi et al., 2003).

$\text{Ca}(\text{OH})_2$ content variation for several syntheses is presented in Table 7.3. It is observed that $\text{Ca}(\text{OH})_2$ content is higher at control mortars in comparison with the mortars with minerals addition. The simultaneously reduction of $\text{Ca}(\text{OH})_2$ accompanied by the increase

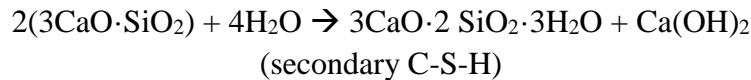
of the CSH (Figure 7.4_{b,c} and 7.5_{b,c}) indicate the pozzolanic reaction. In control mixtures the hydration process results to calcium hydroxide production.

There are two competing reactions that take place at the same time in pozzolanic mortars. Firstly, it occurs the hydration reaction which results to hydrates and calcium hydroxide production. At the same time, active silica of the pozzolans (STG and SF) consume the available calcium hydroxide forming calcium silicate hydrates (Figures 7.4_{b,c} and 7.5_{b,c}). The reduction of Ca(OH)₂ is higher in specimens containing STG than SF indicating higher pozzolanic reactivity of STG (Figures 7.4_d and 7.5_d). Expect from high active silica content, pozzolanic reactivity is also aiming by the higher specific area of STG.

Both the control and the reinforced mortars produce CSH due to primary hydration reaction:



Although, if a pozzolanic material is incorporated in cement pastes, there is a secondary hydration reaction that takes place slowly, since pozzolanic reaction continued till 365 days. This reaction leads to secondary CSH as follows (Vedalakshmi et al., 2003, Tam et al., 2006):



The unreacted Ca(OH)₂ reacts with carbon dioxide under the formation of calcium carbonates, which is the product of lime carbonation. The reaction follows the equation (Černý, et al., 2006):

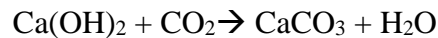


Table 7.3: Percentage of Calcium hydrates content after 90 days of curing

Specimen type	Ca(OH) ₂ (%)
CEMI-control	3.72
CEMI-STG	1.83
CEMI-SF	2.81
CEMII-control	3.69
CEMII-STG	2.06
CEMII-SF	2.80

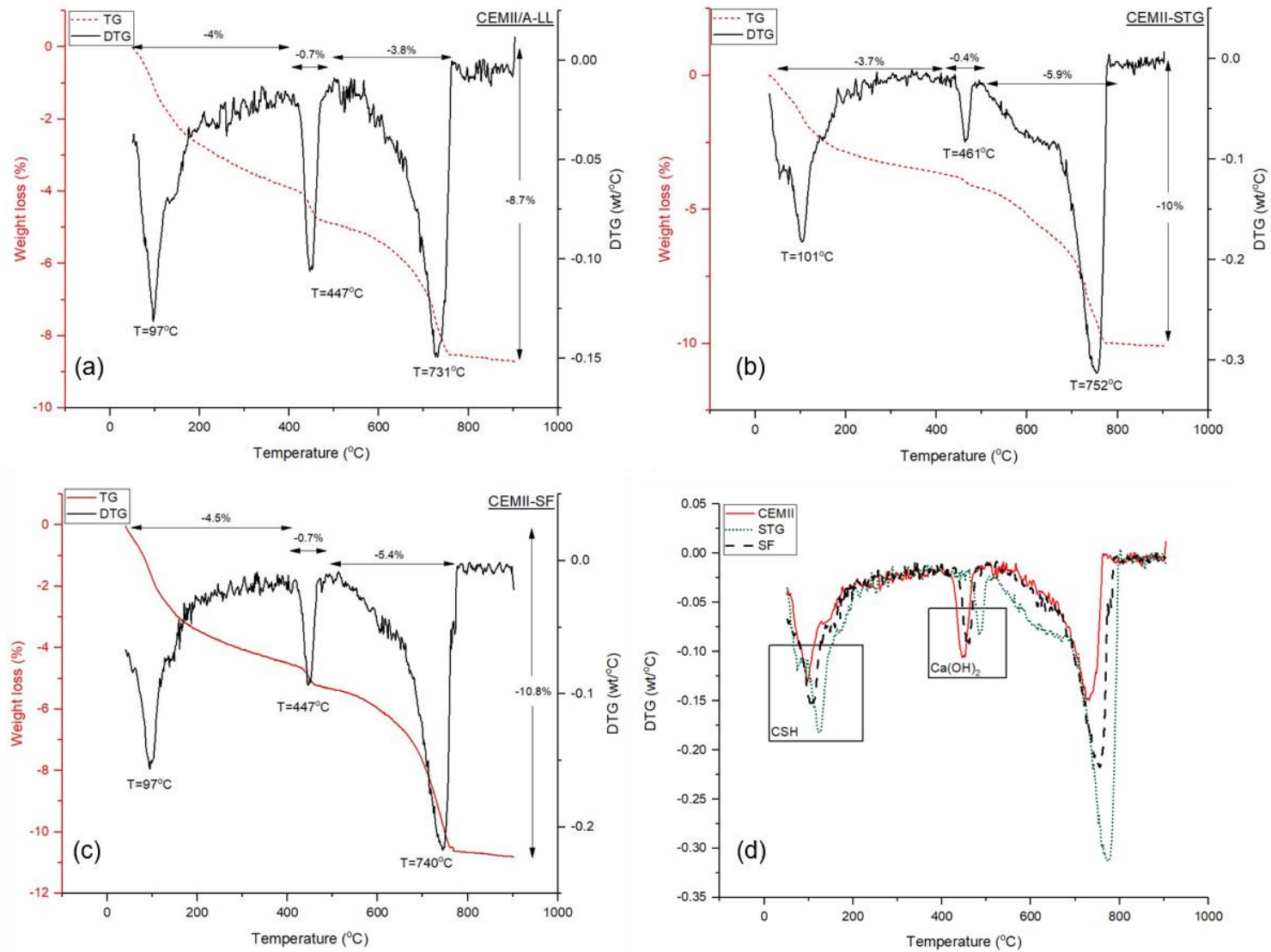


Figure 7.4: DTG/TG thermograms for the CEMII/A-LL based mortars (a-c) for 90 days of curing and comparative DTG curves of three cements syntheses

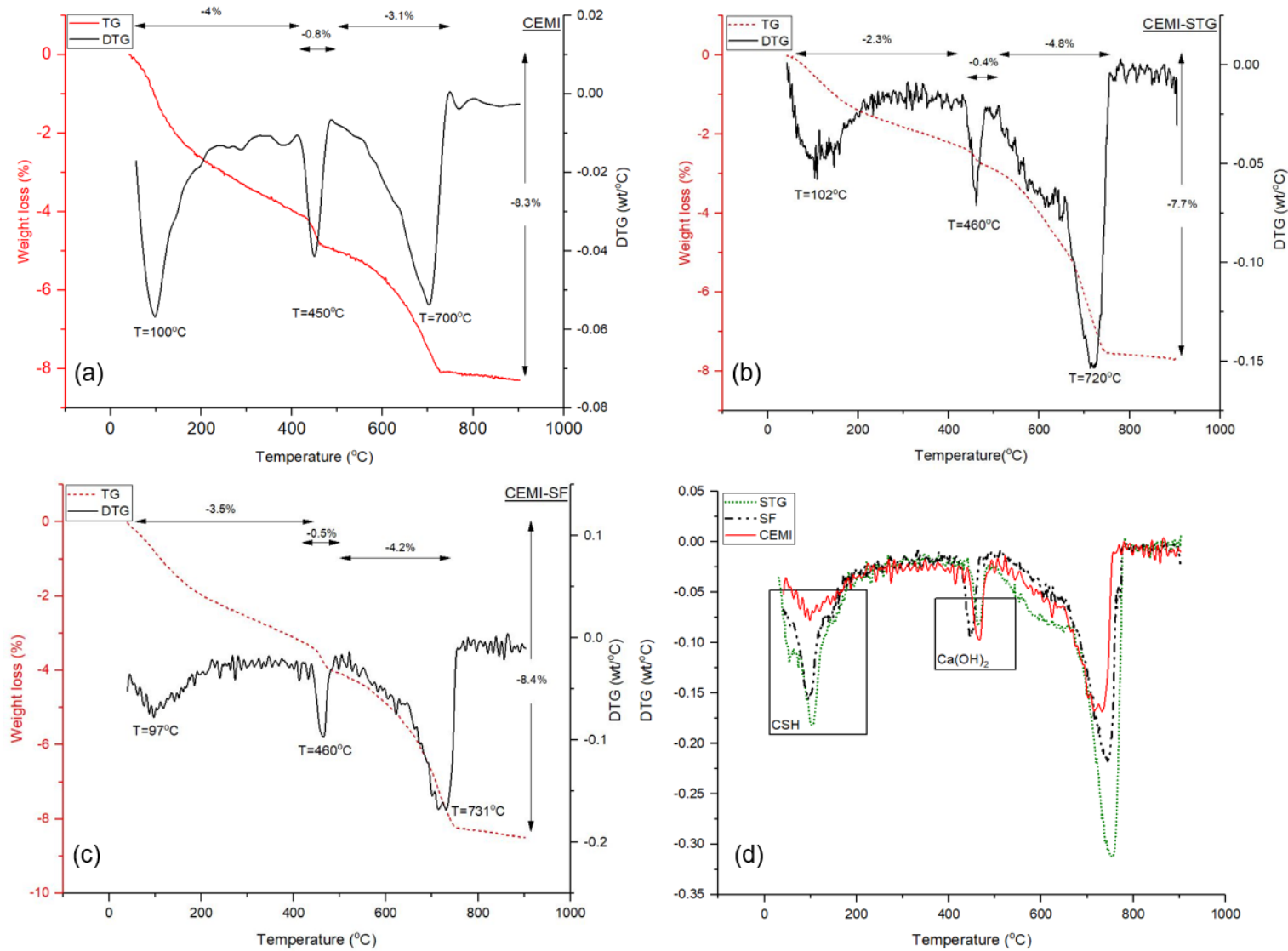


Figure 7.5: DTG/TG thermograms for the CEMI based mortars (a-c) for 90 days of curing and comparative DTG curves of three cements syntheses

Chapter VIII: Recycle of artificial pozzolan as supplementary cementitious material

Abstract

This chapter studies, in a laboratory scale, the possibility of the recycle of the treated material as secondary raw material with pozzolanic properties, to produce building elements with advantageous characteristics. Two commercial types of cement, CEMI 42.5N and CEMII/A-LL 42.5N, standard sand as aggregate and silica fume as additive are used for the mortars production.

Mixing of the materials, casting into moulds and curing were carried out according EN 196-1. After 90 days of curing, specimens are tested (according to EN) for their strength in uniaxial compression, in order to be determined the effect of artificial pozzolan and silica fume as supplementary cementitious materials. Additionally, porosity, density and water absorption are also measured. It is chosen the synthesis which results the most advantageous characteristics on cement mortars concerning each cement type.

8. Recycle of artificial pozzolan as supplementary cementitious material

8.1 Non-Destructive Evaluation of cement mortars using Ultrasonic Pulse Velocity

In order to identify the maximum percentage replacement of cement that does not affect the quality of the mortar, it was produced specimens of different syntheses. The percentage of cement replacement ranged from 1.5 %wt. up to 30 %wt. SF and STG show high wettability as a result of their high specific area, 20694 and 376244 m²/kg respectively. These properties facilitate the development of van der Waals forces between the particles, resulting in agglomeration and increased water demand (Senff et al., 2014). It was observed that the addition of water in the mixture is necessary so as to obtain the desirable workability, when admixtures proportion is higher than 5 %wt. This may be attributed to the small particles size and thereafter high specific surface area of the materials, or agglomeration of the admixtures that can trap water in the agglomerates reducing its contribution to the mixture (Juenger & Siddique, 2015). The water/binder ratio ranged between 0.48 and 0.58.

All the UPV measurements conducted according to BS 1981- 203. Figure 8.1 illustrates the UPV measurements, where it is indicated notable decrease of mortars quality with the increase of water for w/b ratio higher than 0.53. Figure 8.1 demonstrates that the correlation between w/b ratio and the quality of the mortars is significant ($R^2= 0.94$). It is noteworthy that this correlation is representative for both studied materials.

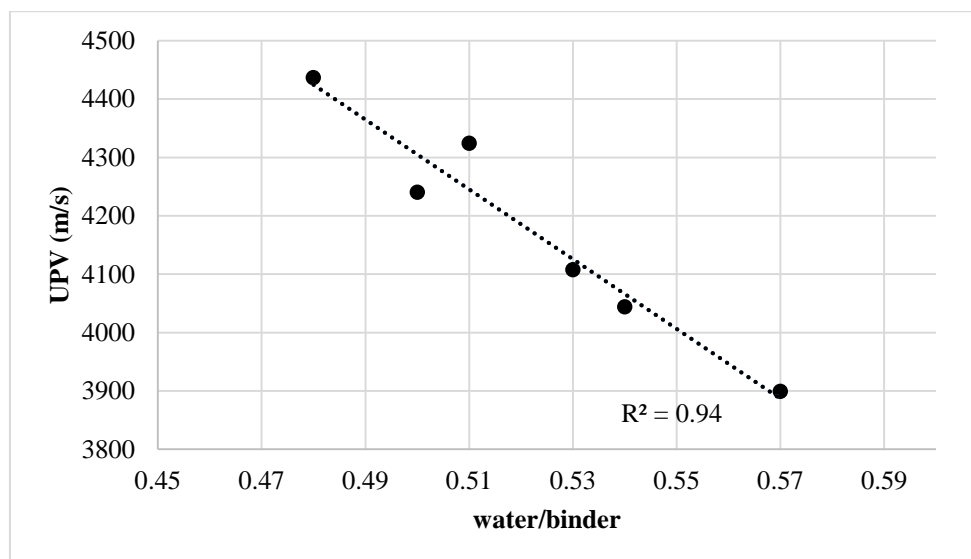


Figure 8.1: Correlation between water/binder ratio and the quality of the mortars

Figures 8.2 and 8.3 illustrate the UPV development during ageing, for specimens produced by replacing cement up to 5 %wt. It is observed that the increase rate of UPV decreases when the proportion of cement replacement increases. Nevertheless, all produced specimens are classified as “good” regarding their quality according to BS 1982-203, rendering their results accurate. There is no indication for internal cracking or excess of trapped air in the voids. The decrease of UPV after cement replacement (in comparison with the control mortar) is considered to be due to the pozzolanic properties of the admixtures. It is well known that

pozzolanic reaction is characterized by slow rate (Yildirim et al., 2018), and the addition pozzolans do not contribute to compressive strength development at early stages. This is attributed to the reaction of pozzolans with calcium hydroxide of Portland cement, which has first to be produced by cement hydration. (Senhadji et al., 2014). So, the admixtures, in this ageing period, contribute to the mortar mainly as filler in the paste. This view is reinforced by the observation of UPV change rate for similar replacement percentages, regardless the material selection (STG or SF).

Comparing the results of the specimens produced using different cements, it is noted that the change rate of UPV of the CEMII/A-LL specimens is lower. This is attributed to the synthesis of cement binder, since CEMII/A-LL has an excess of limestone (approximately 10 %wt.). This content facilitates the rate of pozzolanic reaction, accelerating the cement hydration at early stages.

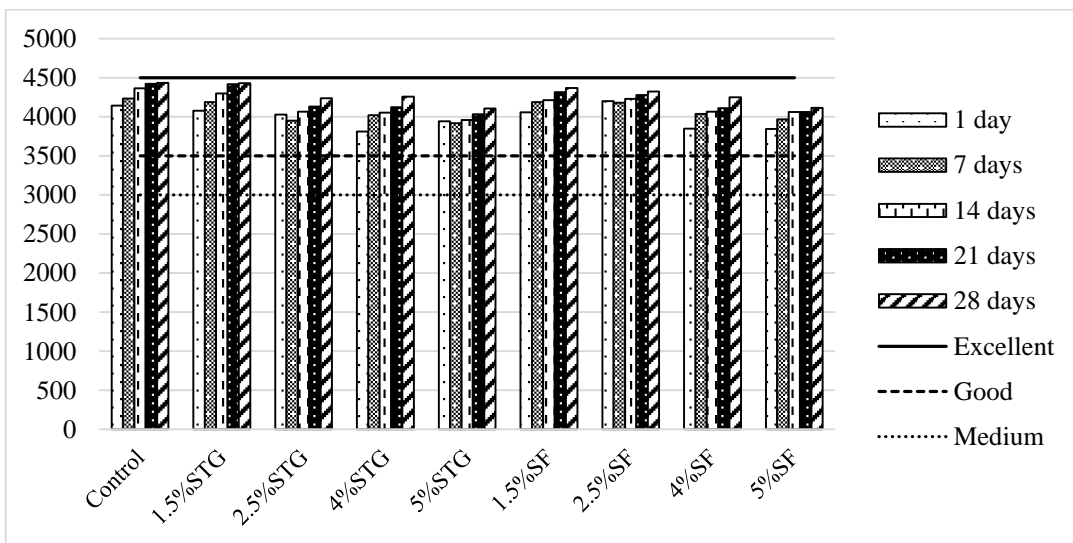


Figure 8.2: UPV measurements of CEMII/A-LL based mortars

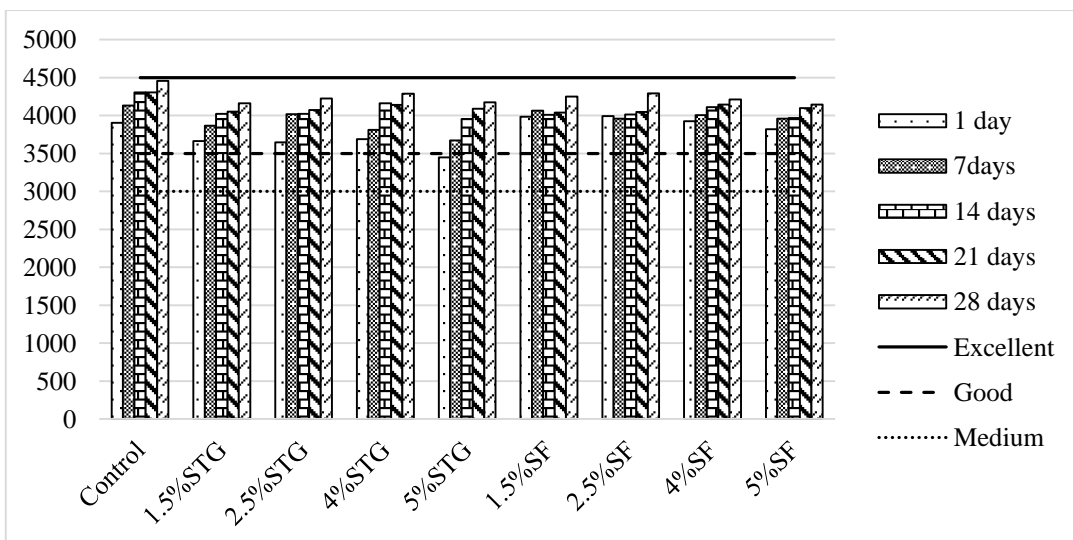


Figure 8.3: UPV measurements of CEMI-based mortars

8.2 Compressive strength

8.2.1 Selection of admixtures proportions

Figure 8.4 shows the effect of fine minerals addition on water demand of the binder. It is noteworthy that the cement type does not affect differently the water requirement of cement paste varying the proportion of fine pozzolanic admixtures. Addition beyond 5 %wt. results increasing water demand at higher ratio than 0.5. Figure 8.4 illustrates the effect of additional water on compressive strength of specimens. The results show that if the ratio of w/b is higher than 0.55 (corresponding at cement replacement higher than 5 %wt.), there is a significant decrease in compressive strength at 25.6%, although the quality of the specimens is classified as “good” according to UPV measurements (Table 4.7). It is observed a high correlation ($R^2=0.942$) between w/b ratio and the obtained compressive strength of cement mortars. Taking under consideration the correlation between w/b and Cs development, specimens synthesized by replacing cement up to 5 % wt. with constant w/b ratio at 0.48 were produced.

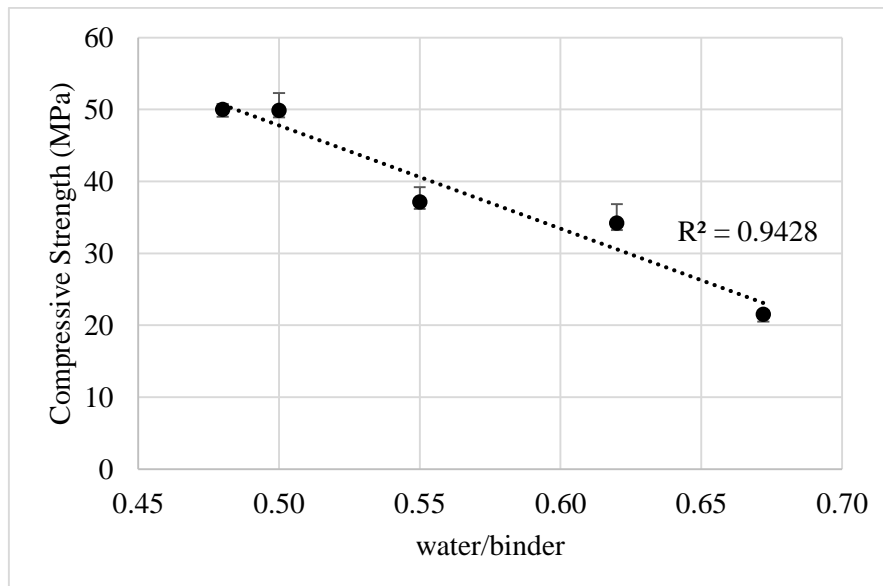


Figure 8.4: Correlation between water/binder ratio and compressive strength

8.2.2 Effect of silica fume

Figure 8.5 shows that the addition of SF at proportions 1.5-5 % wt. does not affect significantly the development of Cs at 28 days. The slight reduction of Cs is coming in accordance with the literature (Khedr & Abou-Zeid, 1994) where it was shown that the replacement of cement by SF results to the reduction of Cs at early stages. The addition of SF at 1.5 %wt. is considered to be the optimum amount of replacement for the mortars produced using CEMI cement. This admixture proportion is responsible for Cs reduction of 5% at 28 days of curing, while after 90 days the Cs is increased by 15%. The increase of SF continues but in a lower rate (8% at 90 days) when SF is added at 2.5 %wt. The addition of higher quantity of SF in the mortar results to the decrease of the Cs, accompanying the indications of UPV measurements referring to the quality of these specimens.

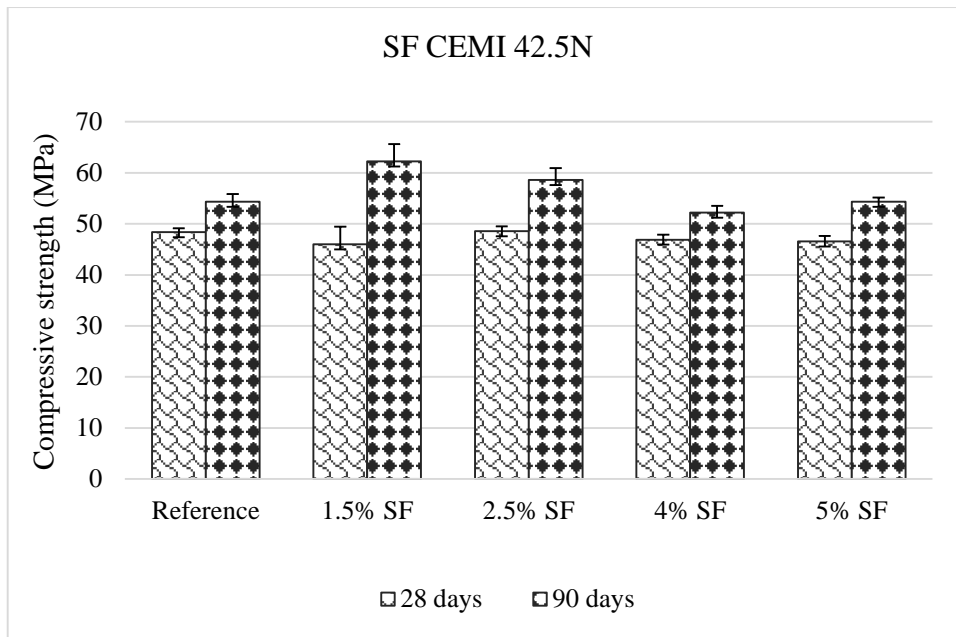


Figure 8.5: Compressive strength (MPa) of CEMI-based mortar specimens produced with SF addition cured for 28 and 90 days

Replacement of CEMII/A-LL cement by SF decreases the Cs at all ages of curing (Figure 8.6). Replacement at 1.5 % wt. does not affect the development of Cs at 28 days ($<1\%$), while at 90 days the Cs reduces by 10%. Higher content of SF in the binder mixture affects similarly the mortars. The Cs of specimens produced with SF addition 1.5-5 % wt. ranged from 50.4 to 56.6 MPa, while the Cs of control specimen amounts to 58 MPa. Furthermore, the decrease rate is increasing during time, in contrast with the results of CEMI cement-based specimens. This is probably attributed to the excess of limestone in CEMII/A-LL binder, which facilitates the pozzolanic reaction at early stages, since the desired calcium is provided. On the other hand, the early consumption of calcium prevents the proper cement hydration and hardening (Senhadji et al., 2014).

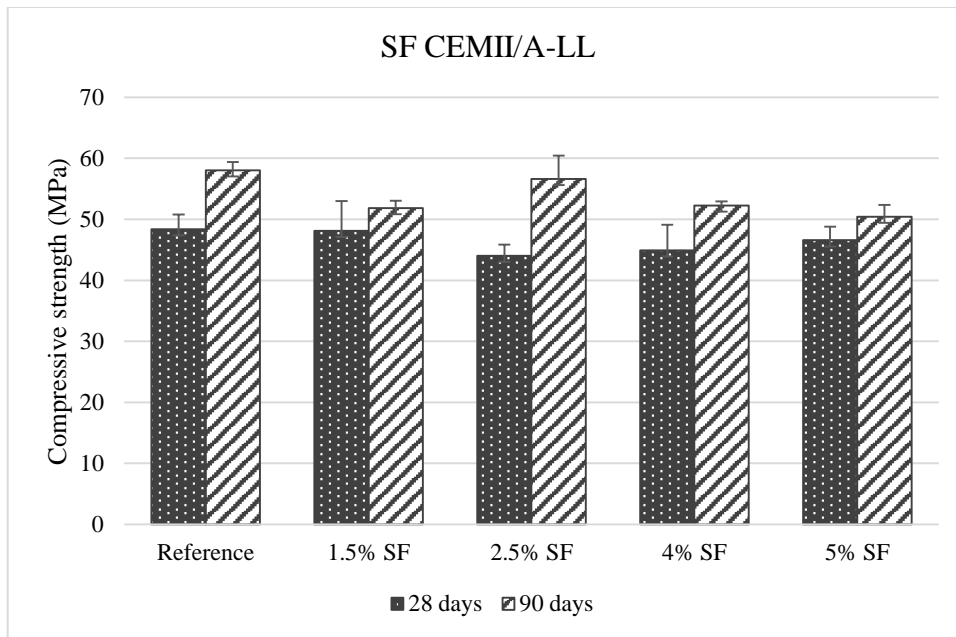


Figure 8.17: Compressive strength (MPa) of CEMII/A-LL based mortar specimens with SF addition cured for 28 and 90 days

8.2.3 Effect of artificial pozzolan STG

The influence of artificial pozzolan on the compressive strength of CEMI and CEMII/A-LL mortars are illustrated in Figures 7.7-7.8 Concerning the CEMI cement mortars (Figure 8.7), STG addition reduced 28 days-compressive strength of specimens produced with 1.5, 2.5 and 5 %wt. cement replacement, with the exception of the specimens with 4 %wt. cement replacement where the 28 days-compressive strength increased. A reduction of 8, 14 and 8% was observed regarding 1.5, 2.5 and 5 %wt. cement replacement, respectively. On the other hand, increase of compressive strength development was observed with increase of curing time at all samples. The most beneficial influence at 90 days of curing was reported at sample with 15 %wt. cement replacement, where the compressive strength was increased 21% comparing with the reference mortar at same curing time. Specifically, this optimal specimen reached a compressive strength value of 66 MPa, while the mortars with the same SF addition and the control specimen reached 62 MPa and 54 MPa., respectively.

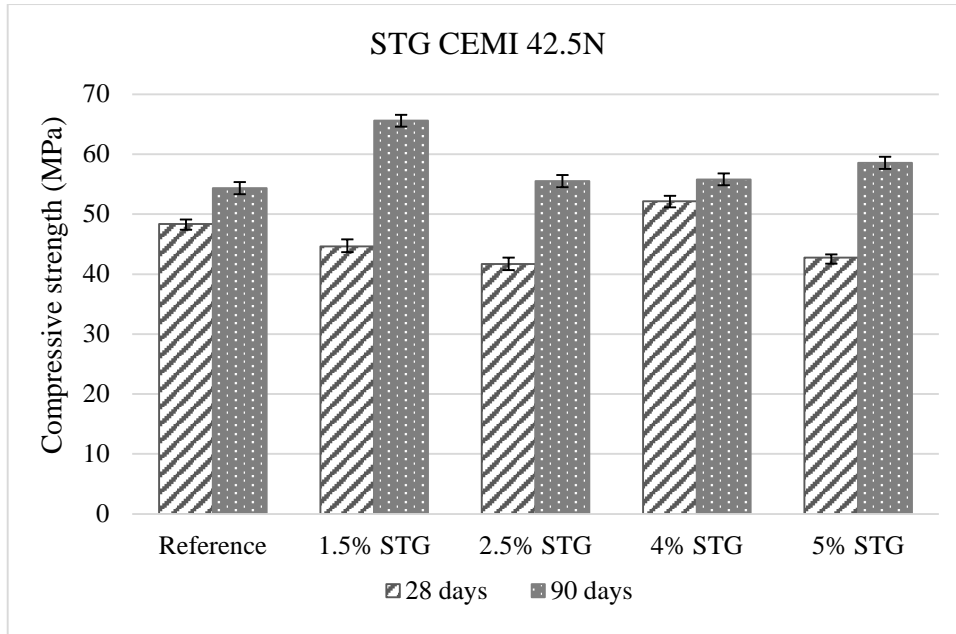


Figure 8.7: Compressive strength (MPa) of CEMI-based mortar specimens produced with STG addition cured for 28 and 90 days

Concerning the mortars produced using CEMII/A-LL cement (Figure 8.8) STG addition induced an increase in the compressive strength up of all specimens cured for 28 days. STG addition in CEMII/A-LL-based mortars is considered beneficial concerning early stage strength (1-14% higher than control), while a reduction of 90 days-compressive strength (3-18% lower than control), with the exception of the specimens with 2.5 %wt. cement replacement where the 90 days-compressive strength slightly increased. Excess limestone accelerates the development of early stage strength. The higher early age compressive strength value was obtained by the specimen with 1.5 %wt. cement replacement with STG, reaching 55 MPa, 13% higher than the control specimen for the same days of curing (48 MPa). However, the compressive strength of the same synthesis at 90 days of curing was 8% lower than the control specimen (58 MPa).

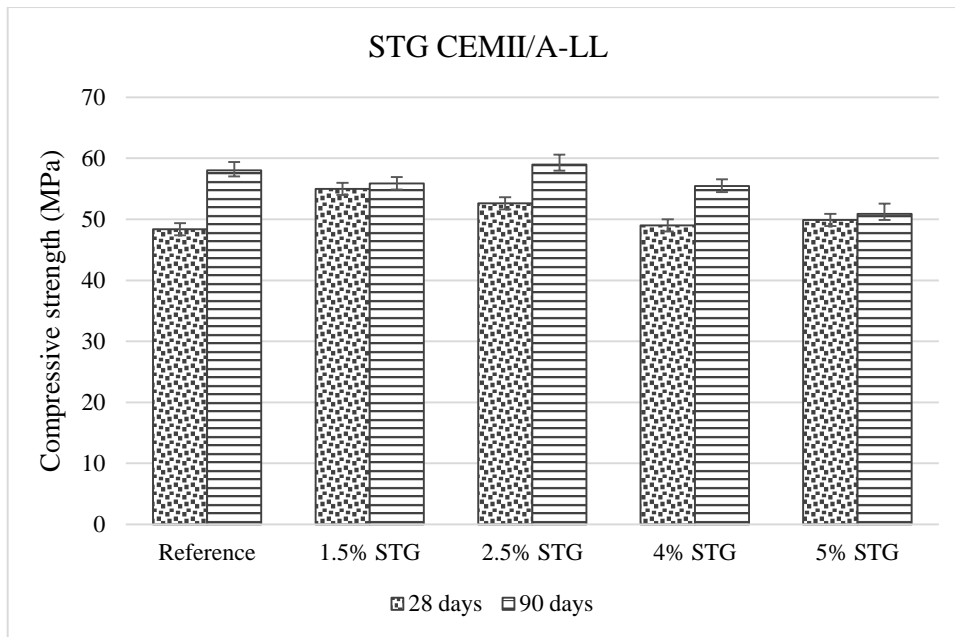


Figure 8.8: Compressive strength (MPa) of CEMII/A-LL-based mortar specimens produced with STG addition cured for 28 and 90 days

8.3 Properties of selective specimens

Table 8.1 summarizes the physical properties, compressive strength, density, porosity, and $\text{Ca}(\text{OH})_2$ content of control mortars and the optimal syntheses with pozzolans. It is noticed that the specimens with STG composite as admixture, which results at higher compressive strength and CSH production, have slightly higher porosity and higher density. Increased density due to SF addition, with round particles, it would be responsible for prevention of the pozzolanic reaction and thus the production of secondary CSH. The simultaneously decreased amount of hydrates and densified pore structure is observed regardless the cement type (CEMI, CEMII/A-LL).

Additionally, the even lower porosity of reference mortars is probably attributed to the high unreactive cement particles, which are not able to produce hydrates and act as fillers of the paste, resulting a beneficial effect on permeability of the mortars without any contribution to the final compressive strength. The lower permeability of blended cement mortars is attributed to more densified pore structure due to additional CSH. (Vedalakshmi et al., 2003).

Table 8.2 presents the minimum compressive strength requirements for different exposure classes according to classification categories (EN 206-1: 2000), while Figure 8.9 illustrates the compressive strength of the optimal specimens that produced in this thesis, after 90 days of curing, compared to these classification categories. The compressive strength of control specimens (CEMI and CEMII/A-LL) is also provided, for comparison. It can be seen that control and blended mortars exceed the requirements of all the demanding categories of exposure.

Table 8.1: Properties of selective specimens

	CEMI		CEMII	
	Control	1.5%STG	Control	2.5%STG
Total Pore Area (m ² /g)	4.20	4.95	3.45	1.91
Median Pore Diameter (nm)	460.23	551.42	111.31	183.65
Average Pore Diameter (nm)	45.03	48.24	46.92	104.43
Bulk Density (kg/m ³)	1967	1963	2073	2090
Apparent Density (kg/m ³)	2171	2226	2266	233
Porosity (%)	9.31	11.71	8.386	10.46
Water Absorption (%)	6.93	9.35	6.74	9.37
Ca(OH) ₂ content (%)	3.70	1.98	3.72	1.82
Compressive strength (MPa)	54	66	58	59

Table 8.2: Exposure classes according EN 206-1, 2000

Exposure classes	Class designation	Informative examples where exposure classes may occur
No risk of corrosion or attack	X0	Concrete inside buildings with very low air humidity
Corrosion induced by carbonation	XC1	Concrete inside buildings with low air humidity. Concrete permanently submerged in water.
	XC2	Concrete surfaces subject to long-term water contact. Many foundations.
	XC3	Concrete inside buildings with moderate or high air humidity. External concrete sheltered from rain.
	XC4	Concrete surfaces subject to water contact, not within exposure Class XC2.
Corrosion induced by chlorides from sea water	XS1	Structures near to or on the coast.
	XS2	Parts of marine structures.
	XS3	
Freeze/thaw attack with or without de-icing agents	XF1	Vertical concrete surfaces exposed to rain and freezing.
	XF2	Vertical concrete surfaces of road structures exposed to freezing and airborne de-icing agents.
	XF3	Horizontal concrete surfaces exposed to rain and freezing.
	XF4	Road and bridge decks exposed to deicing agents. Concrete surfaces exposed to direct spray containing de-icing agents and freezing. Splash zones of marine structures exposed to freezing.
Chemical attack	XA1	Slightly aggressive chemical environment.
	XA2	Moderately aggressive chemical environment.
	XA3	Highly aggressive chemical environment.

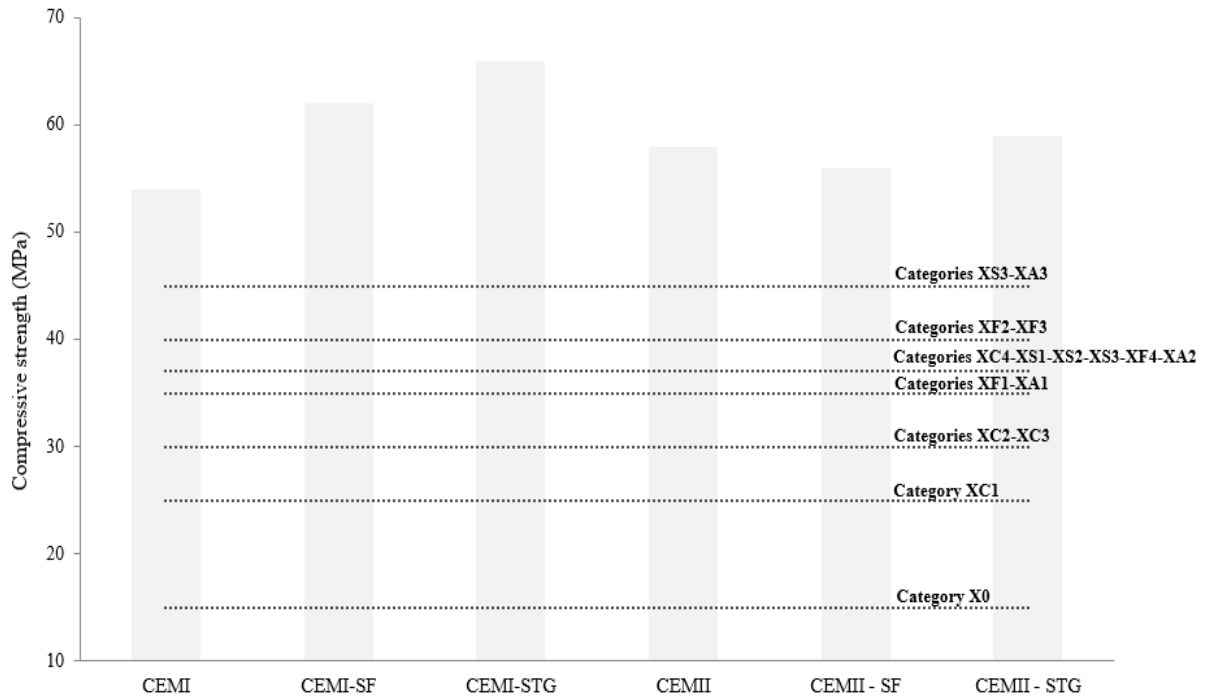


Figure 8.9: Compressive strength of specimens compared to classification categories according to EN 206-1:2000

8.4 Toxicity of the mortars

Table 8.3 presents the toxicity of the control mortar specimens and the mortars produced with STG and SF as admixtures. All the examined specimens produced are not exhibited the lower limits of toxicity as they are specified by the EN 12457-3 test for wastes accepted at landfills for non-hazardous wastes.

These results indicate the use of treated waste does not only contribute to the increase of cement mortars with high compressive strength, but ensure that they contribute to the production of safe materials that they are considered as stable cement matrixes and they do not require special landfilling after their end-of-life.

Table 8.3: Toxicity results according EN 12457-3 results (L/S=10L kg⁻¹).

Element	CEMI	CEM II	CEMI SF	CEMI STG	CEMII SF	CEMII STG	For Wastes Accepted at Landfills for Inert Wastes	For Non-Hazardous Wastes	For Hazardous Wastes Accepted at Landfills for Non-Hazardous Wastes	For Wastes Accepted at Landfills for Hazardous Wastes
	(mg/kg)						Limit values (mg/kg) according 2003/33/EC			
Ni	0.1	0.2	0.12	0.25	0.24	0.13	0.4	10	10	40
Cu	1.09	0.57	0.09	0.41	0.41	0.38	2	50	50	100
Zn	0.39	3.24	0.02	0.34	2.03	2.41	4	50	50	200
As	<D.L	<D.L	<D.L	<D.L	<D.L	<D.L	0.5	2	2	25
Cd	<DL	<DL	<DL	<DL	<DL	<DL	0.04	1	1	5
Cr _{total}	1.26	<DL	1.72	0.73	<DL	<DL	0.5	10	10	50
Pb	0.16	0.11	0.11	0.15	0.11	0.43	0.5	10	10	50

8.5 Discussion

It is well known that the pozzolanic materials do not improve the development of early strength, but worsen it instead. This is attributed to the slow rate of pozzolanic reaction. In order for the pozzolanic reaction to be conducted, calcium hydroxide should be available, since this reaction takes place between the glassy particles of pozzolans and calcium ions. Two competitive reactions take place during hydration of blended cement mortars. The prerequisite calcium hydroxide production due to Portland cement hydration and subsequently the pozzolanic reaction (Kaid et al., 2009).

It becomes understandable that pozzolanic reaction continues long-term, after the 28 days of cement hydration, producing secondary CSH, resulting densification of pore structure and increased density and as a result, thus reducing the permeability of the mortars (Senhadji et al., 2014). All these properties obtained due to pozzolanic reaction render the mortars more durable to deterioration.

Additionally, the formation of CSH gel leads to more effective consumption of the unreactive SiO₂ of the cement pastes. Hubert et al. (2001) noted that the unreacted SiO₂ of Portland cement-based pastes rise up to 15%, while in the pastes of cement blended with pozzolan that percentage varies from 6 to 9%.

Concerning the specimens produced using CEMII/A-LL as a binder, it is noteworthy that better compressive strength at early stages of curing was achieved, even if it is known that the addition of pozzolans do not improve the early strength development. This fact is attributed to the initial synthesis of CEMII/A-LL which is characterized by limestone excess up to 10%. This enables the pozzolanic reaction since at the early days of curing calcium ions are available in the mixture. So, at 28 days of curing higher strength than in control sample is obtained.

The role of limestone excess in the initial clinker of CEMII/A-LL could be either the one of inert filler or of a reactive material that participates in cement hydration. It has been

demonstrated that if excess calcite rises up to 5%, then the whole amount is considered active as a component of cement hydration procedure (Matschei et al., 2007). The cement of this current dissertation was chosen based on the availability of local market. According to Table 4.3 data providing chemical composition of the cements used, it is estimated that the content of CEMII/A-LL to calcium oxides is about 5% higher of the ordinary Portland cement (CEMI).

The reaction between the free calcium ions of calcite containing in the added limestone with available alumina occurs the first days of hydration, resulting the formation of carboaluminates. The carboaluminates accelerate the effect of hydration of predominant cementitious phases of alite (C_3S), belite (C_2S), aluminate phase (C_3A) and induce changes in the formation of CSH gel and the morphology of interfacial transition zone between the cement paste and the aggregates (Heikal et al., 2000). These all affect the development of compressive strength at early and late stages.

Specifically, the increase of compressive strength at early stages is facilitated sine the carboaluminates contribute to strength producing hydrates that reduce the porosity of the mortars. Moreover, the addition of the pozzolanic materials offers to the mixture a proportion of reactive silica able to react with the Ca^+ to the formation of CSH gel.

A significant increase in the early strength of STG and SF reinforced mortars (produced based on CEMII/A-LL) is noted. Specifically, the STG specimens obtained high strength at 28 days, while the SF specimens performed similarly with control mixtures. This is probably attributed to the calcium oxalate presence of STG (9 % wt.) which offers calcium ions to the mixture, facilitating the synergistic reaction of limestone with alumina and the pozzolanic reaction. On the other hand, the pozzolanic reaction of SF samples remains slow, since it follows the cement hydration and the formation of portlandite which contains the available calcium hydroxide.

Chapter IX: Summary and concluding remarks

The objective of this dissertation thesis is the conversion of asbestos cement corrugated sheets to non-hazardous valuable material and reuse it in the construction sector.

In particular, upon the experimental procedure, both chrysotile and crocidolite fibers are destroyed, cement phases are converted and result in secondary minerals recovery. In this line, economic and environmental feasibility are evaluated, through the examination of the most effective reagents concentration, temperature and treatment time, while at the same time, novel options on recycling of end-of-life asbestos cement waste are presented, based on the quality of the secondary raw materials produced.

Oxalic acid is not capable of fully transforming AC into harmless material, even in high concentration of the reagent. In all the proposed syntheses the decrease of asbestos presence is achieved, but the higher quantity of oxalic acid seems to be consumed by calcium, producing a large quantity of calcium oxalate.

The addition of silicate-based reagents to solutions is considered a crucial parameter to this proposed detoxification method. All by-products produced by combined methods in room temperature are considered to be fully detoxified, since chrysotile and crocidolite are not detectable.

Towards the direction of the reuse of treated waste, it is selected the STG as optimal synthesis, since it achieves the complete transformation of asbestos minerals to non-hazardous material, while it is also responsible for the greatest production of amorphous silica.

Asbestos transformation was also achieved in STF sample, but the crystalline phase of calcium oxalate presence is higher to the final product. High presence of calcium oxalate degrades the quality of treated ACW as a valuable secondary raw material. The significantly lower quantity of calcium in STG sample is notable, and it can be assumed that the reaction between oxalic acid, TEOS and ACW is continued after 30 days of treatment.

These results indicated that a valuable material derived from AC transformation. The high percentage of amorphous silica in the secondary raw material STG (90 %wt.) renders it suitability for reuse as a partial replacement or as an additive in binders (cement, pozzolan, lime etc.) for hydraulic mortar production and as raw material for the production of alkali-activated materials, contributing to the protection of the environment, human health and the conservation of natural resources.

The pozzolanic reactivity of studied materials has been evaluated through direct and indirect determination of calcium consumption. Due to silica content of these materials, all of them were investigated over their pozzolanic properties.

According to the Chapelle method (NF P 18 -513), STG, MW and STF samples are pozzolanic reactive. Strength Activity Index (SAI) indicator of pozzolanic activity, estimated according to EN 450-1, confirms the results of the Chapelle test, since SAI is higher than 75% concerning STG, MW and STF samples.

MW promises high pozzolanic reactivity and improvement in Portland cement mortars but asbestos presence, even in low proportions, renders the produced mortars hazardous, and this comes in contrast to the overall approach of this dissertation.

It is noticed that the SAI value of STG sample is higher than the one of SF (94% and 86% respectively), and this is inconsistent with the results of the Chapelle method. Finer particle size and high specific surface area of STG resulted in higher reactivity.

The maximum cement replacement was chosen based on water demand for the mixture. It was calculated that if the ratio of w/b is higher than 0.50 (corresponding to cement replacement higher than 5 % wt.), there is a significant decrease in compressive strength at 25.6%, although the quality of the specimens is classified as “good” according to UPV measurements. High correlation ($R^2= 0.94$) between w/b ratio and the quality of the mortars was estimated. The specimens were produced by replacing cement up to 5 % wt., maintaining a constant w/b ratio at 0.48.

The blended mortars produced using CEMI as a binder after 28 days of curing resulted in the decrease of compressive strength with a range of 1-13%, while after 90 days of curing the compressive strength increased up to 21% using STG as cement replacement. This is attributed to the fact that the slow pozzolanic reaction continues after the 28 days of cement hydration, producing secondary CSH, resulting in increased compressive strength. The formation of CSH gel leads to more effective consumption of the unreactive SiO_2 of the cement pastes.

The specimens produced using CEMII/A-LL as a binder achieved higher compressive strength at early stages of curing, even though it is known that the addition of pozzolans do not improve the early strength development. This fact is attributed to the initial synthesis of CEMII/A-LL which is characterized by limestone excess. This enables the pozzolanic reaction from the early days of curing, due to available calcium ions in the mixture. Compressive strength obtained at 28 days of curing is higher than the control sample.

Additionally, the reaction between the free calcium ions of calcite contained in the added limestone with the available alumina occurs during the first days of hydration, resulting in the formation of carboaluminates. The carboaluminates accelerate the effect of hydration of the predominant cementitious phases of alite (C_3S), belite (C_2S), and aluminate phase (C_3A) and induce changes in the formation of the CSH gel and the morphology of the interfacial transition zone between the cement paste and the aggregates. These alterations affect the development of compressive strength at early and late stages.

Specifically, the increase of compressive strength at early stages is facilitated since the carboaluminates contribute to strength development producing hydrates. Moreover, the addition of the pozzolanic materials offers the mixture a proportion of reactive silica able to react with the Ca^+ in order to form secondary CSH gel.

The reduction of calcium hydroxide in cement pastes containing mineral admixtures is considered a reliable indicator of the pozzolanic reactivity of the materials. TG/DTG investigation determines that $\text{Ca}(\text{OH})_2$ content is higher at control mortars in comparison to the mortars with mineral addition. The reduction of $\text{Ca}(\text{OH})_2$ accompanied by the increase of CSH indicate the pozzolanic reaction. In control specimens the hydration process results in calcium hydroxide production.

Two competing reactions take place at the same time in pozzolanic mortars. At first, the resulted hydration reaction hydrates and calcium hydroxide production occurs. At the same time, active silica of the pozzolans (STG and SF) consumes the available calcium hydroxide formatting calcium silicate hydrates. The reduction of $\text{Ca}(\text{OH})_2$ is higher in specimens containing STG than SF indicating higher pozzolanic reactivity of STG. Apart from the high active silica content this is also attributed to the higher specific area of STG.

The specimens with STG composite as admixture, which result in higher compressive strength and CSH production, have slightly higher porosity and lower density. The increased densified pore structure due to SF addition, with round particles, would be responsible for the prevention of the pozzolanic reaction and, thus, the production of secondary CSH. The simultaneously decreased amount of hydrates and densified pore structure is observed regardless of the cement type (CEMI, CEMII/A-LL).

Lower porosity of control specimens is attributed to the high unreactive cement particles, which are not able to produce hydrates and act as fillers of the paste, resulting in a beneficial effect on permeability of the mortars without any contribution to the final compressive strength.

REFERENCES

- ACI (American Concrete Institute), (2000). ACI 363R-92: State-of-the-Art Report on High-Strength Concrete. American Concrete Institute, Farmington Hill, MI, USA.
- AFNOR, NF P 18-513, (2010). Métakaolin, addition pouzzolannique pour bétons. Définitions, spécifications, critères de conformité, Paris.
- Anastasiadou, K., Axiotis, D., & Gidarakos, E. (2010). Hydrothermal conversion of chrysotile asbestos using near supercritical conditions. *Journal of hazardous materials*, 179(1-3), 926-932.
- ASTM C 150-07, (2009). Standard Specification for Portland Cement, Annual Book of ASTM Standards, Vol. 4.01, ASTM International.
- ASTM C1240 – 15, (2006). Standard Specification for Silica Fume Used in Cementitious Mixtures. Annual Book of ASTM Standards, Vol. 4.02, ASTM International.
- ASTM C125 (2007). Standard terminology relating to concrete and concrete aggregates. ASTM International, West Conshohocken.
- Barberena-Fernández, A. M., Carmona-Quiroga, P. M., & Blanco-Varela, M. T. (2015). Interaction of TEOS with cementitious materials: Chemical and physical effects. *Cement and Concrete Composites*, 55, 145-152.
- Barger, G. S., Hansen, E. R., Wood, M. R., Neary, T., Beech, D. J., & Jaquier, D. (2001). Production and use of calcined natural pozzolans in concrete. *Cement, concrete and aggregates*, 23(2), 73-80.
- Barone-Adesi, F., Ferrante, D., Bertolotti, M., Todesco, A., Mirabelli, D., Terracini, B., & Magnani, C. (2008). Long-term mortality from pleural and peritoneal cancer after exposure to asbestos: Possible role of asbestos clearance. *International journal of cancer*, 123(4), 912-916.
- Bhagat, S. D., & Rao, A. V. (2006). Surface chemical modification of TEOS based silica aerogels synthesized by two step (acid–base) sol–gel process. *Applied Surface Science*, 252(12), 4289-4297.
- Bloise, A., Catalano, M., Barrese, E., Gualtieri, A. F., Gandolfi, N. B., Capella, S., & Belluso, E. (2016). TG/DSC study of the thermal behaviour of hazardous mineral fibres. *Journal of Thermal Analysis and Calorimetry*, 123(3), 2225-2239.
- Bloise, A., Kusiorowski, R., & Gualtieri, A. (2018). The Effect of Grinding on Tremolite Asbestos and Anthophyllite Asbestos. *Minerals*, 8(7), 274.
- Bonifazi, G., Capobianco, G., & Serranti, S., (2018). Asbestos containing materials detection and classification by the use of hyperspectral imaging. *Journal of hazardous materials*, 344, 981-993.

- Boonstra, A. H., & Baken, J. M. E. (1990). Relation between the acidity and reactivity of a teos, ethanol and water mixture. *Journal of Non-Crystalline Solids*, 122(2), 171-182.
- Borges, R., Baika, L. M., Grassi, M. T., & Wypych, F. (2018). Mechanochemical conversion of chrysotile/K₂HPO₄ mixtures into potential sustainable and environmentally friendly slow-release fertilizers. *Journal of environmental management*, 206, 962-970.
- Braga, M., De Brito, J., & Veiga, R. (2012). Incorporation of fine concrete aggregates in mortars. *Construction and Building Materials*, 36, 960-968.
- BS 1881: Part 203, (1986). Recommendations for Measurement of Velocity of Ultrasonic Pulses in Concrete. British Standards Institution, London.
- BS 1881: Part 116, (1983). Method for Determination of Compressive Strength of Concrete Cubes. British Standards Institution, London.
- BS 1881-122 (2011). Testing concrete. Method for determination of water absorption. British Standards Institution, London.
- BS EN 12457-3, (2002). Characterisation of waste. Leaching. In Compliance Test for Leaching of Granular Waste Materials and Sludges. Two Stage Batch Test at a Liquid to Solid Ratio of 2 L/kg and 8 L/kg for Materials with a High Solid Content and with a Particle Size below 4 mm (without or with Size Reduction); British Standards Institution, London.
- BS EN 206-1, (2000). Concrete. Specification, performance, production and conformity, British Standards Institution, London
- Bullard, J. W., Jennings, H. M., Livingston, R. A., Nonat, A., Scherer, G. W., Schweitzer, J. S., & Thomas, J. J. (2011). Mechanisms of cement hydration. *Cement and concrete research*, 41(12), 1208-1223.
- Burgos-Cara, A., Ruiz-Agudo, E., & Rodriguez-Navarro, C. (2017). Effectiveness of oxalic acid treatments for the protection of marble surfaces. *Materials & Design*, 115, 82-92.
- Černý, R., Kunca, A., Tydlitát, V., Drchalová, J., & Rovnaníková, P. (2006). Effect of pozzolanic admixtures on mechanical, thermal and hygric properties of lime plasters. *Construction and Building Materials*, 20(10), 849-857.
- Cherry, K. F. (1988). *Asbestos: engineering, management and control*. CRC Press.
- Cihlář, J. (1993). Hydrolysis and polycondensation of ethyl silicates. 1. Effect of pH and catalyst on the hydrolysis and polycondensation of tetraethoxysilane (TEOS). *Colloids and Surfaces A: Physicochemical and Engineering Aspects*, 70(3), 239-251.
- Colangelo, F., Cioffi, R., Lavorgna, M., Verdolotti, L., & De Stefano, L. (2011). Treatment and recycling of asbestos-cement containing waste. *Journal of hazardous materials*, 195, 391-397.

- Colleoni, C., Esposito, S., Grasso, R., Gulino, M., Musumeci, F., Romeli, D., ... & Scordino, A. (2016). Delayed luminescence induced by complex domains in water and in TEOS aqueous solutions. *Physical Chemistry Chemical Physics*, 18(2), 772-780.
- Cookson, W. O., Glancy, J. J., & Frost, F. A. (1985). Asymmetric rapidly progressive lung fibrosis: a cause of pseudotumour in asbestosis. *British journal of industrial medicine*, 42(5), 350.
- Cyr, M., Lawrence, P., & Ringot, E. (2006). Efficiency of mineral admixtures in mortars: quantification of the physical and chemical effects of fine admixtures in relation with compressive strength. *Cement and concrete research*, 36(2), 264-277.
- Davidovits, J. (1987). Ancient and modern concretes: What is the real difference?. *Concrete International*, 9(12), 23-28.
- Deboucha, W., Leklou, N., Khelidj, A., & Oudjit, M. N. (2017). Hydration development of mineral additives blended cement using thermogravimetric analysis (TGA): Methodology of calculating the degree of hydration. *Construction and Building Materials*, 146, 687-701.
- Dheilily, R. M., Tudo, J., Sebaïbi, Y., & Quéneudec, M. (2002). Influence of storage conditions on the carbonation of powdered Ca (OH) 2. *Construction and Building Materials*, 16(3), 155-161.
- Dias, C. M. R., Cincotto, M. A., Savastano Jr, H., & John, V. M. (2008). Long-term aging of fiber-cement corrugated sheets—The effect of carbonation, leaching and acid rain. *Cement and Concrete Composites*, 30(4), 255-265.
- Ding, M., Chen, F., Shi, X., Yucesoy, B., Mossman, B., & Vallyathan, V. (2002). Diseases caused by silica: mechanisms of injury and disease development. *International immunopharmacology*, 2(2-3), 173-182.
- Directive 2008/98/EC of the European Parliament and of the Council of 19 November 2008 on waste and repealing certain Directives
- Directive 2009/125/EC of the European Parliament and of the Council of 21 October 2009 establishing a framework for the setting of ecodesign requirements for energy-related products
- Directive 80/1107/EEC, (1980). Council Directive 80/1107/EEC of 27 November 1980 on the protection of workers from the risks related to exposure to chemical, physical and biological agents at work
- Directive 83/477/EEC, (1983). Council Directive 83/477/EEC of 19 September 1983 on the protection of workers from the risks related to exposure to asbestos at work
- Donatello, S., Tyrer, M., & Cheeseman, C. R. (2010). Comparison of test methods to assess pozzolanic activity. *Cement and Concrete Composites*, 32(2), 121-127.

- Echigo, T., Kimata, M., Kyono, A., & Shimizu, M. (2005). Re-investigation of the crystal structure of whewellite [Ca (C₂O₄)· H₂O] and the dehydration mechanism of caoxite [Ca (C₂O₄)· 3H₂O]. *Mineralogical Magazine*, 69(1), 77-88.
- EN 196-1:2016 Methods of testing cement. Determination of strength, Brussels, 2005
- EN 450-1: 2012 - Fly ash for concrete. Definition, specifications and conformity criteria, Brussels, 2012
- Feng, D., Lin, Z., Liu, M., Xie, J., Wan, J., Wang, B., ... & Hu, Z. (2016). Silica-alumina gel humidity control beads with bimodal pore structure produced by phase separation during the sol-gel process. *Microporous and Mesoporous Materials*, 222, 138-144.
- Fic, S., Lyubomirskiy, N. V., & Barnat-Hunek, D. (2018). The Influence of the Natural Aggregate Roughness on the ITZ Adhesion in Concrete. In *Materials Science Forum* (Vol. 931, pp. 564-567). Trans Tech Publications.
- Finley, B. L., Pierce, J. S., Phelka, A. D., Adams, R. E., Paustenbach, D. J., Thuett, K. A., & Barlow, C. A. (2012). Evaluation of tremolite asbestos exposures associated with the use of commercial products. *Critical reviews in toxicology*, 42(2), 119-146.
- Gartner, E. M., & Macphee, D. E. (2011). A physico-chemical basis for novel cementitious binders. *Cement and Concrete Research*, 41(7), 736-749.
- Gautam, P. K., Kalla, P., Jethoo, A. S., Agrawal, R., & Singh, H. (2018). Sustainable use of waste in flexible pavement: A review. *Construction and Building Materials*, 180, 239-253.
- Goswami, E., Craven, V., Dahlstrom, D., Alexander, D., & Mowat, F. (2013). Domestic asbestos exposure: a review of epidemiologic and exposure data. *International journal of environmental research and public health*, 10(11), 5629-5670.
- Gualtieri, A. F., Levy, D., Dapiaggi, M., & Belluso, E. (2004). Kinetics of the decomposition of crocidolite asbestos: a preliminary real-time X-ray powder diffraction study. In *Materials Science Forum* (Vol. 443, pp. 291-294). Trans Tech Publications.
- Heikal, M., El-Didamony, H., & Morsy, M. S. (2000). Limestone-filled pozzolanic cement. *Cement and Concrete Research*, 30(11), 1827-1834.
- Hewlett, P. (2003). *Lea's chemistry of cement and concrete*. Elsevier.
- Hewlett, P., & Liska, M. (Eds.). (2019). *Lea's chemistry of cement and concrete*. Butterworth-Heinemann.
- Hu, C., Han, Y., Gao, Y., Zhang, Y., & Li, Z. (2014). Property investigation of calcium-silicate-hydrate (C-S-H) gel in cementitious composites. *Materials Characterization*, 95, 129-139.
- Hubert, C., Wieker, W., & Heidemann, D. (2001). Investigations of hydration products in high-volume fly ash binders. *Special Publication*, 199, 83-98.

- Hyatt, M., MacRae, N. D., & Nesbitt, H. W. (1982). Chemical treatment of chrysotile asbestos in laboratory solutions. *Environment International*, 7(3), 215-220.
- IBAS: The International Ban Asbestos Secretariat, L. Kazan-Allen, (2018). Current asbestos bans. http://www.ibasecretariat.org/lka_alpha_asb_ban_280704.php
- Juenger, M. C. G., Winnefeld, F., Provis, J. L., & Ideker, J. H. (2011). Advances in alternative cementitious binders. *Cement and concrete research*, 41(12), 1232-1243.
- Juenger, M. C., & Siddique, R. (2015). Recent advances in understanding the role of supplementary cementitious materials in concrete. *Cement and Concrete Research*, 78, 71-80.
- Kaid, N., Cyr, M., Julien, S., & Khelafi, H. (2009). Durability of concrete containing a natural pozzolan as defined by a performance-based approach. *Construction and Building Materials*, 23(12), 3457-3467.
- Khedr, S. A., & Abou-Zeid, M. N. (1994). Characteristics of silica-fume concrete. *Journal of Materials in Civil Engineering*, 6(3), 357-375.
- Kim, T., & Olek, J. (2012). Effects of sample preparation and interpretation of thermogravimetric curves on calcium hydroxide in hydrated pastes and mortars. *Transportation Research Record*, 2290(1), 10-18.
- Kusiorowski, R., Zaremba, T., & Piotrowski, J. (2016). Influence of the type of pre-calcined asbestos containing wastes on the properties of sintered ceramics. *Construction and Building Materials*, 106, 422-429.
- Kusiorowski, R., Zaremba, T., Piotrowski, J., & Gerle, A. (2013). Thermal decomposition of asbestos-containing materials. *Journal of Thermal Analysis and Calorimetry*, 113(1), 179-188.
- Kusiorowski, R., Zaremba, T., Piotrowski, J., & Podwórny, J. (2015). Utilisation of cement-asbestos wastes by thermal treatment and the potential possibility use of obtained product for the clinker bricks manufacture. *Journal of materials science*, 50(20), 6757-6767.
- Lavkulich, L. M., Schreier, H. E., & Wilson, J. E. (2014). Effects of natural acids on surface properties of asbestos minerals and kaolinite. *Journal of Environmental Science and Health, Part A*, 49(6), 617-624.
- Lawson, I., Danso, K. A., Odoi, H. C., Adjei, C. A., Quashie, F. K., Mumuni, I. I., & Ibrahim, I. S. (2011). Non-destructive evaluation of concrete using ultrasonic pulse velocity. *Research Journal of Applied Sciences, Engineering and Technology*, 3(6), 499-504.
- Lázár, M., Čarnogurská, M., Brestovič, T., Jasminská, N., Kmeťová, Ľ., Kapustová, Ľ., & Jezný, T. (2016). High-Temperature Processing of Asbestos-Cement Roofing Material in a Plasma Reactor. *Polish Journal of Environmental Studies*, 25(5), 2027-2033.
- Lea, F. M. (1971). *Chemistry of Cement and Concrete*, Arnold.

- Leonelli, C., Veronesi, P., Boccaccini, D. N., Rivasi, M. R., Barbieri, L., Andreola, F., & Pellacani, G. C. (2006). Microwave thermal inertisation of asbestos containing waste and its recycling in traditional ceramics. *Journal of hazardous materials*, 135(1-3), 149-155.
- Li, J., Dong, Q., Yu, K., & Liu, L. (2014). Asbestos and asbestos waste management in the Asian-Pacific region: trends, challenges and solutions. *Journal of cleaner production*, 81, 218-226.
- Liu, J., & Wang, D. (2017). Influence of steel slag-silica fume composite mineral admixture on the properties of concrete. *Powder technology*, 320, 230-238.
- Lothenbach, B., & Nonat, A. (2015). Calcium silicate hydrates: solid and liquid phase composition. *Cement and Concrete Research*, 78, 57-70.
- Marchon, D., & Flatt, R. J. (2016). Impact of chemical admixtures on cement hydration. In *Science and technology of concrete admixtures* (pp. 279-304). Woodhead Publishing.
- Markowitz, S. B., Levin, S. M., Miller, A., & Morabia, A. (2013). Asbestos, asbestosis, smoking, and lung cancer. New findings from the North American insulator cohort. *American journal of respiratory and critical care medicine*, 188(1), 90-96
- Massazza, F. (1998). Pozzolana and pozzolanic cements. *Lea's chemistry of cement and concrete*, 4, 471-636.
- Matschei, T., Lothenbach, B., & Glasser, F. P. (2007). The role of calcium carbonate in cement hydration. *Cement and Concrete Research*, 37(4), 551-558.
- McArthur, H., & Spalding, D. (2004). *Engineering materials science: Properties, uses, degradation, remediation*. Elsevier
- Moropoulou, A., Bakolas, A., & Aggelakopoulou, E. (2004). Evaluation of pozzolanic activity of natural and artificial pozzolans by thermal analysis. *Thermochimica Acta*, 420(1-2), 135-140.
- Murdock, L. J., & Brook, K. M. (1979). *Concrete materials and practice*, 5th edition, Arnold (Edward) Publishers, Limited, London.
- Nagrockienė, D., Girskas, G., & Skripkiūnas, G. (2017). Properties of concrete modified with mineral additives. *Construction and Building Materials*, 135, 37-42.
- Nam, S. N., Jeong, S., & Lim, H. (2014). Thermochemical destruction of asbestos-containing roofing slate and the feasibility of using recycled waste sulfuric acid. *Journal of hazardous materials*, 265, 151-157.
- Paglietti, F., Malinconico, S., della Staffa, B. C., Bellagamba, S., & De Simone, P. (2016). Classification and management of asbestos-containing waste: European legislation and the Italian experience. *Waste management*, 50, 130-150.

- Paglietti, F., Malinconico, S., della Staffa, B. C., Bellagamba, S., & De Simone, P. (2016). Classification and management of asbestos-containing waste: European legislation and the Italian experience. *Waste management*, 50, 130-150.
- Paglietti, F., Malinconico, S., Molfetta, V. D., Bellagamba, S., Damiani, F., Gennari, F., ... & Giangrasso, M. (2012). Asbestos risk: From raw material to waste management: The Italian experience. *Critical reviews in environmental science and technology*, 42(17), 1781-1861.
- Paglietti, F., Malinconico, S., Molfetta, V. D., Bellagamba, S., Damiani, F., Gennari, F., & Giangrasso, M. (2012). Asbestos risk: From raw material to waste management: The Italian experience. *Critical reviews in environmental science and technology*, 42(17), 1781-1861.
- Paiva, H., Silva, A. S., Velosa, A., Cachim, P., & Ferreira, V. M. (2017). Microstructure and hardened state properties on pozzolan-containing concrete. *Construction and Building Materials*, 140, 374-384.
- Panizza M., Natali M., Garbin E., Tamburini S. and Secco M. (2018). Assessment of geopolymers with Construction and Demolition Waste (CDW) aggregates as a building material, *Construction and Building Materials* 181, 119–133, doi: 10.1016/j.conbuildmat.2018.06.018
- Parale, V. G., Han, W., Lee, K. Y., & Park, H. H. (2018). Ambient pressure dried tetrapropoxysilane-based silica aerogels with high specific surface area. *Solid State Sciences*, 75, 63-70.
- Park, E. K., Takahashi, K., Jiang, Y., Movahed, M., & Kameda, T. (2012). Elimination of asbestos use and asbestos-related diseases: A n unfinished story. *Cancer science*, 103(10), 1751-1755.
- Park, E. K., Takahashi, K., Jiang, Y., Movahed, M., & Kameda, T. (2012). Elimination of asbestos use and asbestos-related diseases: A n unfinished story. *Cancer science*, 103(10), 1751-1755.
- Pawelczyk, A., Bożek, F., Grabas, K., & Chęcmanowski, J. (2017). Chemical elimination of the harmful properties of asbestos from military facilities. *Waste Management*, 61, 377-385.
- Plescia, P., Gizzi, D., Benedetti, S., Camilucci, L., Fanizza, C., De Simone, P., & Paglietti, F. (2003). Mechanochemical treatment to recycling asbestos-containing waste. *Waste Management*, 23(3), 209-218.
- Quarcioni, V. A., Chotoli, F. F., Coelho, A. C. V., & Cincotto, M. A. (2015). Indirect and direct Chapelle's methods for the determination of lime consumption in pozzolanic materials. *Revista Ibracon de Estruturas e Materiais*, 8(1), 1-7.
- Rao, A. V., & Bhagat, S. D. (2004). Synthesis and physical properties of TEOS-based silica aerogels prepared by two step (acid–base) sol–gel process. *Solid State Sciences*, 6(9), 945-952.
- Resolution EU-P7_TA, 2013

- Rivera-Villarreal, R., & Kraymer, S. (1996). Ancient structural concrete in Mesoamerica. *Concrete International*, 18(6), 67-70.
- Ro, J. C., & Chung, I. J. (1989). Sol-gel kinetics of tetraethylorthosilicate (TEOS) in acid catalyzed. *Journal of non-crystalline solids*, 110(1), 26-32.
- Roskill Information Services Ltd, 1986
- Rostami, V., Shao, Y., Boyd, A. J., & He, Z. (2012). Microstructure of cement paste subject to early carbonation curing. *Cement and Concrete Research*, 42(1), 186-193.
- Roszczyński, W. (2002). Determination of pozzolanic activity of materials by thermal analysis. *Journal of Thermal Analysis and Calorimetry*, 70(2), 387-392.
- Rozalen, M., & Huertas, F. J. (2013). Comparative effect of chrysotile leaching in nitric, sulfuric and oxalic acids at room temperature. *Chemical Geology*, 352, 134-142.
- Rozalen, M., & Huertas, F. J. (2013). Comparative effect of chrysotile leaching in nitric, sulfuric and oxalic acids at room temperature. *Chemical Geology*, 352, 134-142.
- Ruiz, A. I., Ortega, A., Fernández, R., Miranda, J. F., Samaniego, E. L., & Cuevas, J. (2018). Thermal treatment of asbestos containing materials (ACM) by mixing with Na₂CO₃ and special clays for partial vitrification of waste. *Materials Letters*, 232, 29-32.
- Sakulich, A. R. (2011). Reinforced geopolymer composites for enhanced material greenness and durability. *Sustainable Cities and Society*, 1(4), 195-210.
- Sanjuan, M. A., Argiz, C., Gálvez, J. C., & Moragues, A. (2015). Effect of silica fume fineness on the improvement of Portland cement strength performance. *Construction and Building Materials*, 96, 55-64.
- Sanjuan, M. A., Argiz, C., Gálvez, J. C., & Moragues, A. (2015). Effect of silica fume fineness on the improvement of Portland cement strength performance. *Construction and Building Materials*, 96, 55-64.
- Schreier, H. (1989). *Asbestos in the natural environment* (Vol. 37). Elsevier.
- Sekkoum, K., Cheriti, A., Taleb, S., & Belboukhari, N. (2016). FTIR spectroscopic study of human urinary stones from El Bayadh district (Algeria). *Arabian Journal of Chemistry*, 9(3), 330-334.
- Senff, L., Modolo, R. C. E., Silva, A. S., Ferreira, V. M., Hotza, D., & Labrincha, J. A. (2014). Influence of red mud addition on rheological behavior and hardened properties of mortars. *Construction and Building Materials*, 65, 84-91.
- Senhadji, Y., Escadeillas, G., Mouli, M., & Khelafi, H. (2014). Influence of natural pozzolan, silica fume and limestone fine on strength, acid resistance and microstructure of mortar. *Powder technology*, 254, 314-323.

- Siddique, R. (2011). Utilization of silica fume in concrete: Review of hardened properties. *Resources, Conservation and Recycling*, 55(11), 923-932.
- Silva, R. V., De Brito, J., & Dhir, R. K. (2017). Availability and processing of recycled aggregates within the construction and demolition supply chain: A review. *Journal of cleaner production*, 143, 598-614.
- Skinner, H. C. W., Ross, M., & Frondel, C. (1988). *Asbestos and other fibrous materials: mineralogy, crystal chemistry, and health effects*. Oxford University Press.
- Spasiano, D., & Pirozzi, F. (2017). Treatments of asbestos containing wastes. *Journal of environmental management*, 204, 82-91.
- Spasiano, D., Luongo, V., Race, M., Petrella, A., Fiore, S., Apollonio, C., & Piccinni, A. F. (2019). Sustainable bio-hydrothermal sequencing treatment for asbestos-cement wastes. *Journal of hazardous materials*, 364, 256-263
- Sugama T., Sabatini R., Petrakis L., 1998. Decomposition of Chrysotile Asbestos by Fluorosulfonic Acid, *Ind. Eng. Chem. Res.* 5885, 79–88.
- Sugama, T., Sabatini, R., & Petrakis, L. (1998). Decomposition of chrysotile asbestos by fluorosulfonic acid. *Industrial & engineering chemistry research*, 37(1), 79-88.
- Theodosoglou, E., Koroneos, A., Paraskevopoulos, K. M., Christofides, G., Papadopoulou, L., & Zorba, T. (2007). Comparative infrared spectroscopic study of natural amphiboles. *Bulletin of the Geological Society of Greece*, 40(2), 984-995.
- Thomaidis, E., & Kostakis, G. (2015). Synthesis of cordieritic materials using raw kaolin, bauxite, serpentinite/olivinite and magnesite. *Ceramics International*, 41(8), 9701-9707.
- Thomaidis, E., & Kostakis, G. (2015). Synthesis of cordieritic materials using raw kaolin, bauxite, serpentinite/olivinite and magnesite. *Ceramics International*, 41(8), 9701-9707.
- Triantafyllou A. *Δομικά Υλικά, Εκδόσεις Gotsis*, ISSN: 978-960-9427-65-4
- Valouma, A., Verganelaki, A., Maravelaki-Kalaitzaki, P., & Gidaracos, E. (2016). Chrysotile asbestos detoxification with a combined treatment of oxalic acid and silicates producing amorphous silica and biomaterial. *Journal of hazardous materials*, 305, 164-170.
- Valouma, A., Verganelaki, A., Tectoros, I., Maravelaki-Kalaitzaki, P., & Gidaracos, E. (2017). Magnesium oxide production from chrysotile asbestos detoxification with oxalic acid treatment. *Journal of hazardous materials*, 336, 93-100.
- Veblen, D. R., & Wylie, A. G. (1993). *Mineralogy of amphiboles and 1: 1 layer silicates* (No. CONF-9310406-Vol. 28). Mineralogical Society of America, Washington, DC (United States).
- Vedalakshmi, R., Raj, A. S., Srinivasan, S., & Babu, K. G. (2003). Quantification of hydrated cement products of blended cements in low and medium strength concrete using TG and DTA technique. *Thermochimica Acta*, 407(1-2), 49-60.

- Verganelaki A., Kilikoglou V., Karatasios I., Maravelaki-Kalaitzaki P., 2014. A biomimetic approach to strengthen and protect construction materials with a novel calcium-oxalate-silica nanocomposite. *Constr. Build. Mater.* 62, 8–17.
- Viani, A., & Gualtieri, A. F. (2014). Preparation of magnesium phosphate cement by recycling the product of thermal transformation of asbestos containing wastes. *Cement and Concrete Research*, 58, 56-66.
- Viani, A., Gualtieri, A. F., Secco, M., Peruzzo, L., Artioli, G., & Cruciani, G. (2013). Crystal chemistry of cement-asbestos. *American Mineralogist*, 98(7), 1095-1105.
- Virta R. L. & Flanagan D.M., (2014). US Geological Survey 2013 minerals yearbook: asbestos. US Department of the Interior.
- Virta, R. L. (2006). Worldwide asbestos supply and consumption trends from 1900 through 2003. US Geological Survey.
- Wagner, J.C.; Sleggs, C.A.; Marchand, P. Diffuse pleural mesothelioma and asbestos exposure in the north western Cape Province. *Brit. J. Ind. Med.* **1960**, 17, 260-271.
- Wang, D., Shi, C., Farzadnia, N., Shi, Z., Jia, H., & Ou, Z. (2018). A review on use of limestone powder in cement-based materials: Mechanism, hydration and microstructures. *Construction and Building Materials*, 181, 659-672.
- Weiss, W. (1999). Asbestosis: a marker for the increased risk of lung cancer among workers exposed to asbestos. *Chest*, 115(2), 536-549.
- Wendehorst, R. (1975). *Materials of Construction*, 2nd edition, Construction Press, London.
- Wille D., (2016). STATE OF THE ART ASBESTOS Possible treatment methods in Flanders: constraints and opportunities. 3, 1–142. Retrieved from www.ovam.be
- Yajun, J., & Cahyadi, J. H. (2003). Effects of densified silica fume on microstructure and compressive strength of blended cement pastes. *Cement and Concrete Research*, 33(10), 1543-1548.
- Yamamoto, T., Kida, A., Noma, Y., Terazono, A., & Sakai, S. I. (2014). Development of a testing method for asbestos fibers in treated materials of asbestos containing wastes by transmission electron microscopy. *Waste management*, 34(2), 536-541.
- Yıldırım, G., Khiavi, A. H., Yeşilmen, S., & Şahmaran, M. (2018). Self-healing performance of aged cementitious composites. *Cement and Concrete Composites*, 87, 172-186.
- Yvon, Y., & Sharrock, P. (2011). Characterization of thermochemical inactivation of asbestos containing wastes and recycling the mineral residues in cement products. *Waste and Biomass Valorization*, 2(2), 169-181.

Zaremba, T., Krzakała, A., Piotrowski, J., & Garczorz, D. (2010). Study on the thermal decomposition of chrysotile asbestos. *Journal of Thermal Analysis and Calorimetry*, 101(2), 479-485.

Zhang, Z., Zhang, B., & Yan, P. (2016). Hydration and microstructures of concrete containing raw or densified silica fume at different curing temperatures. *Construction and Building Materials*, 121, 483-490.

Αναστασιάδου Κ., (2011). Υδροθερμική επεξεργασία αμιαντούχων υλικών σε υπό/υπερκρίσιμες συνθήκες, Διδακτορική διατριβή, Πολυτεχνείο Κρήτης

Γιδαράκος Ε., (2006). Επικίνδυνα Απόβλητα, Διαχείριση – Επεξεργασία -Διάθεση, Εκδόσεις Ζυγός, Θεσσαλονίκη

Links

<https://www.asbestos.com/mesothelioma/related-diseases/>

<https://www.chegg.com>

<http://ibasecretariat.org/>

www.statista.com

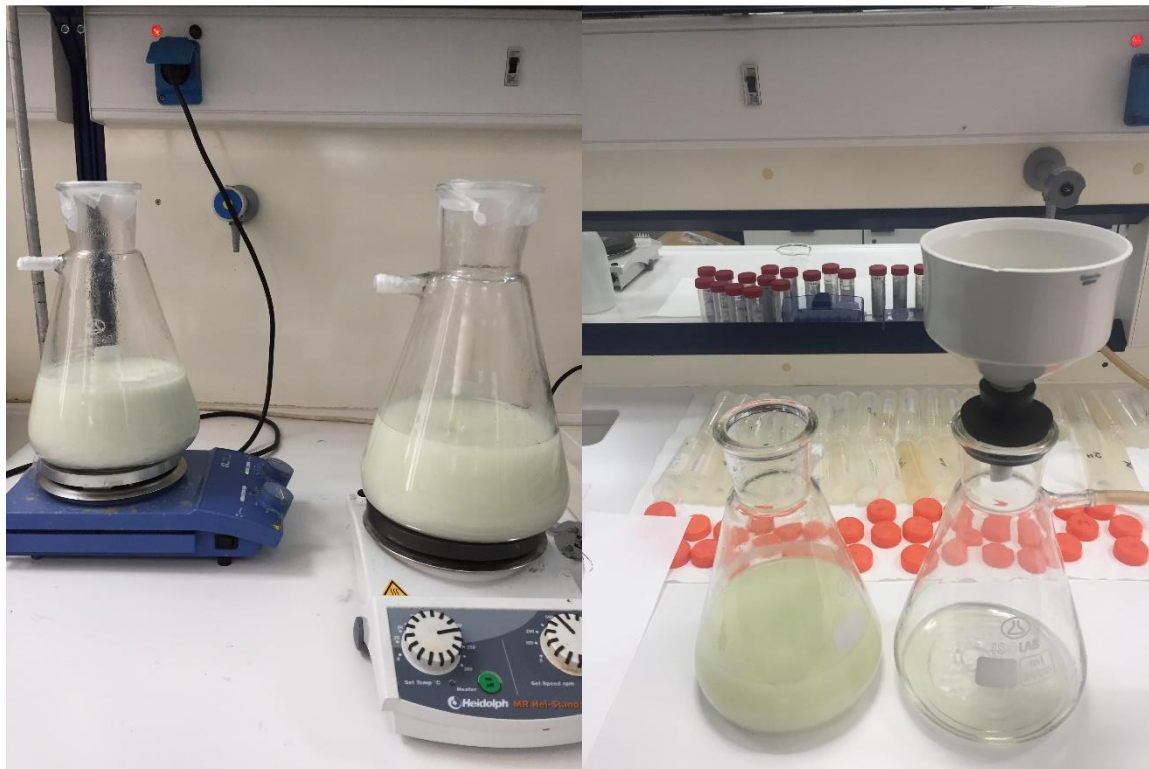
APPENDIXPhotos of the experimental procedure

Figure 1: Chemical treatment of asbestos containing waste with oxalic acid and tetraethyl orthosilicate.



Figure 2: The precipitate by-product of the combined treatment

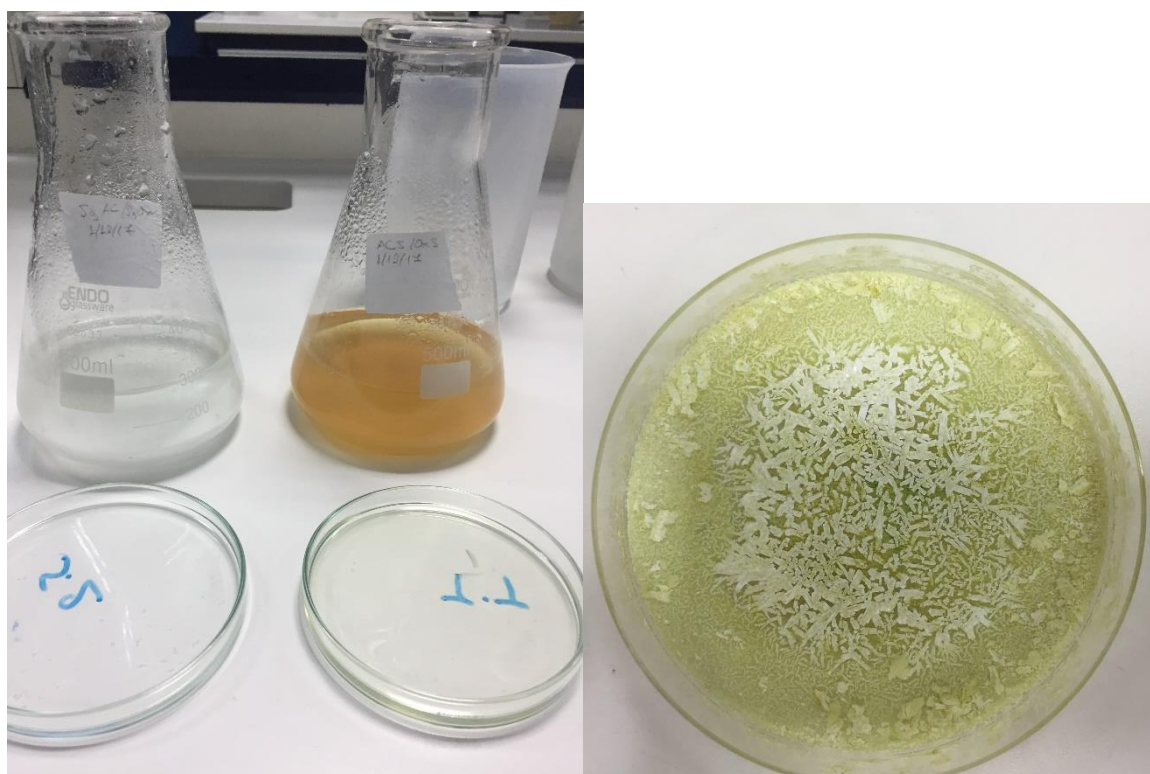


Figure 3: The supernatant of the treatment with oxalic acid and dried sample.

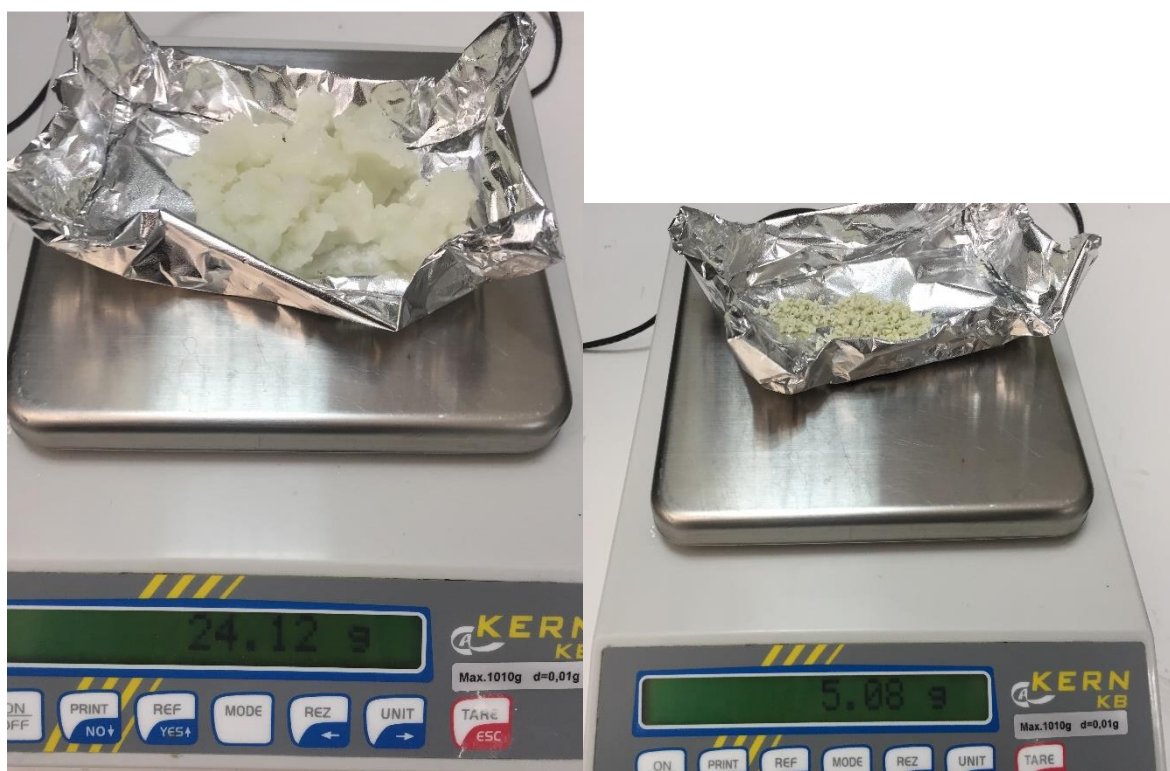


Figure 4: The precipitate of the treatment with oxalic acid and tetraethyl orthosilicate and dried sample



Figure 5: The apparatus of Chapelle test



Figure 6: Titration for CaO consumption measurement



Figure 7: Preparation of cement mortars



Figure 8: Casting of cement mortars into prismatic steel moulds $4 \times 4 \times 16 \text{ cm}^3$



Figure 9: Demoulding of specimens after 24 hours



Figure 10: Specimens of mortars after 90 days of curing in a curing chamber (E139, MATEST) with stable conditions at 27-30 °C and relative humidity of 90%.

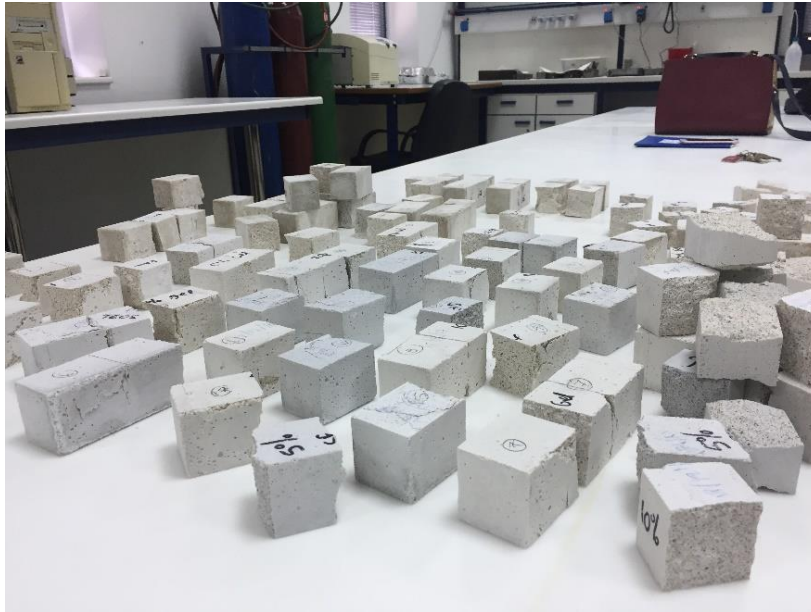


Figure 11: Specimens after measurement for compressive strength evaluation using a Matest type compression and flexural machine with dual range 500/15 kN.